Lawrence Berkeley Laboratory
UNIVERSITY OF CALIFORNIA

Materials & Molecular Research Division

NOVEL GRAPHITE SALTS OF HIGH OXIDIZING POTENTIAL

Eugene Michael McCarron III
(Ph.D. thesis)

August 1980

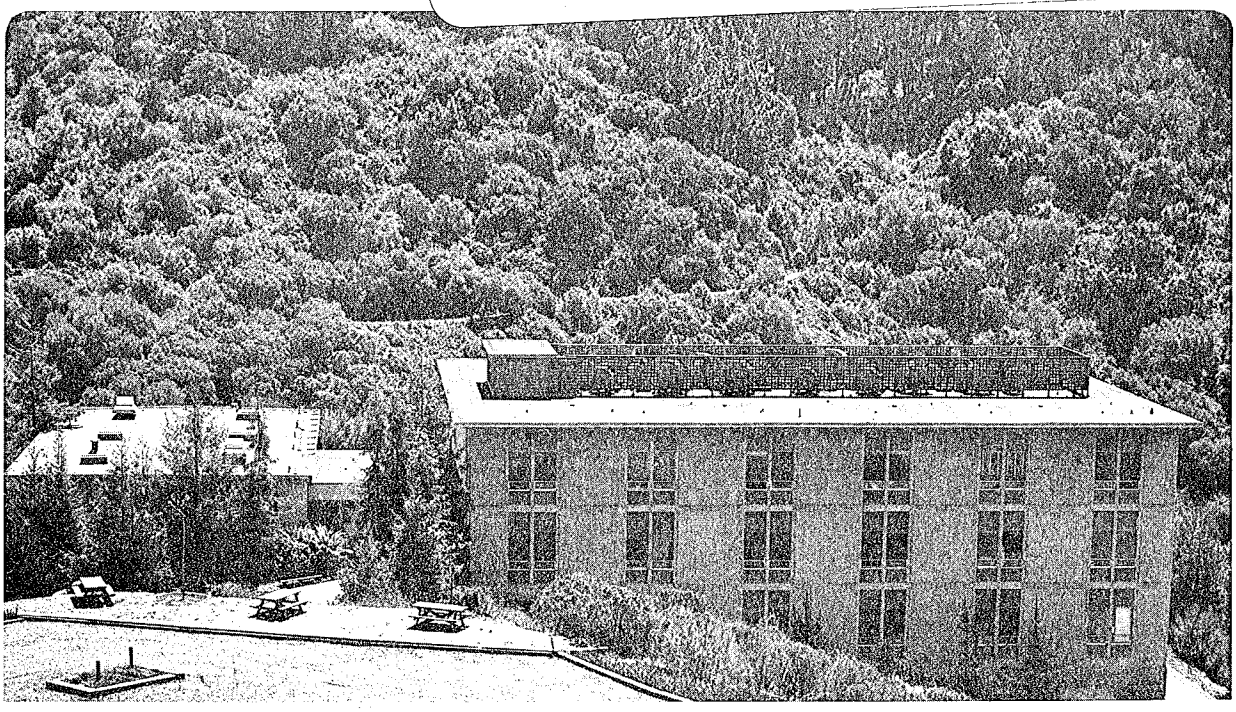

Prepared for the U.S. Department of Energy under Contract W-7405-ENG-48

LBL-11272

NOVEL GRAPHITE SALTS OF HIGH OXIDIZING POTENTIAL

Eugene Michael McCarron III

Materials and Molecular Research Division
Lawrence Berkeley Laboratory
and
Department of Chemistry
University of California
Berkeley, California 94720

This work was supported by the U.S. Department of Energy
under contract No. W-7405-ENG-48

For those special people:

"I have a feeling we're not in Kansas any more."

NOVEL GRAPHITE SALTS OF HIGH OXIDIZING POTENTIAL

Table of Contents

Table of Contents (continued)

Table of Contents (continued)

Table of Contents (continued)

List of Tables

List of Tables (continued

List of Figures

List of Figures (continued)

ACKNOWLEDGMENTS

I would like to especially thank Professor Neil Bartlett. He smoothed out the few rough times and accentuated the many good ones. I will always consider him, professionally, a true scientist and, personally, a true friend.

I would like to thank Dr. Tom Thompson of SRI International for his time and effort in making the conductivity studies. His physical measurements provided much of the impetus for my synthetic work; Professor Rudi Wenk of the Geology Department for his help with the x-ray diffraction studies and also his time spent in judging my candidacy; Professor Leo Brewer for reading critically my thesis through to the last period.

Special thanks go to Drs. Jean Grannec and Josik Portier of the Laboratoire de Chemie du Solide du CNRS, Bordeaux, France. They not only provided for some interesting dabblings into both pure and applied electrochemistry, but also made France come alive for a total stranger. Especially Jean, for without whom, my shirts would still be at the laundry.

Finally, thanks to all my friends, who form the memories of that time in my life that I call Berkeley (August 1976 - September 1980).

This work was supported by the U.S. Department of Energy under contract No. W-7405-ENG-48.

NOVEL GRAPHITE SALTS OF HIGH OXIDIZING POTENTIAL

Eugene Michael McCarron III

Materials and Molecular Research Division
Lawrence Berkeley Laboratory
and
Department of Chemistry
University of California
Berkeley, California 94720

ABSTRACT

The intercalation of graphite by the third-transition-series metal hexafluorides has yielded the graphite salts, $C_8^+OsF_6^-$, $C_8^+IrF_6^-$ and $C_{12}^{2+}PtF_6^{2-}$. The fluoroplatinate salt represents the highest electron withdrawal from the graphite network yet achieved.

Analogues to the Os and Ir salts have been obtained both by fluorination of Group V pentaflouride intercalates, C_8MF_5 (M = As, Sb), and by the interaction of the dioxygenyl salts with graphite ($8C + O_2MF_6 \rightarrow C_8MF_6 + O_2\uparrow$). Non-intercalating binary fluorides have been observed to intercalate in the presence of a fluorine-rich environment (e.g., $8C + PF_5 + 1/2\ F_2 \rightarrow C_8PF_6$).

GeF_4, which also does not spontaneously intercalate graphite, has been observed to interact with graphite in the presence of 2 atmospheres of fluorine overpressure to give the fluoroplatinate salt analogue, $C_{12}^{2+}GeF_6^{2-}$. This material is in equilibrium with the pentafluorogermanate at ordinary pressures and temperatures:

$$C_{12}^{2+}GeF_6^{2-} \rightarrow C_{12}^{+}GeF_5^{-} + 1/2\ F_2 \quad .$$

$C_{12}GeF_6$ must have an oxidizing potential close to that of fluorine itself.

The graphite fluorometallate salts are both electronic and ionic (F^-) conductors. For the $C_8^+MF_6^-$ salts, a maximum electronic conductivity an order of magnitude greater than the parent graphite has been observed for stage two. The high oxidizing potential, coupled with the fluoride ion transport capability of the graphite salts, has been exploited in the construction of solid-state galvanic cells. These cells use the graphite fluorometallate salts as electrode materials in combination with a superionic fluoride-ion-conducting solid electrolyte.

CHAPTER I

GENERAL INTRODUCTION

The 'bare bones' of this thesis are the graphite fluorometallate salts. Summarily, this thesis can be broadly divided into two parts: (1) the synthesis and characterization of novel graphite salts (Chapters III through VII) and (2) studies of the intriguing physical characteristics (electronic and electrochemical) of these salts (Chapters VIII and IX). The division is somewhat arbitrary, in that often, the interesting physical features of a particular system dictated the direction of new synthetic efforts.

Techniques and apparatus involved in working with graphite salts, and high energy oxidizers in general, are described in Chapter II, as are descriptions of the instrumentation used in the experimental work.

Chapter III deals with the interaction of graphite with the third-series platinum metal hexafluorides. These hexafluorides, MF_6 (M = W → Pt), represent a unique series of compounds of well-graded oxidizing power. Likewise, the dioxygenyl salts, $O_2^+MF_6^-$ (M = As, Pt, Au), which are very potent oxidizers, react with graphite to produce salts with liberation of oxygen (Chapter IV). It has also been found that, in certain cases where a metal fluoride will not spontaneously intercalate graphite, the provision of fluorine-rich atmosphere will promote salt formation (Chapter V).

Chapters VI and VII describe the important graphite fluoroarsenate and graphite fluorogermanate systems. These systems are complicated by the presence of more than one guest species and these different species are in equilibrium with one another. The fluoroarsenate systems is

undoubtedly the most studied of all graphite-acceptor intercalation compounds. The fluorogermanate system involves an equilibrium with gaseous F_2 at ordinary temperatures and pressures, and is the first substance known to be in equilibrium with the most powerfully oxidizing of the elements.

All graphite salts conduct electricity. The graphite fluorometallates are both electronic (Chapter VIII) and ionic, F^- (Chapter IX), conductors. The potential of these graphite fluormetallate salts, with respect to electrochemical applications, is discussed briefly in these Chapters.

CHAPTER II

GENERAL APPARATUS AND HANDLING TECHNIQUES

A. Apparatus

1. General

Central to the chemistry of high energy oxidizers is the need to maintain a rigorously dry, inert environment. Hence, all of the experiments outlined in this thesis required the use of a metal high-vacuum line and an inert-atmosphere box. Methods for handling air-sensitive materials are described in detail by Shriver.[1]

The manipulation of volatile compounds was accomplished using a vacuum line consisting of: (1) a high-pressure region constructed from Autoclave Engineering 30VM6071 Monel valves (rated to 30,000 psi) and appropriate connectors; (2) a low-pressure region constructed from Whitey IKS4 stainless steel valves connected with 1/4 inch swage-locked stainless steel pipe.

In the high-pressure region which serviced the fluorine cylinder, pressures (0-500 psia) were measured with an Acco Helicoid gauge (Bridgeport, Connecticut). A second Helicoid gauge (0-1500 torr Hg) was located in the low-pressure portion of the system.

Vacuum was provided throughout the system by three separate pumps: (1) a small mechanical pump for drawing corrosive materials through a soda lime tower for disposal; (2) a large mechanical pump for high speed rough-pumping; and (3) a two-inch Consolidated Vacumn Corporation silicone oil diffusion pump coupled to a large-bore manifold for high-vacuum capacity. Vacuum was measured throughout the system with Varian (type 0531) thermocouple gauges.

Reaction vessels, blown from quartz tubing and capped with Whitey valves via teflon-Swagelok compresion fitting, were attached to ports on the vacuum system. The loading of solid materials into the quartz tubes was done in a Vacuum Atmospheres Corporation Dri-Lab (North Hollywood, California) which housed a Metler H311 analytical balance. A dry nitrogen atmosphere (checked by glowing tungsten filament) was maintained by two circulating trains; an oxygen scavenger, and a water scrubber. These trains were regenerated on a regular schedule.

All newly assembled or reassembled reaction systems were leak tested using a Consolidated Electrodynamics Corporation quadrupole mass spectrometer helium leak detector.

Finally, high pressure/high temperature reactions were carried out in Monel metal bombs, tested to 500 atmospheres of gaseous fluorine at 600^{o}C.

2. In-Situ Sample Shroud for X-Ray Diffractometer Studies

To observed structural rearrangements in HOPG (highly oriented pyrolytic graphite) samples as intercalation proceeds, a reaction shroud was designed which fits over a goniometer head for use with a General Electric XRD5 x-ray diffractometer. The schematic is given in Fig. II-1.

The shroud was milled from an aluminum block down to a dome thickness of 15/1000ths of an inch. Aluminum was chosen for the shroud material because of its relatively weak x-ray absorption and its ability, once passivated with elemental fluorine, to withstand extremely oxidizing environments.

The shroud, containing the HOPG sample, is evacuated through the port (1/8 inch, i.d.), through which volatile reactants are subsequently

introduced. The HOPG sample is held in position by draping teflon tape over the sample and securing the tape to the center teflon post with a teflon-coated o-ring. This allows for the expected c-axis expansion of the sample (normal to the sample-post interface).

3. Battery Casing for Solid Electrolyte Cells

The schematic for a solid electrolyte battery is given in Fig. II-2. Screwing down on the teflon body brings the gold current collectors into contact with the electrodes (powder or HOPG) which are separated by the solid electrolyte plug. The solid electrolyte used was $PbF_2 \cdot SbF_3$.[2] Due to the moisture sensitivity of the materials involved, the cell was put together in the Dri-Lab and potential measurements were made via leads run through jacks in the Dri-Lab wall to the outside. The cells could be brought out of the Dri-Lab, however, if Kel-F grease was liberally applied to the case threads and lead holes to insure an air-tight seal.

4. Teflon FEP - Quartz Capillary Seals

Teflon to quartz seals permitted the reaction/growth of air sensitive single-crystals within a quartz capillary, upon which, the subsequent x-ray precession work could be done directly. This eliminated the painstaking task of handling small crystals in the Dri-Lab.

The seals were made by first drawing down a 9 mm pyrex tube and breaking it so that a 1.5 mm quartz capillary could just be inserted into the draw-down end. From the other end of the pyrex tube, 1/4 inch teflon FEP tubing (Chemplast Inc., Wayne, New Jersey) was slid in (see Fig. II-3.). The draw-down end was then heated just until the FEP became translucent. Pushing the FEP forward at this time caused the FEP to extrude from the draw-down end of the pyrex tube forming, with luck, a

vacuum-tight seal upon cooling. The teflon FEP tube was then capped with a Whitey valve using teflon Swagelok compression fittings.

B. Reagents

1. Graphite

The graphite used in these studies was of three types: (1) HOPG (highly oriented pyrolytic graphite); (2) powder; (3) natural single crystals.

HOPG was suplied by Dr. Authur Moore of Union Carbide, Parma, Ohio. It is produced by stress-annealing cracked methane at high temperature (>2000°C). It is exceptionally pure (99.9%) and well ordered, having a c-axis spread of <1°.

Graphite powder used for large scale and tensiometric work was obtained by "filing" monolithic pieces of NASA "nose-cone" graphite. The powder produced in this manner was better than 200 mesh. After vacuum heating this graphite in a quartz tube with a hand torch to a cherry-red glow for 15-20 minutes, a typical CHN analysis gave: C-98.5%, H-0.5%, N-0.1%. After fluorination with 2 atmospheres pressure F_2 at room temperature for 1/2 hour and subsequent vacuum heating, this graphite analyzed as 100% carbon.

Naturally occurring single crystals of graphite used in x-ray precession work were obtained from a calcite marble of the Santa Lucia formation, Big Sur, California.[3] The single crystals were freed by dissolution of the marble matrix in concentrated hydrochloric acid. They were then washed with water, dried, and selected by x-ray precession photography. The selection process was notoriously tedious as a result of facile twinning in the graphite system.

Prior to any reaction, the graphite was treated with elemental fluorine to remove any reducing species remaining after the vacuum drying procedure; graphite itself being inert to fluorine at ordinary pressures and temperatures.[4]

2. Metals

The metals used in the preparation of binary fluorides and dioxygenyl salts were all used as supplied without further purification. As list of the metals along with their supplier follows:

Metal	Supplier
Gold	Engelhard Industries (Union, NJ)
Platinum	Engelhard Industries (Union, NJ)
Iridium	Engelhard Industries (Union, NJ)
Osmium	Engelhard Industries (Union, NJ)
Rhenium	Engelhard Inudstries (Union, NJ)
Arsenic	B & A, Allied Chemical (Morristown, NJ)
Germanium	Alfa Inorganics Inc. (Beverly, MA)
Silicon	Matheson, Coleman & Bell (Norwood, OH)

All metals were specified at least 99.99% pure.

3. Metal Hexafluorides

The transition metal hexafluories listed below were prepared by standard procedures. The literature references are also cited. Characterization was done by infrared spectroscopy.

MF_6	Reference
PtF_6	Wienstock, Malm, and Weaver[5]
IrF_6	Ruff and Fisher[6]
OsF_6	Wienstock and Malm[7]
ReF_6	Malm and Selig[8]

Tungsten hexafluoride was used as supplied by Matheson Gas Products (East Rutherford, New Jersey).

4. Rhenium Heptafluoride

ReF_7 was prepared according to Malm and Selig[8] and confirmed by infrared spectroscopy.

5. Dioxygenyl Hexafluorometallate Salts

O_2MF_6 salts were prepared by standard procedures. The salts along with their literature references are listed below. The salts were characterized by Raman spectroscopy.

Salt	References
O_2AuF_6	Leary and Bartlett[9]
O_2PtF_6	Bartlett and Lohman[10]
O_2AsF_6	Shamir and Binerbouym[11]

6. Gases and Volatile Liquids

All volatile reactants were checked for purity by infrared spectroscopy prior to reaction.

Fluorine was supplied by Matheson Gas Products. Traces of hydrogen fluoride were removed by passing the F_2 through a copper coil immersed in liquid nitrogen. Arsenic pentafluoride, supplied by Ozark-Mahoning (Tulsa, Oklahoma), was purified by a brief pumping at 78°C (dry ice - acetone bath). Arsenic trifluoride was produced by reacting AsF_5 and As metal (excess) at ~200°C in a Monel bomb for 12 hours. Germanium tetrafluoride was obtained by reacting the elements in a Monel bomb. CAUTION! Because of the extreme exothermicity of this reaction, the F_2 was added in aliquots with extreme caution at first, until F_2 uptake became impreceptibly slow. Excess F_2 was then added, and the bomb heated to 200°C for 12 hours to insure complete reaction. Silicon tetrafluoride was produced in a manner analogous to GeF_4. Phosphorous pentafluoride

was obtained by reacting phosphorus trifluoride (Pennisular Chemresearch, Inc., Gainsville, Florida) with F_2 (in excess) at 200°C in a Monel bomb for 12 hours.

Peroxydisulfuryl difluoride was produced by the method of Wechsburg, Bulliner, Sladky, Mews, and Bartlett.[12] The resulting $S_2O_6F_2$ was stored over graphite, which appeared to inhibit decomposition.

The solvent, hydrogen fluoride (Matheson Gas Products), was treated with 2 atmospheres F_2 pressure before being condensed onto and stored over K_2NiF_6, a water scavenger. Sulfuryl chlorofluoride, also used as a solvent, was supplied by Ozark Machoning. SO_2ClF was distilled immediately before reaction. To remove oxidizable impurities, SO_2ClF was condensed onto O_2AsF_6 and allowed to warm to -45°C (chlorobenzene slush). All volatiles produced were removed at -78°C. The SO_2ClF was then held at -78°C until condensed into the reaction vessel.

C. Instrumentation

1. X-Ray Powder Diffraction

X-ray diffractometer tracings of intercalated HOPG samples were recorded with a Phillips-Norelco powder diffractometer equipped with a graphite monochromator (Cu - K_α radiation). An inert-atmosphere sample holder was designed to fit into the diffractometer's spinning sample holder. The schematic is given in Fig. II-4. The sample, loaded in the Dri-Lab, was centered on the teflon post, covered with a thin plastic "Baggie" wrap, and secured with an o-ring compression seal. The sample, aligned with its c-axis normal to the powder plane, limited observable reflections to 00ℓ. Scans were normally run from $2\theta = 3^\circ$ to 90°.

2. X-Ray Powder Photography

X-ray powder photographs were taken using a General Electric Precision Powder Camera of 45 cm circumference (Straumanis loading) equipped with a grahite monochromator (Cu - K_α radiation). Finely powdered samples were loaded in the Dri-Lab into 0.3 - 0.5 mm thin-walled quartz capillaries (Charles Supper Company, Inc., Natick, Massachusetts). The sample-containing capillaries were temporarily sealed in the Dri-Lab with a plug of Kel-F grease. Once outside the Dri-Lab, the capillaries were drawn down and sealed with a microflame torch. X-ray films were measured on a Norelco film-measuring device.

3. Single Crystal Precession Photography

Precession work was performed on a Enraf-Nonius camera, type Y925-67 (Delft, Holland), equipped with a Polaroid XR-7 film cassette, using zirconium filtered Mo radiation. Single crystals of graphite were suspended in a quartz wool within a 1.5 mm quartz capillary (see Fig. II-5). The quartz wool allowed for the c-axis expansion which results from intercalation. The intercalation was performed in a system as described in Chapter II, section A.3. After reaction, the specimen-containing quartz capillary was drawn down and sealed with a microflame torch.

4. Magnetic Susceptibility

Magnetic susceptibility measurements were made using a Princeton Applied Research Vibrating Sample Magnetometer over the temperature range 4^{o}-77^{o}C. Powdered samples, typically 0.15-0.25 gram, were loaded into specially fabrication Kel-F tubes. A tight-fitting plug was pressed firmly down onto the sample to insure dense packing of the sample while

protecting the sample from moisture. $Hg(Co(SCN_4)_2$ was used as the calibration standard.[13]

5. Infrared Spectroscopy

Infrared spectra were recorded with a Perkin-Elmer Model 597 spectrometer over the range 4000-200 cm^{-1}. Gas spectra were obtained with a 10 cm path length Monel cell fitted with silver chloride windows. These windows were cut from a 1 mm sheet of AgCl supplied by Harshaw Chemical Company (Cleveland, Ohio). The cell was also fitted with a side arm which permitted condensation of volatiles into the cell under static or dynamic vacuum.

6. Raman Spectroscopy

Raman spectra were recorded using a Jubin-Yvon Ramanor double monachromator. Two lasers, a Spectra Physics Model 165 krypton ion and a Coherent Radiation Model CR-2 Argon ion, were used as sources for three excitation wavelengths:

blue	488.0 nm
green	514.5 nm
red	647.1 nm

Powdered samples were loaded into quartz capillaries as described under X-Ray Powder Photography.

7. Chemical Analysis

i) CHN: Routine CHN analyses were performed on powder samples by the Microanalytic Laboratory in the College of Chemistry, University of California, Berkeley.

ii) Platinum: Platinum analysis was done by roasting samples containing C, Pt and F in a flowing oxygen stream at 800°C. The sample was contained in a platinum boat. Analysis was by gravimetry.

8. Electrical Conductivity Measurement

Measurement of basal plane electrical conductivities was made by the contactless radio frequency (1 kHz) inductive technique described by Zeller, Denenstein and Foley.[14] The technique is illustrated in Fig. II-6. For these measurements, HOPG was air-abraided into pieces, each roughly square, approximately 5 mm on edge (ab-plane) and 1/2 mm thick (along the c-axis). Calibration of the instrument was accomplished using a copper standard of nearly the same dimensions.

The induced eddy current (Fig. II-7) was sensed in a secondary circuit and the conductivity was derived from the empirically evaluated relationship:

$$\Delta V = K\,(\text{area})^2\, t \cdot \sigma$$

where ΔV represents the voltage change (sample in field - sample out); K, a proportionality constant; area, the ab-plane surface area; t, the sample thickness; and σ, the specific conductivity.

With the arrangement shown in Fig. II-6, it was possible to monitor the conductivity of a sample as the intercalation proceeded. The reaction vessel was made to fit between the jaws (1.0 cm gap) of the magnet by joining 7 mm flat quartz tubing (sample region) to 9 mm quartz tubing. The vessel was capped by a Whitey valve using the appropriate Swagelok connectors with teflon ferrules. Weighing the entire assembly allowed for the determination of stoichiometry by gravimetry.

9. t/t_o Measurement

Measurement of the c-axis expansion, t/t_o, of HOPG samples upon intercalation was performed directly on vacuum stable samples in the Dri-Lab using a digital micrometer (Series 193) supplied by Mitutoyo Mfg. Co., Ltd. (Japan). The micrometer had an accuracy of $\pm$ 0.001 mm.

On samples known to lose intercalate to a vacuum, t/t_o measurements were obtained using a microscope, equipped with a calibrated sliding scale, by focusing directly on the sample which was standing on edge (at right angles to the c-axis) in a reaction vessel made of flat quartz tubing (as described in Chapter II, section C.8.). The vessel, capped with a Whitey valve, permitted a positive pressure of the intercalant to be maintained over the sample while the t/t_o measurement was taken. Optical abberations caused by the quartz tubing limited accuracy to an estimated $\pm$ 0.05 mm.

10. Electrochemical Potential Measurement

Potential measurements on batteries constructed as outlined in Chapter II, section A.3.) were made using a Keifhley model 210 Electrometer (Cleveland, Ohio). A check on the reversibility of the various cells produced was obtained by discharging the cells to zero potential, and then recharging using a standard variable (0-30 volts) D.C. power source (General Electric). Normally, the cells were recharged for one hour at 5 volts output.

References

1. D. F. Shriver, The Manipulation of Air-Sensitive Compounds, McGraw-Hill, New York, 1969.

2. Supplied by Dr. Josik Portier, Laboratoire de Chimie du Solide du CNRS, Universite de Bordeaux 1, Talence, France.

3. Exact location supplied by Dr. H. R. Wenk, Department of Geology, University of California, Berkeley.

4. L. B. Erbert, Ann. Rev. Mat. Sci., 6, 181 (1976).

5. B. Wienstock, J. G. Malm and E. E. Weaver, J. Amer. Chem. Soc., 83, 4310 (1961).

6. O. Ruff and J. Fisher, Z. Anorg. Allgem. Chem., 179, 161 (1929).

7. B. Wienstock and J. G. Malm, J. Amer. Chem. Soc., 80, 4466 (1958).

8. J. G. Malm and H. Selig, J. Inorg. Nucl. Chem., 20, 189 (1961).

9. K. Leary and N. Bartlett, J. Chem. Soc., Chem. Comm., 903 (1972).

10. N. Bartlett and D. H. Lohman, J. Chem. Soc., 5253 (1962).

11. J. Shamir and J. Binerboyum, Inorg. Chem. Chem. Acta., 2, 37 (1968).

12. M. Wechsberg, P. A. Bulliner, F. O. Sladky, R. Mews and N. Bartlett, Inorg. Chem., 11, 3063 (1972).

13. B. N. Figgis and R. S. Noholym, J. Chem. Soc., 4190 (1958).

14. C. Zeller, A. Denestein and G. M. T. Foley, Rev. Sci. Instrum., 50, 602 (1979).

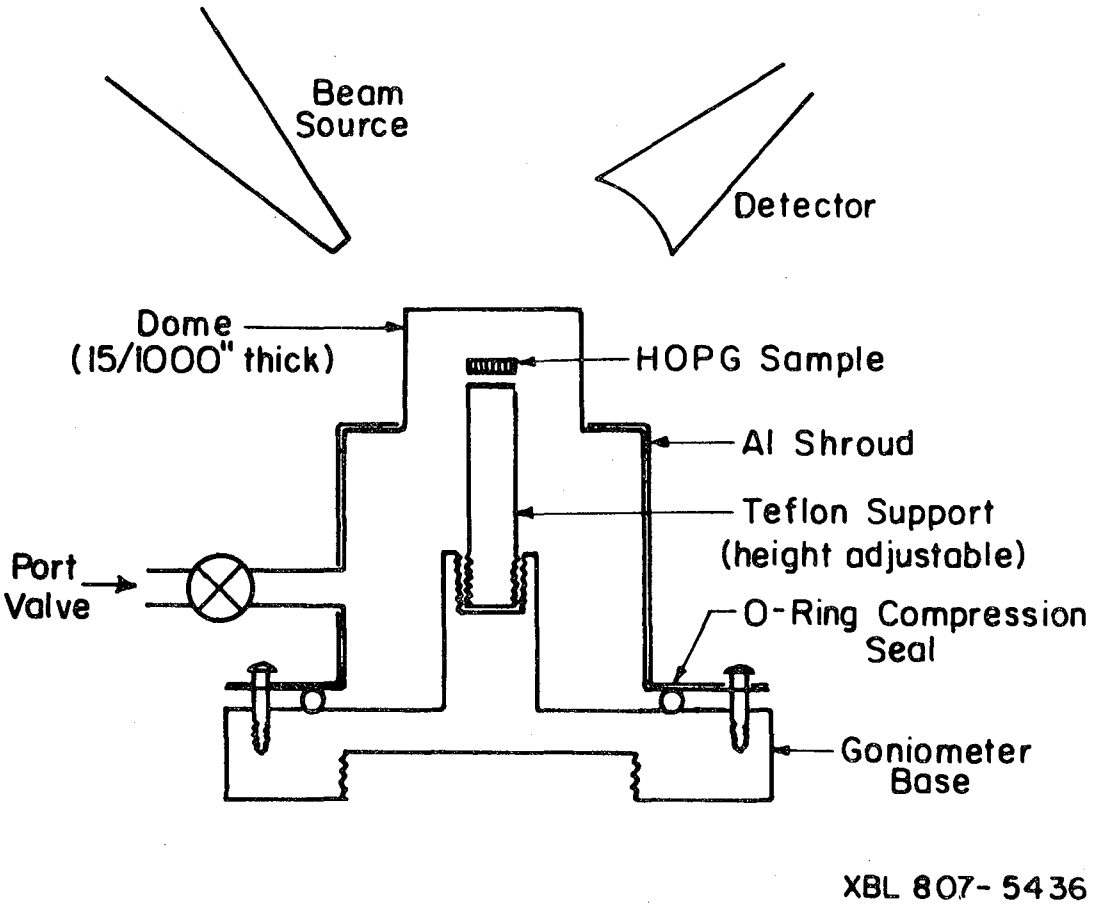

Figure II-1. In-situ sample shroud for x-ray diffractometer studies.

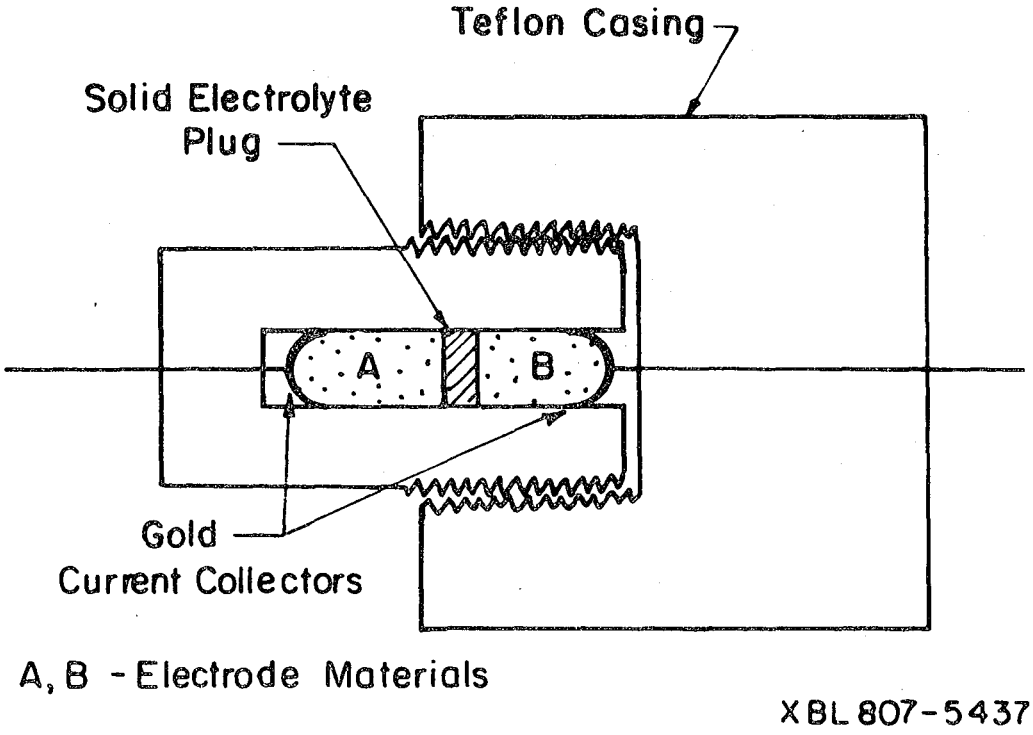

Figure II-2. Battery casing for solid electrolyte cells.

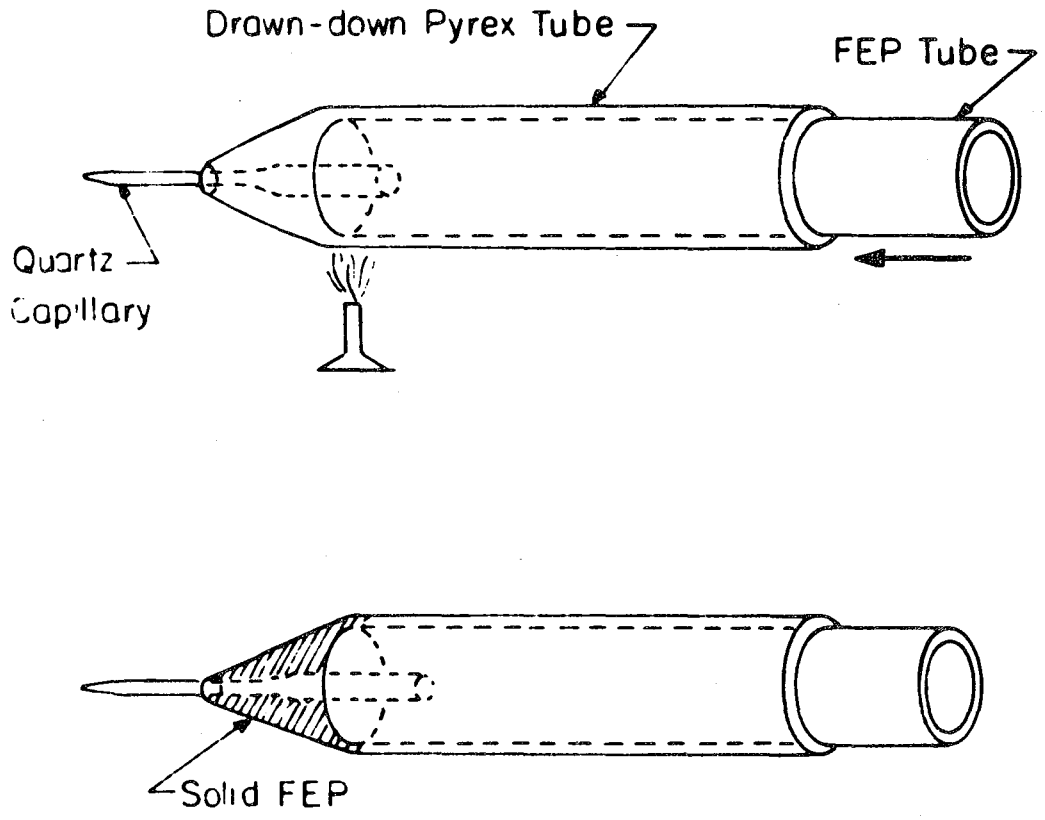

Figure II-3. Teflon FEP - Quartz capillary seals.

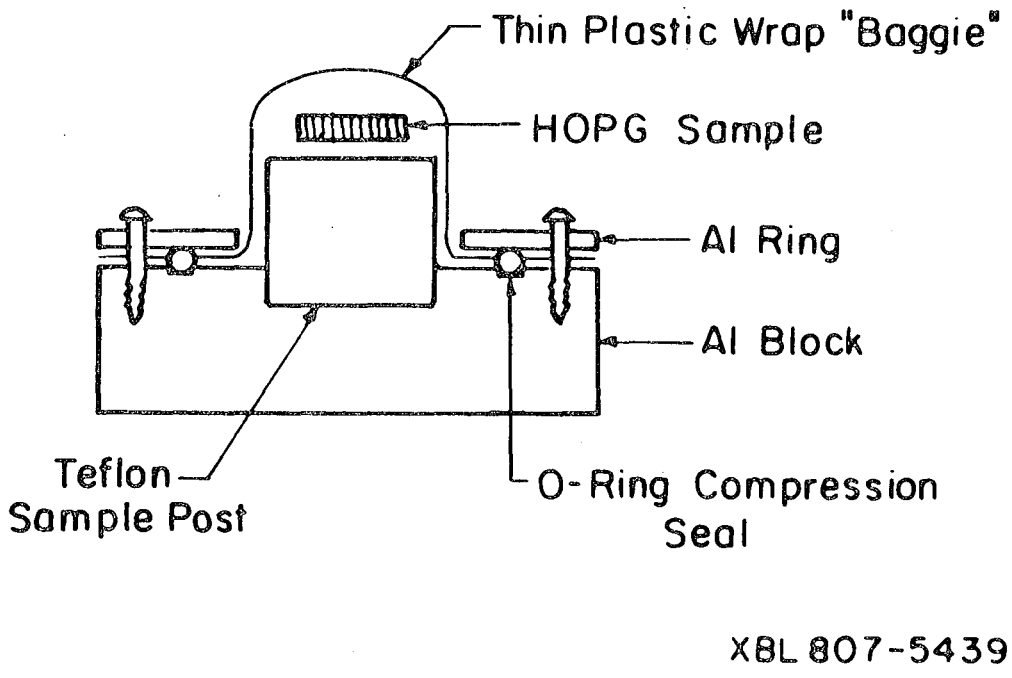

Figure II-4. Inert-atmosphere HOPG intercalate sample holder for powder diffractometer.

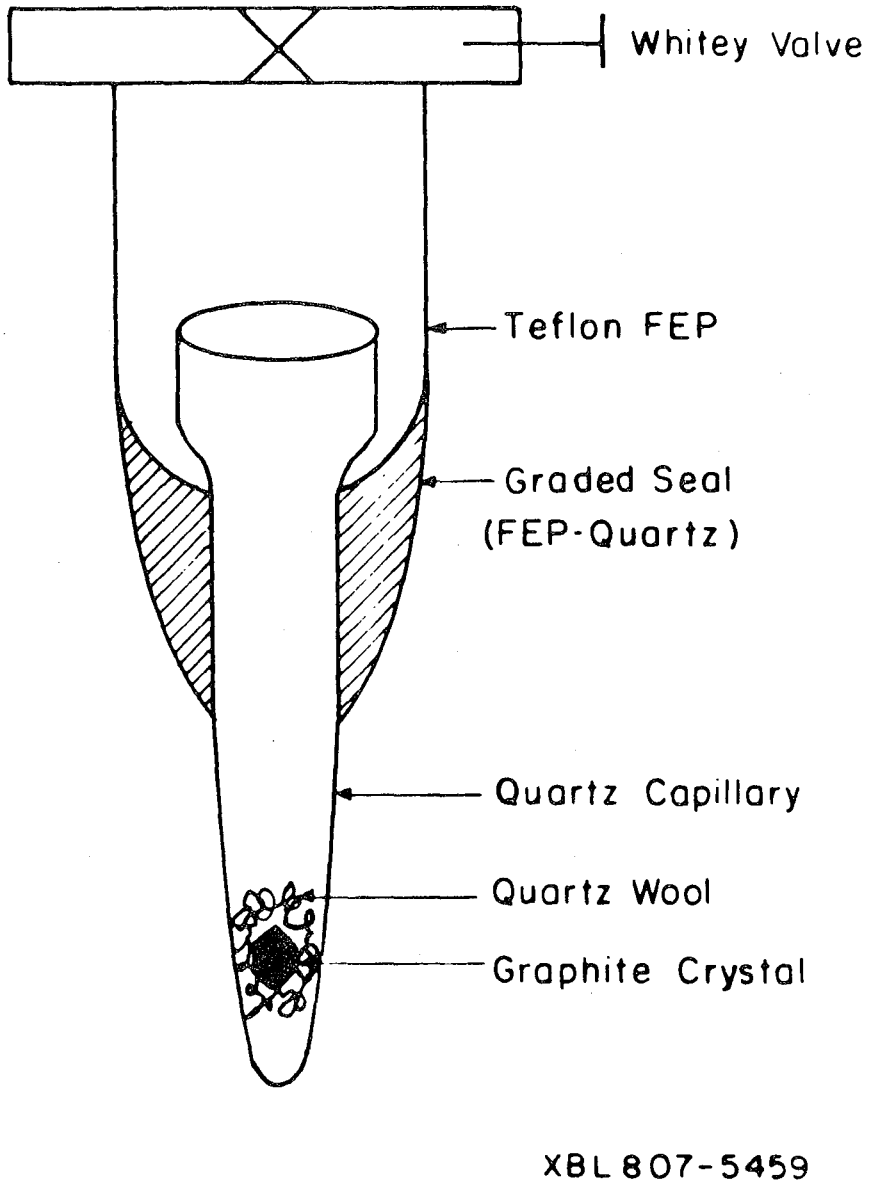

Figure II-5. In-situ reaction apparatus for single crystals of graphite.

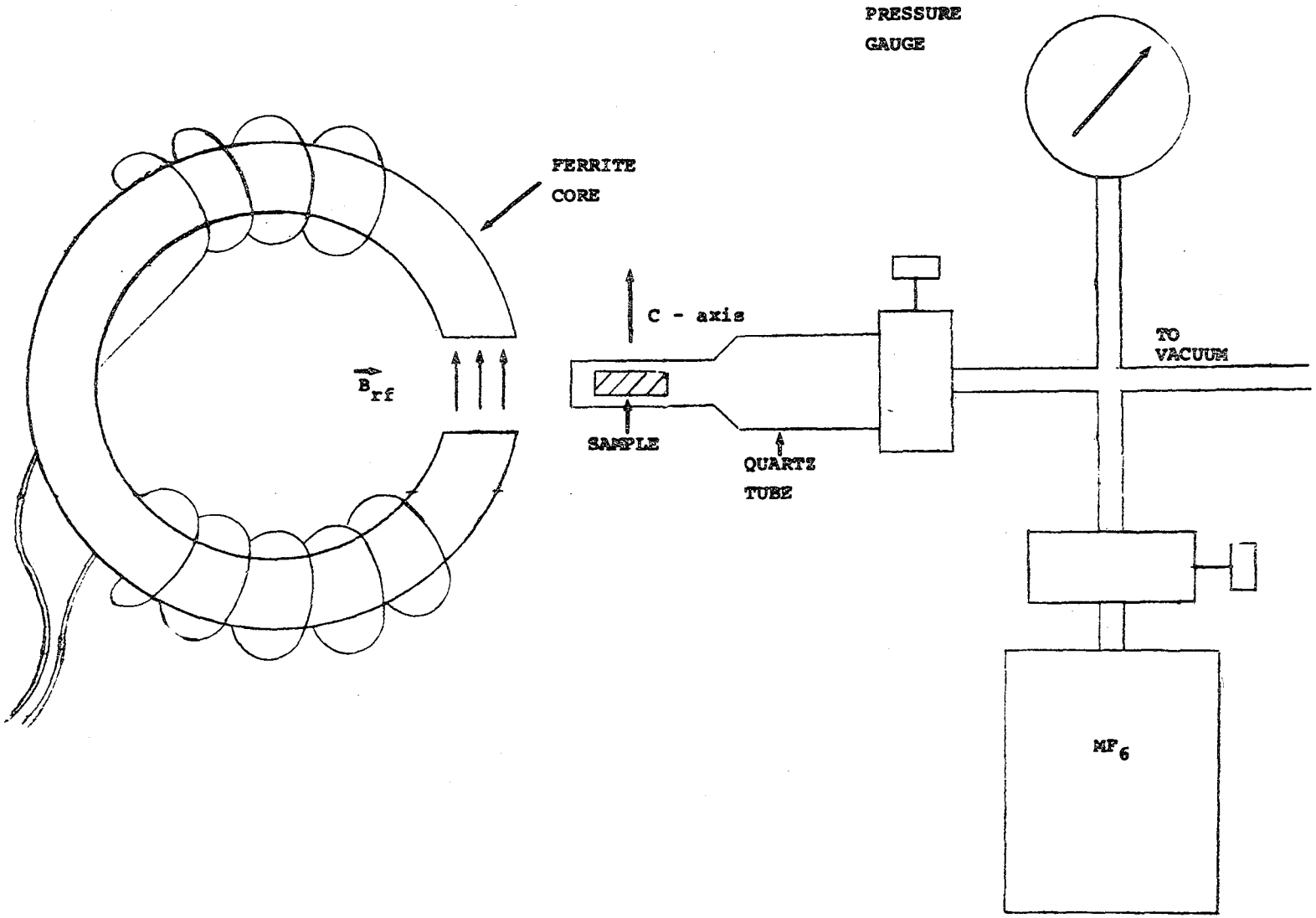

Figure II-6. Apparatus for in-situ measurement of conductivity on HOPG/intercalates.

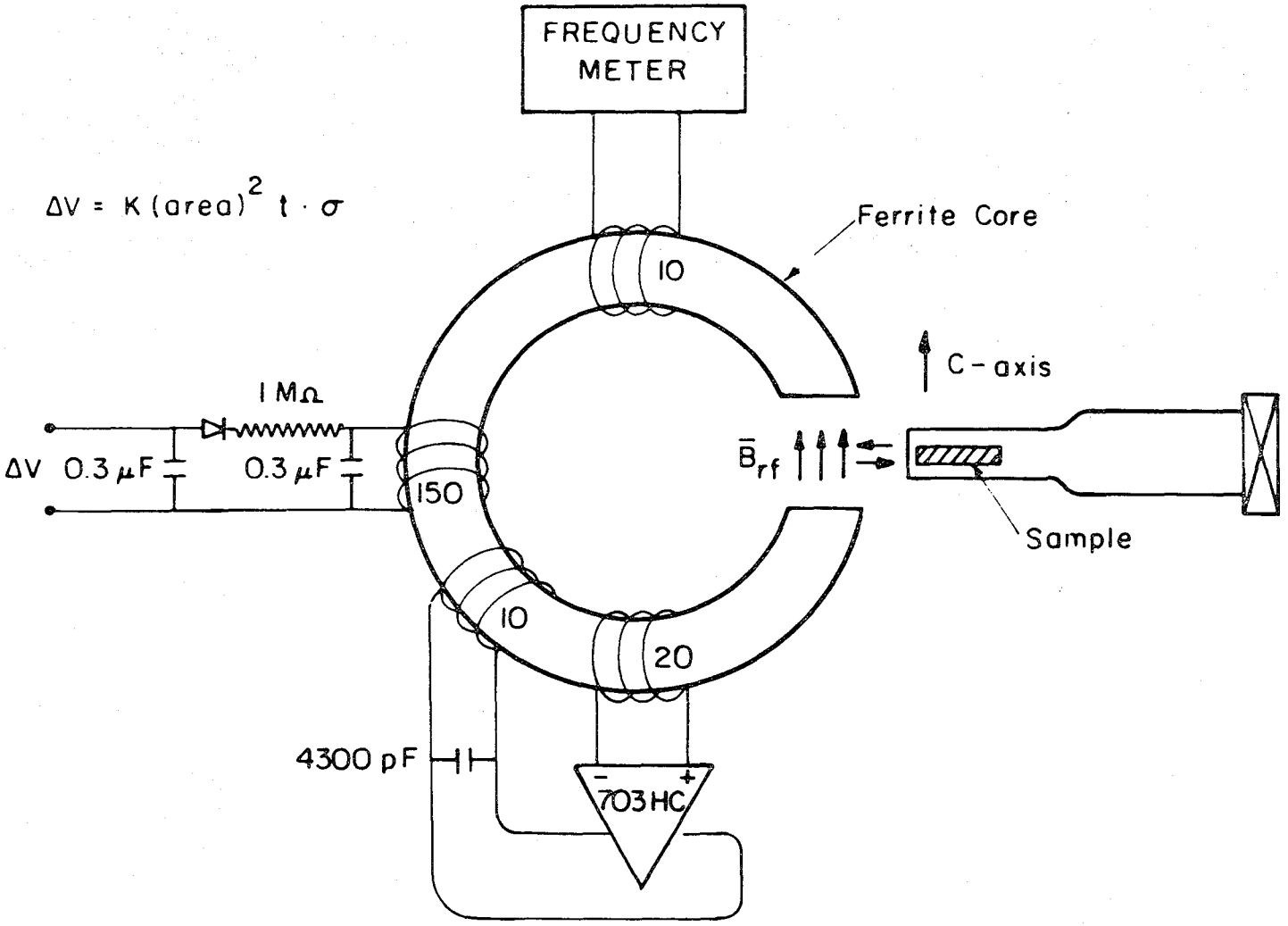

Figure II-7. Contactless inductive technique for measurement conductivity.

CHAPTER III

REACTIONS OF THE PLATINUM METAL HEXAFLUORIDES

A. Introduction

Ubbelohde was the first to propose graphite salt formulations (see Table III-1) for certain mineral acid-graphite intercalation compounds as a result of his electrochemical studies.[1] Unfortunately, his systems were structurally complicated by the fact that in addition to the anionic guest species, neutral molecule "spacers"[2] were also incorporated into the galleries.

The specific ab-plane electrical conductivities for these salts are also listed in Table III-1. The simplest model for the conductivity, σ, of a graphite salt, $C_x^+A^-$, is

$$\sigma \propto n \equiv \rho(A^-) \propto C^{+/x} \qquad (1)$$

where the carrier density, n, is equal to the total charge transfer per unit volume. This implies that as the anion density increases--as the formal charge on the graphite increases--the conductivity normalized per graphite plane should likewise increase.

It was the need for a structurally simple graphite salt coupled with the lure of exceedingly high conductivities that lead naturally to an investigation of graphite intercalation by high energy oxidizers. It was hoped that powerful oxidizers would produce graphite salts containing only densely-packed anionic guests, thus providing the desired structural simplicity and high formal charge on the graphite network.[1]

The platinum metal hexafluorides were ideal for such a study for the following reasons: (1) as Bartlett[3] has shown, they represent a

a series of compounds of well characterized, graded oxidizing potential; (2) they are essentially isodimensional; and (3) they are easily characterized by their magnetic data. These points are clearly set out in Table III-2.

The smooth increase in electron affinity from WF_6 (3.5 eV) to PtF_6 (9.2 eV) is a result of the increasing nuclear charge, Z, on the metal, while the associated electrons occupy the rather poorly screening dt_{2g} orbitals (see Table III-2).

B. Experimental

1. Graphite/Tungsten Hexafluoride

Graphite, either powder or HOPG, was not observed to react spontaneously with WF_6. In fact, WF_6 was used as a solvent for the more highly oxidizing members of the series (MF_6; M = Os, Ir, Pt). In these reactions, it was indeed possible that WF_6 was incorporated. But the absence of any magnetic behavior attributable to a d^1-system discounted any electron transfer to the WF_6. Hence, WF_6, if it were present, must act as a neutral spacer separating charged species,

$$G + MF_6 \xrightarrow{WF_6} C_x^+MF_6^- \cdot \delta WF_6 \quad .$$

From evidence presented in Chapter VII, one would postulate the existence of materials, $C_{12n}^+ MF_6^- \cdot 1/2\ WF_6$ and $C_{12n}^{++} MF_6^= \cdot 1/2\ WF_6$. These materials have not been confirmed.

2. Graphite/Rhenium Hexafluoride

ReF_6 was not observed to react spontaneously with graphite nor was it used as a solvent.

3. Graphite/Osmium Hexafluoride

Graphite, both powder and HOPG, were observed to react with OsF_6 (in excess) to form a deep blue (gun-metal blue) material of limiting composition, C_8OsF_6 (see Table III-3). Three preparative procedures were followed: (1) OsF_6 stored in a Monel can was condensed onto graphite, powder (~1/2 g) or HOPG (~25 mg), in a quartz bulb at -196°C and allowed to warm to room temperature. The reaction was exceedingly fast (~3 min) and would cause HOPG to cleave. (2) The reaction could be slowed by using WF_6 as a solvent. WF_6 in large excess (10 cc liq.) was condensed onto the graphite in a quartz vessel. OsF_6 was then condensed into the vessel in aliquots. Visual inspection of the liquid (held at 0°C) was used as a criterion for completeness of reaction, OsF_6 being yellow while the WF_6 is colorless. Also towards completion, the sample, which initially floated on the WF_6 liquid, sank[4] to the bottom of the vessel. Questions regarding the inclusion of solvent in the sample, which were not resolved, made this preparation suspect. (3) Slow reaction of HOPG which avoided sample cleaving could be obtained by direct reaction with the gas at low pressures. Typically cooling the Monel storage can to -23°C, at which OsF_6 has a vapor pressure of 15 torr, would effect reaction without cleaving. This was especially important for reactions carried out while monitoring the conductivity as a function of composition.

4. Graphite/Iridium Hexafluoride

Graphite reacted with IrF_6 in a manner analogous with OsF_6 produced a gun-metal blue material of limiting composition, C_8IrF_6 (Table III-3). Holding the IrF_6 at 23°C at which it has a vapor pressure of 11 torr

inhibited HOPG sample cleaving. Additionally, when WF_6 was used as a solvent, the material sank towards completion of the reaction.[4]

5. Graphite/Platinum Hexafluoride

Because of the extreme oxidizing power of PtF_6 (PtF_6 spontaneously oxidizes molecular O_2 forming $O_2^+PtF_6^-$) glass reaction vessels were inadequate. Quartz was also inadequate because of photolysis:

$$PtF_6 \xrightarrow{h\nu} PtF_5 + 1/2\ F_2 \quad .$$

Therefore reactions were carried out in Monel vessels made by drilling out a 3/8" Monel rod. The preps followed those outlined for OsF_6, except that PtF_6 reactions with HOPG were very slow. Typically, these reactions were run for 12-24 hours. Graphite powders produced a gun-metal blue material of limiting composition, $C_{12}PtF_6$ (Table III-3). HOPG samples never reached this composition, instead these samples exhibited a marked dishing with compositions ranging from C_{24} to $C_{36}PtF_6$. Samples of $C_{12}PtF_6$ were observed to float on WF_6 liquid.

6. Hydrolysis of G/MF_6 Salts

Spreading the powders on a mortar and adding water resulted in hydrogen fluoride production in all cases. It was also evident that the hydroxides or hydrated oxides of the metals were also formed as indicated by their characteristic colors:

Os - black solution
Ir - deep purple solution
Pt - faint yellow solution

X-ray powder diffraction photographs of the powdered graphite residues, once dried, indicated the parent graphite. Hence, hydrolysis appears to lead to removal of the guest species from the galleries.

7. G/IrF_6 Reduction with Hydrogen

C_8IrF_6 (from HOPG) was reduced by heating to 250°C under 1 atm of H_2 in a Monel bomb for 12 hours. Hydrogen fluoride was pumped from the bomb and shown by infrared spectroscopy to be the major infrared active volatile. The remaining material was iridium-coated graphite. X-ray diffraction showed patterns attributable to both iridium metal and the parent graphite. No lines attributable to an intercalated lower fluoride were observed. The iridium coating was remarkably uniform.

C. Magnetic Studies on Graphite/MF_6

The magnetic data for both the osmium and iridium hexafluoride-intercalated graphites have been obtained and show that the metals are quinquevalent. The C_8OsF_6 magnetic susceptibility obeys a Curie-Weiss relationship indicative of a t_{2g}^3-system and has a magnetic moment similar to that of the simple cubic salt $SF_3^+OsF_6^-$ (Fig. III-1). Similarly, C_8IrF_6 shows a temerature independent paramagnetism, indicative of t_{2g}^4, akin to that of $H_3O^+IrF_6^-$ (Fig. III-2).[5] Thus the materials are formulated as graphite salts, $C_8^+OsF_6^-$ and $C_8^+IrF_6^-$.

On the other hand, the platinum material, $C_{12}PtF_6$ was essentially non-magnetic, the diamagnetic term approximately cancelling a Pauli-type paramagnetism. This indicates that the platinum is tetravalent (t_{2g}^6 system). The salt formulation is therefore $C_{12}^{++}PtF_6^{=}$.

D. Structural Studies on Graphite/MF_6

Both single crystal and HOPG 00ℓ diffraction data on both C_8OsF_6 and C_8IrF_6 showed these materials to be first stage with c-spacing or "gallery heights" of 8.10(3) Å and 8.06(3) Å, respectively. This is in agreement,[6] within experimental error, with the smaller volume of IrF_6 relative to OsF_6 (Table III-2). Diffraction tracings of these HOPG salts are shown in Fig. III-3. Also precession photographs have shown that both salts are primitive hexagonal, the a_o value of 4.92(3) Å being twice that of hexagonal graphite.[7]

Powder diffraction of $C_{12}PtF_6$ indicated a first-stage salt of c-space 7.56 Å. This value appears anomalously small[6] with respect to the change in molecular volume going from OsF_6 to PtF_6 (see Table III-2).

E. Results and Discussion

The ease of incorporation of the third-transition-series hexafluorides into graphite and the stability of the resultant salt, appears to depend simply upon the electron affinity of the hexafluoride as shown in Tables III-2 and III-3. Neither WF_6 nor ReF_6 is incorporated massively into graphite. The more powerful oxidizers OsF_6 and IrF_6 each intercalate easily up to a limiting composition C_8MF_6. The most powerful oxidizer, PtF_6, is readily intercalated by powdered graphite but to a limiting composition of $C_{12}PtF_6$. This anomaly is explained by the magnetic data.

These data for C_8OsF_6 and C_8IrF_6, which are presented in Figs. III-1 and III-2, show that in each case the dominant guest species has to be the MF_6^- ion. For each salt the appropriate formula is $C_8^+MF_6^-$. Moreover, since the volume of the hexagonal C_8MF_6 unit cell, which is 170.9(1) $Å^3$,

is essentially the sum of the volume of eight carbon atoms, as in hexagonal graphite[7] (= 70.00 $Å^3$) and the volume of a hexafluoride (= ~ 105 $Å^3$), it is evident that the MF_6^- species must be close packed in the graphite galleries. It seems therefore that the degree of oxidation of the graphite is not the composition-limiting factor for C_8OsF_6 and C_8IrF_6, but it does appear to be important in the PtF_6 case. The diamagnetism of $C_{12}PtF_6$ confirms that the guest is PtF_6^{2-}. This means that the graphite is more highly oxidized in $C_{12}PtF_6$ than in the C_8IrF_6 or C_8OsF_6 cases. It is probable that the incomplete filling of the galleries in $C_{12}PtF_6$ is a consequence of the much greater energy needed to yield the average carbon atom charge of +1/6 relative to +1/8. There is a possibility that the true intercalation limit for PtF_6 has not been reached in this work. It is difficult to intercalate HOPG pieces (5 x 5 x 0.5 mm) to produce uniform first-stage sample. Evidently the intercalated PtF_6^{2-} is not very mobile with the consequence that each HOPG sample is invariably concave at the center. The finely powdered samples do intercalate quickly to an impressively constant composition close to $C_{12}PtF_6$, as the findings given in Table III-3 indicate.

Single crystal precession photographs of both C_8OsF_6 and C_8IrF_6 show that the salts are primitive hexagonal, the $\underline{a}_o$ value of 4.92(2) Å being twice that of hexagonal graphite.[7] The $\underline{c}_o$ value of ~8.1 Å is consistent with the MF_6^- being oriented with a threefold axis parallel to $\underline{c}_o$. With this orientation the effective height[8] of MF_6^- is ~4.7 Å. Since the effective thickness of a graphite sheet[7] is 3.35 Å the anticipated $\underline{c}_o$ value for the primitive unit cell is the sum of these values, i.e. ~8 Å. These and other considerations suggest the unit cell

represented in Fig. III-4. Furthermore, $C_{12}PtF_6$ may also be rationalized on the basis of a comparison of nearest neighbor interactions derived from the C_8MF_6 structure. The $C_{12}X$ structure is simply generated from the C_8X structure by removal of one third of the X species from each filled gallery. For a doubly charged anion, like $PtF_6^{=}$, electrostatic repulsions would favor a $C_{12}X$ packing, since it has one half the number of nearest neighbor interactions present in C_8X (3 vs. 6; see Fig. III-4). Moreover, the increased packing density of C_8MF_6 (M = Os, Ir) [$\rho \sim 3.9$ g/cc] versus $C_{12}PtF_6$ [$\rho \sim 3.0$ g/cc] is reflected in the observation that both C_8MF_6 salts sink in liquid WF_6 [$\rho \sim 3.44$ g/cc], whereas $C_{12}PtF_6$ floats.[4] Indeed, the packing density of MF_6^- in the C_8MF_6 salts must far exceed that in the liquid MF_6, since the anion density must compensate for the much less dense graphite host lattice [$\rho \sim 2.2$ g/cc].

Although HOPG samples of the first-stage PtF_6^{2-} salt have not been obtained, powder data for $C_{12}PtF_6$ and second- and third-stage HOPG/PtF_6 00ℓ reflections indicate that the PtF_6^{2-}-occupied gallery height is 7.55(3) Å (see Table III-3). Evidently the greater Coulomb attraction between graphite sheet and guest, consequent upon the higher positive charge of the former and the double negative charge of the latter, is responsible for the appreciable contraction when compared with C_8IrF_6;[6] where $\underline{c}_o = 8.06$ Å. Indeed other observations also indicate that the gallery height is somewhat sensitive to the charging. The results given in Chapter VI, Table III-3, for first-stage $C_xAsF_6^-$ salts, show that as the concentration of AsF_6^- in the graphite galleries increases (as x decreases), the $\underline{c}_o$ value (obtained from 00ℓ reflections from HOPG samples) decreases.

Finally, the observations, that both the hydrolysis and hydrogen reduction of the graphite/MF_6 salts massively remove guest and restsore the graphite host lattice, imply that reduction of the graphite by electron transfer from water or hydrogen to the hexafluorometal species is external to the graphite. There appears to be no inclusion of neutral or partially reduced species within the galleries. A plausible scheme for the hydrogen reduction being:

Step 1: $1/2\ H_2 + C_n^+MF_6^- \rightarrow H^+ + C_n^+[MF_6^-]_{internal}$

Step 2: $C_n[MF_6^-]_{internal} \rightarrow C_n[MF_6^-]_{surface}$

Step 3: $C_n[MF_6^-]_{surface} + H^+ + 5/2H_2 \rightarrow M_{(s)} + 6HF$

where in step 2 the MF_6^- anion presumably migrates from within the gallery to the edge surface region. A similar scheme is expected for the hydrolysis.

References

1. a) A. R. Ubbelohde, Proc. Roy. Soc., 309, 297 (1969). b) A. R. Ubbelohde, Proc. R. Soc. Lond. A, 327, 289 (1972).

2. M. L. Dzurus and G. R. Hennig, J. Amer. Chem. Soc., 79, 1051 (1957).

3. N. Bartlett, Angew. Chem. Internat. Ed., 7, 433 (1968).

4. WF_6 liquid at 0°C has a density of 3.44 g/cm^3. C_8OsF_6 and C_8IrF_6 have calculated densities, based on a_o = 4.92 Å and c_o = 8.1 Å, of 3.93 and 3.94 g/cm^3, respectively. $C_{12}PtF_6$, presumed to have a structure as in Fig. 4(b), would have a density of 3.00 g/cm^3. (a_o = 8.51 Å and c_o = 7.56 Å).

5. H. Selig, W. A. Sunder, F. A. Disaluo, and W. E. Falconer, J. Fluorine Chem., 11, 602 (1978).

6. Taking as a first approximation:

$$\Delta\ c\text{-spacing} = 2[r(MF_6) - r(M'F_6)]$$

where

$$r(MF_6) = \sqrt[3]{\frac{3}{4\pi}\ (\text{Molecular Volume})_{MF_6}}$$

	calculated	observed
c-spacing (OsF_6) =	--	8.10(3) Å
c-spacing (IrF_6) =	8.09 Å	8.06(3) Å
c-spacing (PtF_6) =	8.07 Å	7.56(3) Å

7. R. W. G. Wyckoff, Crystal Structures, vol. 1, 2nd Ed., Interscience Pub., New York, p. 27 (1963).

8. Since in OsF_6^- the M-F internuclear distance is approximately 1.82 Å [M. A. Hepworth, K. H. Jack and G. J. Westland, J. Inorg. Nucl. Chem., 2, 79 (1956).], the effective packing length (along c) should be {2 x 1.82/$\sqrt{3}$} + {2 x van der Waals radii of the F ligands (which is taken to be 1.3 Å)}.

Table III-1. Conductivity of some graphite salts.

	$\sigma_{ab}(295^{o}K)$ $(10^{4}\Omega^{-1}\ cm^{-1})$	σ_{ab}/σ_{Cu}
$C_{24}^{+}NO_{3}^{-}\cdot 3HNO_{3}$	31.8	0.53
$C_{24}^{+}HSO_{4}^{-}\cdot 2H_{2}SO_{4}$	15.9	0.27
$C_{24}^{+}ClSO_{3}^{-}\cdot nHClSO_{3}$	14.4	0.24
$C_{24}^{+}AlCl_{4}^{-}\cdot AlCl_{3}$	16.1	0.27
Graphite	2.7	0.05
Copper	59.8	1

Table III-2. Third transition series hexafluorides: the nonbonding electron configurations, molecular volumes and electron affinities.

	WF_6	ReF_6	OsF_6	IrF_6	PtF_6
dt_{2g}^n	n = 0	1	2	3	4
Molecular volume ($Å^3$) orthorhombic phase[a]	108.5	106.5	105.7	105.4	104.6
E (eV)	3.5[b]	5[d]	6.5[d]	8[d]	9.2[c]

[a] S. Siegel and D. A. Northrop, Inorg. Chem., 5, 2187 (1966).

[b] P. M. George and J. L. Beauchamp, Chem. Phys., 36, 345 (1979).

[c] P. Barberi and N. Bartlett, unpublished results based on $\Delta H_f\{O_2PtF_6$ (cryst.) from O_2 (g) and PtF_6 (g)$\}$ = -60 kcal mol^{-1}.

[d] Estimated values.

Table III-3. Maximum intercalation of HOPG graphite by metal hexafluorides.

Hexa-fluoride	Form of Graphite	Gravimetry	Analyses	Stage, c_o(Å) ±0.03
WF_6		does not intercalate		
ReF_6		does not intercalate		
OsF_6	powder	(a) C_9OsF_6 (b) $C_{7.72}OsF_6$	(a) $C_{8.13}OsF_6$ (b) $C_{7.81}OsF_6$	1st, 8.10
	HOPG (5 x 5 x 1 mm)	(a) $C_{9.9}OsF_6$* (b) $C_{11.6}OsF_6$*		1st, 8.10
IrF_6	powder	(a) $C_{8.01}IrF_6$ (b) $C_{8.01}IrF_6$	(a) $C_{7.98}IrF_6$ (b) $C_{8.05}IrF_6$	1st, 8.05
	HOPG (5 x 5 x 1 mm)	(a) $C_{8.3}IrF_6$* (b) $C_{10.8}IrF_6$* (c) $C_{10.6}IrF6$*		1st, 8.06
PtF_6	powder	(a) --- (b) $C_{12.0}PtF_6$ (c) $C_{11.0}PtF_6$	(a) $C_{12.4}PtF_6$ (b) $C_{12.0}PtF_6$ (c) $C_{12.4}PtF_6$	1st, 7.56
	HOPG (5 x 5 x 1 mm)	(a) $C_{24.1}PtF_6$ (b) $C_{36.3}PtF_6$		2nd, 10.88† 3rd, 14.25†

*experiment terminated prior to achieving a limiting composition

†implies a 1st stage spacing of ~7.54 Å;
for 2nd stage: 10.88 Å - 3.35 Å = 7.54 Å;
for 3rd stage: 14.25 Å - 2(3.35Å) = 7.55 Å;
since c-spacing of a stage n material is equal to
[1st-stage spacing + (n-1)(3.35 Å)]
where 3.35 Å is the graphite gallery height.

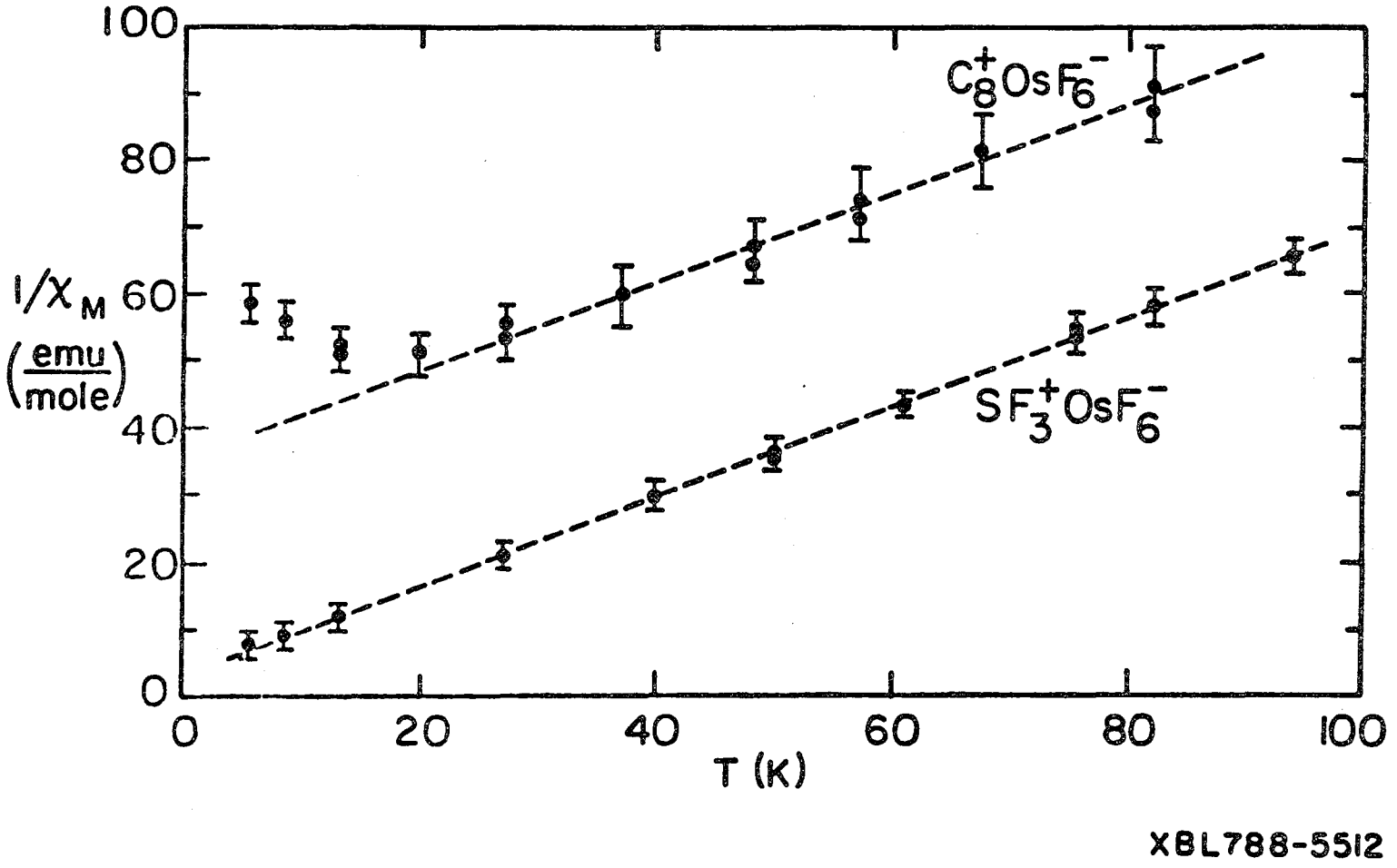

Figure III-1. Magnetic susceptibility-temperature relationships for $C_8^+OsF_6^-$ and $SF_3^+OsF_6^-$.

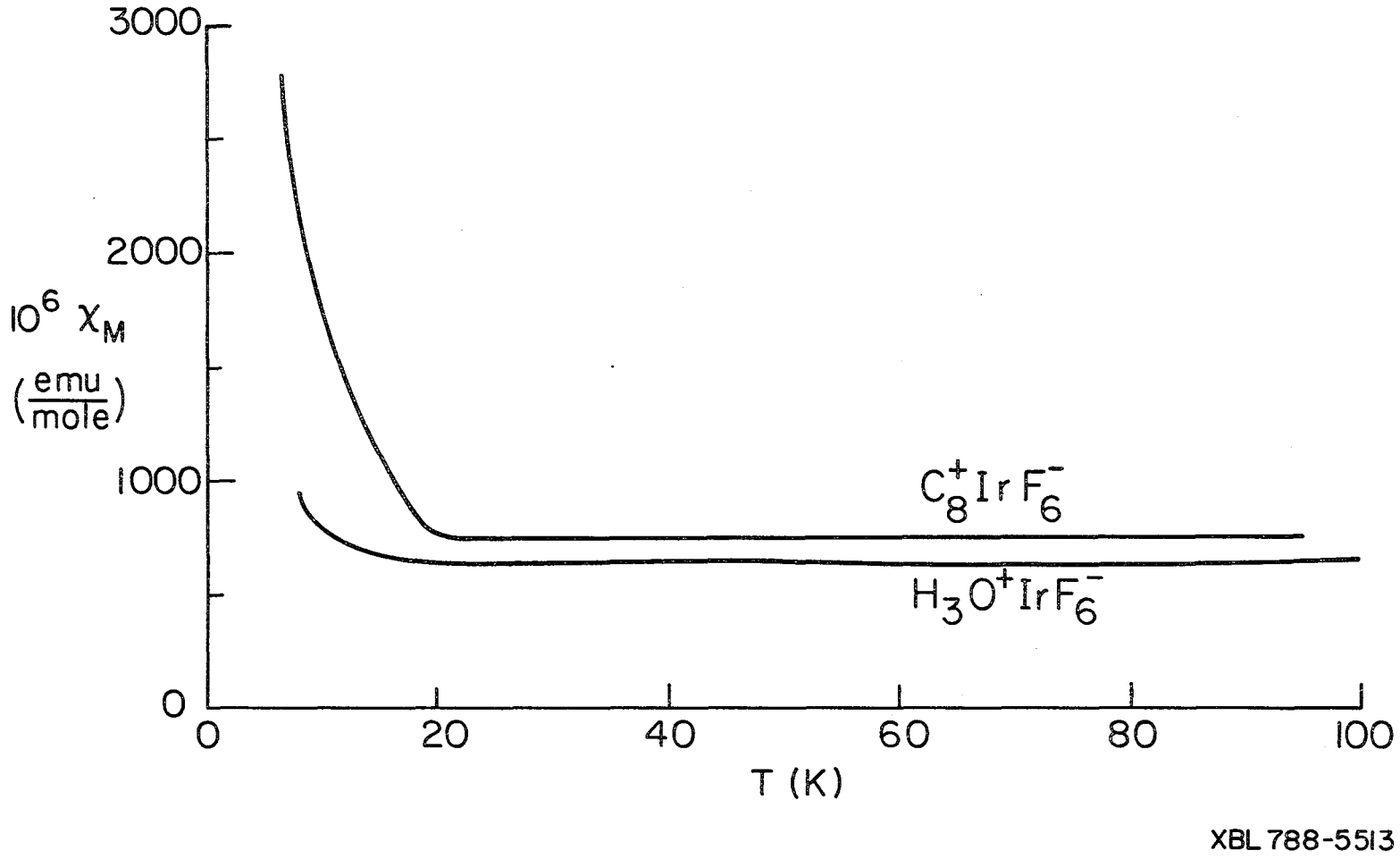

Figure III-2. Magnetic susceptibility-temperature relationships for $C_8^+IrF_6^-$ and $H_3O^+IrF_6^-$.

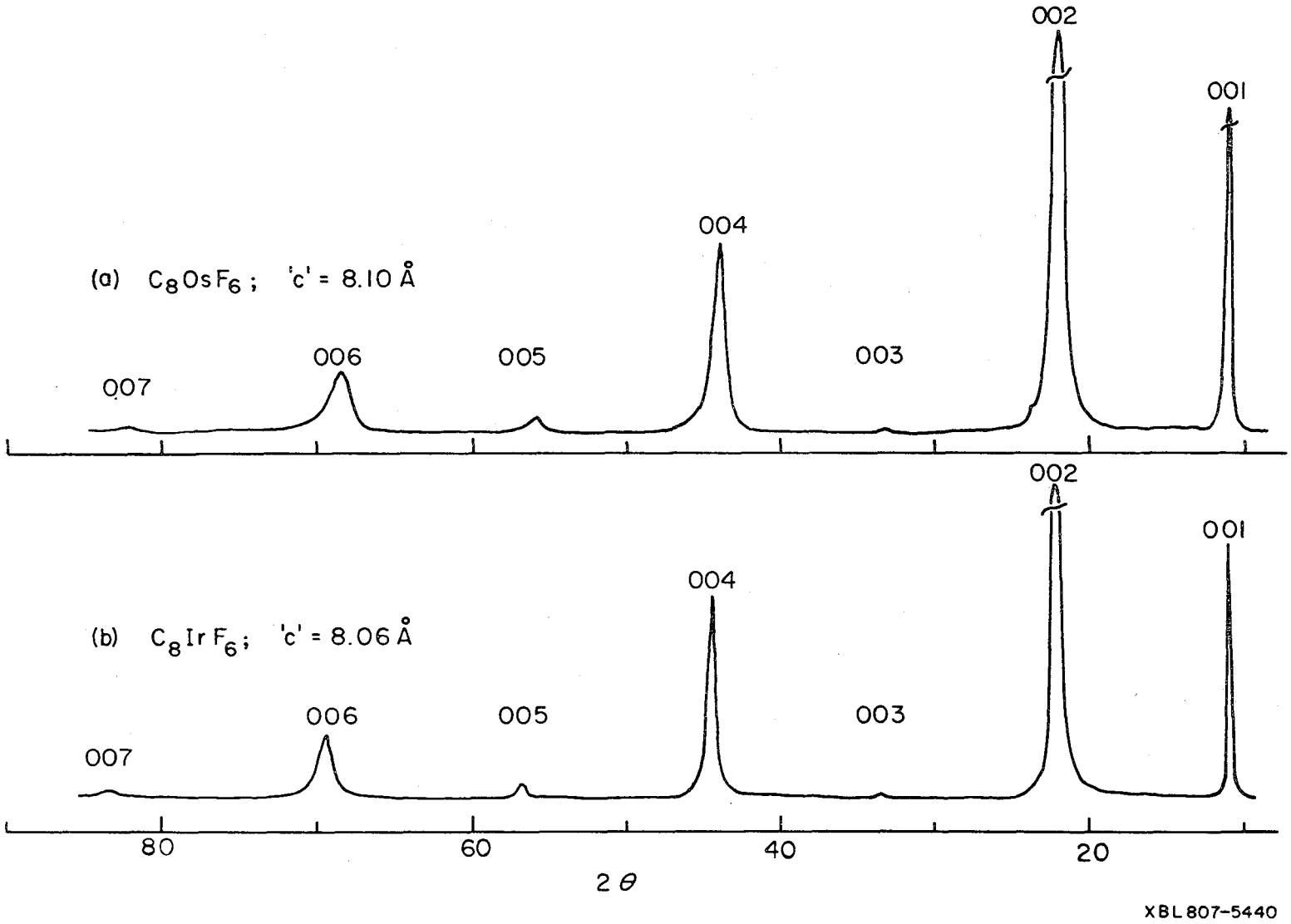

Figure III-3. Diffraction tracings of (a) C_8OsF_6 and (b) C_8IrF_6.

(a)

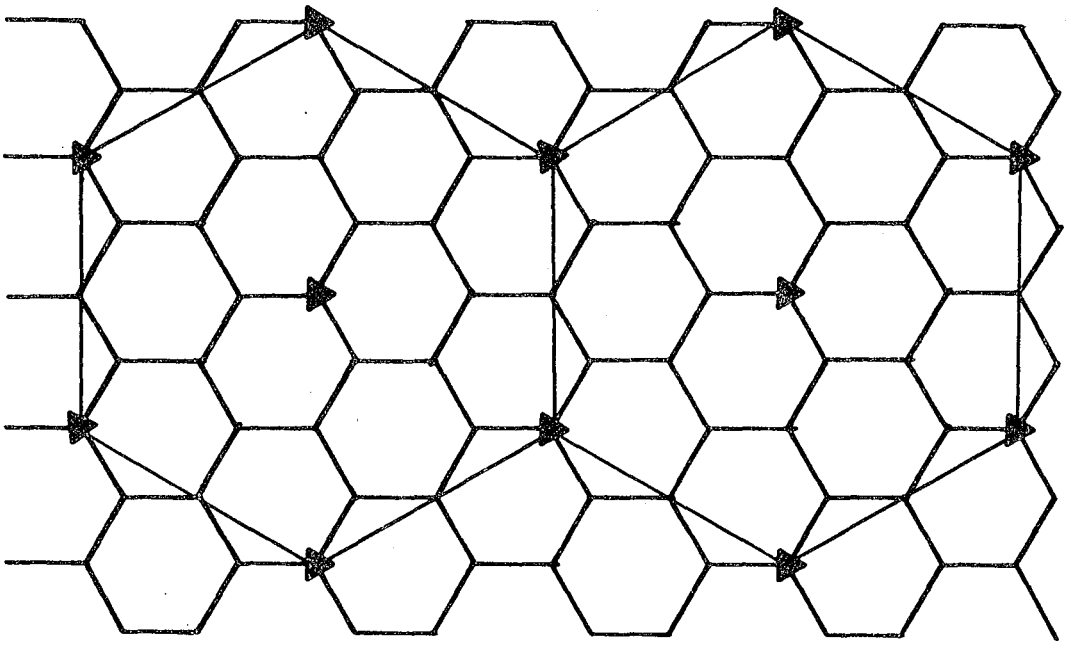

(b)

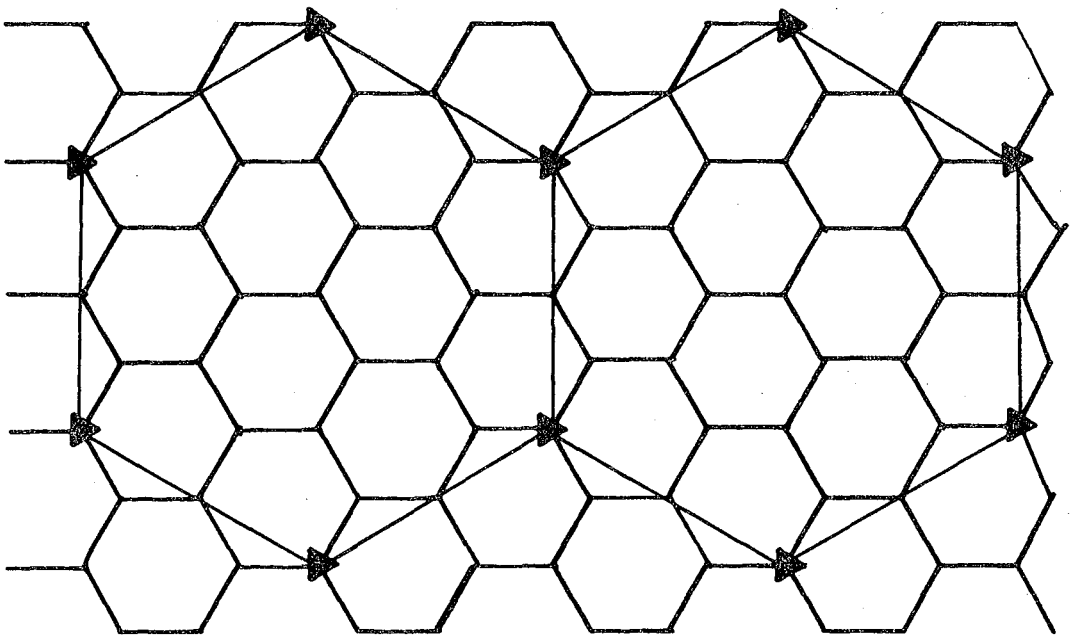

Figure III-4. Proposed structures for (a) C_8X and (b) $C_{12}X$.

CHAPTER IV

DIOXYGENYL SALTS WITH GRAPHITE

A. Introduction

AuF_6 is as yet unknown. From an extrapolation of the electron affinities for the third-series transition metal hexafluorides, AuF_6 would be expected to have an electron affinity in excess of 10 eV! The relationship of the E_a to the nuclear charge, Z, and the t_{2g} electron configuration is discussed in the introduction to Chapter III.

One plausible scheme for the generation of AuF_6 involves the electrochemical oxidation of low-melting Au(V) salts recently discovered in this laboratory.[1] Melts of $XeF_2 \cdot XeF_5^+ AuF_6^-$, for example, would be cathodically oxidized. Suitable gases (Ar, N_2) could then be bubbled past this cathode in the hope of forming such exotic materials as $ArF^+AuF_6^-$ or even $N_2^+AuF_6^-$! Molecular AuF_6 itself is expected to be unstable with respect to AuF_5 and 1/2 F_2 at ordinary temperatures.

Obviously, any attempt along these lines would require a most robust electrode in order to withstand the extremely oxidizing conditions involved. $C_8^+AuF_6^-$ might well be just such an electrode, since the guest is oxidatively robust and such positively charged graphite, $C^{+1/8}$, will not be readily oxidized further. Also, the salt, C_8AuF_6, is expected to conduct electricity at least as well as graphite itself (see Chapter VIII).

The intercalation of graphite by dioxygenyl salts was studied. These salts could be expected to yield a graphite salt after the established pattern of perfluoroaromatic molecule oxidations[2] according to the equation:

$$\text{Graphite} + O_2MF_6 \rightarrow C_nMF_6 + O_2\uparrow \qquad (1)$$

B. Experimental

1. Graphite/O_2PtF_6

An approximately 50% excess, by weight, of O_2PtF_6 was transferred in the Dri-Lab into a quartz vessel containing approximately 1/4 gram of graphite powder. Evolution of O_2 occurred spontaneously without the addition of solvent. This was presumably due to a dissociation vapor pressure of PtF_6, since mass spectroscopic studies by Falconer and co-workers have shown[3] that the important vapor species are:

$$O_2PtF_{6(cryst)} \rightarrow O_{2(g)} + PtF_{6(g)} \qquad (2)$$

The powder pattern of the gun-metal-blue reaction product was identical to that of the material, $C_{12}PtF_6$, formed from graphite plus $PtF_{6(g)}$ (see Chapter III). Excess O_2PtF_6 was also visible in the pattern.

2. Graphite/O_2AsF_6

i) HOPG (~30 mg) was observed to react with O_2AsF_6 (in 100-fold excess, by weight) without solvent over a period of about 21 days. Again this was most likely due to a small dissociation vapor pressure:[4]

$$O_2AsF_{6(cryst)} \rightarrow O_2F(O_2 + 1/2\ F_2) + AsF_5 \qquad (3)$$

The final product, $C_{30}AsF_6$ (by gravimetry), was not a deep blue color (indicative of a first-stage salt) but a lighter steel-blue characteristic of a lower stage salt. A t/t_o measurement of 1.59 supported the gravimetry [t/t_o (ideal, $C_{30}AsF_6$) = 1.59; see Chapter VI]. X-ray diffraction tracings of this material indicated a mixture of second- and third-stage materials consistant with the t/t_o ratio from micrometer measurements.

ii) HOPG (~30 mg) reacted with a ten-fold excess of O_2AsF_6 in SO_2ClF at -23°C (CCl_4 slush bath) for 12 hours to produce a deep blue material, $C_{15}AsF_6$, along with the liberation of an incondensible gas (O_2). t/t_o was measured to be 2.25, in accord with the diffractometer findings (a mixture of first and second stage). t/t_o ideal for $C_{15}AsF_6$ is 2.25 (see Chapter VI).

iii) HOPG (~30 mg) was reacted with a ten-fold excess, by weight, of O_2AsF_6 in HF. The graphite grossly exfoliated. The material, when pumped to dryness, had a stoichiometry, assuming that HF is not taken up, of C_9AsF_6 by gravimetry. The assumption that HF is not taken up was not evaluated. The final material was gun-metal-blue. During the reaction the solution took on a red-orange tint (indicative of O_2F)[5] and a noncondensible gas, presumably O_2, was evolved.

3. Graphite/O_2AuF_6

O_2AuF_6 did not react with graphite in the absence of solvent. Reaction in SO_2ClF of a three-fold excess, by weight, of O_2AuF_6 with HOPG (~30 mg) was slow at -23°C (CCl_4 slush bath). After 24 hours the composition was $C_{15.5}AuF_6$ by gravimetry (t/t_o = 2.26; compare with $C_{15}AsF_6$, section B.2.ii). Removing SO_2ClF and condensing in HF accelerated intercalation (completion reached in ~1/2 hour). The HOPG sample appeared grossly exfoliated. O_2 evolution was observed as the solution developed a red-orange coloration. A small residue of AuF_3 was revealed by its characteristic x-ray powder pattern. Presumably this AuF_3 was due to interaction of O_2AuF_6 with SO_2ClF. The final product, assuming no HF uptake, was $C_{8.8}AuF_6$, by gravimetry.

C. Results and Discussion

Both O_2PtF_6 and O_2AsF_6 were observed to react with graphite to give products which are identical to those produced from PtF_6 and AsF_5/ 1/2 F_2 gases. The observation that these salts appeared to form graphite salts with the liberation of O_2 as a result of a solid-solid reaction suggested that reaction was governed by dissociation of the dioxygenyl salt at RT:

$$O_2PtF_{6(cryst)} \rightarrow O_{2(g)} + PtF_{6(g)} \quad (4)$$

$$\text{Graphite} + PtF_{6(g)} \rightarrow C_{12}PtF_6 \quad (5)$$

and

$$O_2AsF_6 \rightarrow O_2F(O_2 + 1/2\ F_2) + AsF_{5(g)} \quad (6)$$

$$\text{Graphite} + AsF_{5(g)} + 1/2\ F_{2(g)} \rightarrow C_8AsF_6 \quad (7)$$

Both O_2PtF_6[3] and O_2AsF_6[4] can be stored in closed vessels, hence, equilibrium vapor pressures are established (4 and 6). Consumption of the gases produced (5 and 7) drives the reaction towards completion.

O_2AuF_6, on the other hand, was not observed to react with graphite in the absence of solvent. O_2AuF_6 apparently has a very low equilibrium vapor pressure at room temperature. The vapor species detected by Falconer and coworkers[5] suggest dissociation according to the equation:

$$O_2AuF_6 \rightarrow O_2F\ (O_2 + 1/2\ F_2) + AuF_5 \quad (8)$$

with the resulting

$$\text{Graphite} + AuF_5 + 1/2\ F_2 \rightarrow C_nAuF_6 \quad . \quad (9)$$

So parallels with O_2AsF_6 are anticipated, although the greater thermal stability of O_2AuF_6 is probably responsible for the slowness of this reaction. Another feature which distinguishes the AuF_6^- case from the AsF_6^- is the well known ease of reduction of AuF_5:[5]

$$AuF_5 \rightarrow AuF_3 + F_2 \qquad (10)$$

Separate experiments established that graphite will not intercalate crystalline AuF_3, which is polymeric.

Additionally, tetrameric RuF_5 (Ru_4F_{20}) was not observed to intercalate graphite. Presumably, the energy cost to break up the MF_5 tetrameric unit is unfavorble to intercalation. It seems unlikely therefore that tetrameric or polymeric AuF_5 can be involved in the intercalation of hexafluoroaurate. A monomeric AuF_5, derived in the first step of O_2AuF_6 dissociation (equation 8) could intercalate and particularly in the presence of fluorine derived from O_2F. The observation of some AuF_3 product even allows for the possibility of oxidation according to the equation:

$$2\bar{e} + 3\ AuF_5 \rightarrow 2AuF_6^- + AuF_3 \qquad (11)$$

as in the well established AsF_5 analogue (see Chapter VI), but it seems more likely that this AuF_3 derives from reduction of either O_2AuF_6 or AuF_5 by the SO_2ClF solvent, which was in contact with the Au(V) materials for many hours.

SO_2ClF appears to be a poor solvent for dioxygenyl salts. The need to work at low temperatures ($<0^oC$) in order to prevent formation of SO_2F_2 from SO_2ClF further restricts solubility.

In the AsF_5 system, control of the vapor pressure, hence the chemical potential, of the guest has been shown to control the stage[6] of the graphite/AsF_5 material. The inability to produce first-stage graphite salts from dioxygenyl salts in SO_2ClF may be a consequence of solubility and hence the chemical potential. Pure first-stage materials did not result from this work and even after exposure of graphite to excess O_2AuF_6 for many hours the resulting material was a mixture of first- and second-stage compounds of composition $C_{15.5}AuF_6$.

Attempts to produce a pure first-stage material by utilizing a solvent, HF, with a higher solubility for O_2MF_6 resulted in exfoliation of the HOPG samples. HF by itself is not known to intercalate graphite. But perhaps solution of the guest species by solvent within the graphite itself was responsible for the sample degradation. Pumping on these exfoliated materials suggests that limiting first-stage compositions, C_8MF_6, may have been reached, but this composition, from gravimetry, assumes that all HF was removed under vacuum. Clearly, to attain pure first-stage C_8AuF_6, a new solvent system with high O_2AuF_6 solubility, which itself does not intercalate graphite, must be found.

CHAPTER V

FLUORINE INDUCED INTERCALATION OF GRAPHITE BY BINARY METAL FLUORIDES

A. Introduction

In sharp contrast to the increasing electron affinity for the sequence, $WF_6 < ReF_6 < OsF_6 < IrF_6 < PtF_6$ (see Chapter III), the fluoride ion acceptor ability[1] decreases from left to right. This must be due to an increase in ligand crowding and a decrease in the d orbital availability for σ bonding as the series is ascended. Although the effective nuclear charge is increasing from W to Pt, the filling of the t_{2g} symmetry d orbitals reduces the availability of these orbitals for bonding. Over the entire third transition metal fluoride series, these two opposing trends, the increasing effective nuclear charge and the decreasing d t_{2g} orbital availability, result in a maximum in the fluoride ion affinity at tungsten and rhenium.

As was demonstrated in Chapter III, the electron affinity played a major role in determining whether a particular MF_6 species would intercalate graphite spontaneously. For non-intercalating binary fluorides the question naturally arose: Could the fluoride ion affinity of the species tip the thermodynamic balance in favor of intercalation, provided that a fluorine-rich oxidizing environment was maintained? Indeed, WF_6 does not react with nitric oxide, but does react[1] with nitrosyl fluoride to yield salts, $NO^+WF_7^-$ (1:1 gas mixture) and $(NO^+)_2WF_8^=$ (NOF in excess). Therefore, the fluoride ion affinity of WF_6 is shown to promote salt stabilization in fluorine-rich systems.

References

1. N. Bartlett, A. K. Cheetham, D. H. Templeton, A. Zalkin and B. Zemva, Lawrence Berkeley Laboratory Report LBL-10232 (1979).

2. N. Bartlett, R. N. Biagioni, E. M. McCarron, B. W. McQuillan and F. L. Tanzella, Molecular Metals, W. E. Hatfield, ed., Plenum Publishing Corp., 293 (1979); T. J. Richardson and N. B. Bartlett, J. C. S. Chem. Comm., 427 (1974).

3. M. J. Vasile and W. E. Falconer, J. C. S. Dalton, 316 (1975).

4. The dissociation, $O_2MF_6 \rightarrow O_2F\ (O_2 + 1/2\ F_2) + MF_5$ (M = Sb, Bi) was shown by Falconer.[3] Although no result is given for O_2AsF_6 itself, a similar result is expected. Moreover, the observation of a red solution species (O_2AsF_6 in HF) is indicative of O_2F. See J. J. Turner, Endeavour, 27, 42 (1968).

5. M. J. Vasile, T. J. Richardson, F. A. Frederick and W. E. Falconer, J. C. S. Dalton, 351 (1976).

6. E. R. Falerdeau, L. R. Hanlon and T. J. Thompson, Inorg. Chem., 17, 301 (1978).

In the case of non-intercalating MF_x species, the availability of fluorine atoms to produce a metastable $[MF_{x+1}]$ species may lead to graphite salts by fast electron transfer from the graphite to $[MF_{x+1}]$;

$$MF_x + F \rightarrow [MF_{x+1}] \qquad (1)$$

$$G + [MF_{x+1}] \rightarrow C_n^+MF_{x+1}^- \quad . \qquad (2)$$

Equations (1) and (2) are equivalent to fluoride ion capture. Therefore, for MF_x species with high F^- affinities, it should be possible to favor salt formation by photolysis, since ultraviolet light will break the relatively weak (38 kcal/mole) F - F bond. Therefore, in marginal-stability cases, photolysis of fluorine in graphite/MF_x/F_2 systems may yield graphite salts.

The systems, graphite/MF_5/F_2 (P, As, Sb), graphite/GeF_4/F_2 and graphite/BF_3/F_2, stand out as being exceptionally promising ones, because the MF_{x+1}^- anions derived from the MF_x parent are all capable of stabilizing O_2^+.[2-6] As was seen in Chapter IV, all the dioxygenyl salts attempted were observed to intercalate graphite with liberation of O_2. Hence, the dioxygenyl salts, $O_2^+MF_{x+1}^-$, should provide an alternative preparation for the graphite salts. But in the case of O_2BF_4[2], O_2GeF_5[6] and O_2PF_6[2], marginal stabilities would unnecessarily complicate the experimental details versus the graphite/MF_x/F_2 systems.

The graphite/AsF_5/F_2 and graphite/GeF_4/F_2 systems are discussed at length in Chapters VI and VII because of their special importance. They are mentioned, for completeness, only briefly in the Results and Discussion section of this chapter.

B. Experimental

1. Graphite/WF_6/F_2

Graphite powder (~1/2 gram) and HOPG (~30 mg) were reacted with a large excess of WF_6 (10 cc. liquid) at 0°C under 2 atmospheres pressure of fluorine. Reaction was not apparent. Photolysis of the mixture in a quartz vessel with a high pressure mercury ultraviolet lamp produced a blue material. Problems with the vacuum stability of the material hindered the determination of the limiting composition. But by removing the excess WF_6 in a static system with the receiving trap cooled to liquid nitrogen temperature (270 torr F_2 overpressure), a powder stoichiometry of approximately $C_{24}WF_{6+x}$ was obtained. Facile loss of WF_6 to vacuum resulted in a stable material of approximate composition $C_{36}WF_{6+x}$. HOPG samples irradiated for 3 hours reached a composition of approximately $C_{60}WF_{6+x}$.

2. Graphite/ReF_6/F_2

Graphite was reacted with ReF_6 and F_2 in a manner analogous to that dscribed for WF_6/F_2 above. Without ultraviolet irradiation no reaction was apparent. With U.V. irradiation, results were identical to those obtained by reacting graphite with ReF_7 (see below).

3. Graphite/ReF_7

HOPG (~30 mg) spontaneously reacted with ReF_7 (in excess) at room temperature to produce a deep blue first-stage material, $C_{10.3}ReF_7$. t/t_o was measured by micrometer to be 2.45 (see Chapter VI). The c-spacing determined from x-ray diffraction tracings was 8.18 Å. The material was vacuum stable at room temperature.

4. Graphite/PF_5/F_2

HOPG (~30 mg) was reacted with PF_5 (in excess) under 2 atmospheres of F_2 at room temperature for 12 hours to produce a deep blue material of limiting composition, C_8PF_6. t/t_o, from micrometry, was 2.27. The c-axis gallery spacing was 7.78 Å as determined by x-ray diffraction.

5. Graphite/SiF_4/F_2

HOPG (~30 mg) with excess SiF_4 under 2 atmospheres of F_2 pressure was not observed to react at room temperature, nor was reaction observed at 250°C.

6. Graphite/SnF_4/F_2

HOPG (30 mg) with excess SnF_4 under 2 atmospheres F_2 pressure was not intercalated at room temperature, nor at 250°C.

C. Results and Discussion

Rhenium is unique among the third transition series elements in forming a neutral molecular heptacoordinate, ReF_7.[7] ReF_7 is expected to have a larger electron affinity than ReF_6. As seen in Chapter III, ReF_6 does not intercalate spontaneously into graphite but OsF_6 does. Thus, the threshold electron affinity for graphite intercalation by MF_6 lies between 5.0 eV (ReF_6) and 6.5 eV (OsF_6) (see Chapter III, Table III-2). Assuming that the difference in the latice energetics between intercalated MF_6 and MF_7 are small, the spontaneous intercalation of ReF_7 is not surprising. The apparently anomalous limiting composition, $C_{10}ReF_7$, is easily explained.

As shown in Chapter III, C_8MF_6 represents a closest-packing of MF_6^- octahedra within the graphite galleries. Therefore, the larger volume of ReF_7^- (by approximately 18 $Å^3$) would preclude a C_8 packing.

Indeed, assuming a closest packing of F-ligands, $C_{9.3}ReF_7$ is calculated to be the limiting composition.[8] The possibility of forming $C_n^{++}ReF_8^{=}$ by disproportionation:

$$nC + 2ReF_7 \rightarrow C_n^{++}ReF_8^{=} + ReF_6 \qquad (4)$$

is discounted by the C_{10} packing ($C_{12}^{++}PtF_6^{=}$ limit established, Chapter III) and the large c-axis spacing, 8.18 Å ($C_{12}PtF_6$ - 7.55 Å; Chapter III). Neither was ReF_6 observed in infrared spectra of the gases after reaction.

The systems $G/MF_6/F_2$ (M = W and Re) in the absence of photolysis were ill-characterized and not rigorously persued. These reactions were performed in liquid hexafluoride at 0^oC with 2 atmospheres of fluorine overpressure. The absence of a reaction may be attributed to kinetic problems. Activation by photolysis probably generated reactive species by F atom attack on the hexafluoride. The intermediate in the ReF_6 case could simply be ReF_7. Although WF_7 seems less likely, F atom attachment to WF_6 may produce a sufficiently long-lived molecule for the abstraction of an electron from the graphite (which must be a very fast process) to occur. Unfortunately, MF_7^- and $MF_8^{=}$ cannot be distinguished by magnetic data, and some doubt as to the nature of the intercalant, especially in the tungsten case, must remain.

The graphite/MF_5/F_2 systems (M = P, As, Sb) all have large fluoride ion affinities and all yield closest-packed, first-stage salts according to the equation:

$$\text{Graphite} + MF_5 + 1/2\ F_2 \rightarrow C_8MF_6 \qquad (5)$$

This is hardly surprising since all of the MF_6^- anions stabilize O_2^+.[2-4] Dioxygenyl hexafluoroarsenate was observed (Chapter IV) to react with graphite with liberation of O_2.

The results for the intercalation by the Group IV tetrafluorides/F_2 systems of graphite were not so easily anticipated. GeF_5^- anion stabilizes O_2^+,[5] and, indeed, $C_{12}GeF_5$ was observed, but in conjunction with the related salt, $C_{12}GeF_6$ (see Chapter VII). A dioxygenyl salt of SiF_5^- is not known, and all attempts to intercalate SiF_4, in like fashion to GeF_4, have failed. Although SiF_4 will form SiF_5^- and SiF_6^{2-} salts, it appears that the work required to oxidize the graphite is not compensated for by the fluoride ion affinities and the lattice energy (which should be slightly more favorable than the Ge cases because of the smaller size of the silicon species). Since SiF_4 will not form even the salt $SF_3^+SiF_5^-$ with the fluoride-ion donor SF_4, whereas GeF_4 spontaneously generates $(SF_3^+)_2GeF_6^{2-}$:

$$2SF_{4(g)} + GeF_{4(g)} \rightarrow (SF_3)2GeF_{6(c)} \qquad (6)$$

it is clear that the enthalpies $\Delta H_{(1)}$ $(GeF_{4(g)} + F_{(g)}^- \rightarrow GeF_{5(g)}^-)$ and $\Delta H_{(2)}$ $(GeF_{5(g)}^- + F_{(g)}^- \rightarrow GeF_{6(g)}^{2-})$ must be more exothermic (or less endothermic) than for SiF_4.

SnF_4, on the other hand, should have a greater fluoride ion affinity than GeF_4, yet it does not intercalate graphite in the presence of F_2 even at high pressures and temperatures. Here, the energy required to break up the SnF_4 polymer may be a decisive adverse factor. Likewise, PbF_4 is a three dimensional lattice and the activation energy, to produce molecular PbF_4 essential to the formation of any discreet PbF_5^- or

$PbF_6^{=}$ species, are major obstacles to direct intercalation of PbF_4 with F_2. It should be possible to produce graphite salts containing $SnF_6^{=}$ and $PbF_6^{=}$ electrochemically, since these anions are well characterized and highly stable.[9]

Finally, $G/BF_3/F_2$ should intercalate graphite, since O_2BF_4[6] is known, and a reaction analogous to O_2MF_6 (M = As, Pt, Au) plus graphite (Chapter IV) is expected. Reports of HF or F_2 "catalyzed" BF_3 intercalations of graphite have been reported.[10]

References

1. N. Bartlett, Angew. Chem., Int. Ed., 7, 433 (1968).

2. I. J. Solomon, R. I. Brabets, R. K. Uenishi, J. N. Keith and J. M. McDonough, Inorg. Chem., 3, 457 (1964).

3. A. R. Young, T. Hirata and S. I. Morrow, J. Amer. Chemc. Soc., 86, 20 (1964).

4. J. Shamir and J. Binerboym, Inorg. Chem., 2, 37 (1968).

5. J. B. Beal, C. Pupp and W. E. White, Inorg. Chem., 8, 828 (1969).

6. K. O. Christe, R. D. Wilson and I. B. Goldberg, Inorg. Chem., 15, 1271 (1976).

7. J. G. Malm and H. Selig, J. Inorg. Nucl. Chem., 20, 189 (1961).

8. C_8MF_6 represents essentially a close-packing of F ligands. If the same close-packing is assumed for MF_7 then C_8MF_6 ($\equiv C_{56}(MF_6)_7$) equates to $C_{56}(MF_7)_6$ which gives $C_{9.3}MF_7$. The differing geometry of ReF_7 versus ReF_6 can only increase the C/M ratio. Therefore, a $C_{10}ReF_7$ packing limit is plausible.

9. F. A. Cotton and G. W. Wilkinson, Advanced Inorganic Chemistry, 3rd ed., p. 326 (1972).

10. J. E. Griffiths, W. A. Sunder and W. E. Falconer, Spectrochim. Acta, Part A, 31, 1207 (1975).

CHAPTER VI

COMPOSITION AND STAGING IN THE GRAPHITE/AsF_6 SYSTEM AND ITS RELATIONSHIP TO GRAPHITE/AsF_5

A. Introduction

Claims of exceptionally high conductivities (in excess of that of silver metal!) for certain graphite/AsF_5 intercalates[1] have focused much attention on these materials. Early speculation on the exact nature of the intercalated species leaned toward the guest residing within the graphite galleries as molecular AsF_5. This view was based on mass spectromeric[2,5] and NMR results.[3,5]

Subsequently, Bartlett and coworkers proposed[4] that the intercalation proceeded via an oxidation of the graphite according to the equation:

$$3AsF_5 + 2e^- \rightarrow 2AsF_6^- + AsF_3 \qquad (1)$$

where the electons are supplied by the graphite host. This proposal was supported by x-ray As - K edge absorption studies,[4,5] the preabsorption edge features of which clearly indicated the presence of AsF_3 and AsF_6^- in the graphite/AsF_5 materials (see Fig. VI-1).

Because of the high fluoride ion affinity of AsF_5,[6] salts analogous to those obtained from graphite plus O_2AsF_6 (Chapter IV) should be produced by the reactions:

$$\text{Graphite} + AsF_5 + 1/2\ F_2 \rightarrow C_xAsF_6 \qquad (2)$$

$$C_xAsF_5 + 1/2\ F_2 \rightarrow C_xAsF_6 \qquad (3)$$

It was believed that a comparison of the fluorinated materials with their AsF_5 relatives would shed some light on the nature of the latter. Moreover, it was also recognized that it should be possible to convert the hexafluoroarsenate salts to AsF_5 intercalated materials by addition of AsF_3 if the proposal of Bartlett and his coworkers[1] is valid:

$$C_xAsF_6 + 1/2\ AsF_3 \rightarrow C_{2/3x}AsF_5 \qquad (4)$$

where $x \geqslant 12$.

B. Experimental

1. Graphite/AsF_5

Apart from prefluorination of the graphite to remove any reducing species present (1 atmosphere F_2 for 1/2 hour at room temperature), the synthesis of graphite intercalation compounds containing AsF_5 employed was essentially that of Falerdeau et al.[7] The reactions were carried out in quartz vessels at room temperature.

The ratio of final to initial thickness for samples prepared from HOPG are given in Table VI-1. The theoretical t/t_o values given are based on 00ℓ diffraction data and single crystal precession photography which indicate a gallery spacing of 8.05(3) Å for graphite/AsF_5 materials.

The details of the subsequent removal of arsenic-containing species from these graphite/AsF_5 materials under vacuum are listed in Table VI-2. The volatiles were collected as a function of pumping time and characterized by infrared spectroscopy. Representative I.R. spectra of the volatiles versus pumping time are given in Fig. VI-2.

2. Graphite/AsF_6

Prefluorinated graphite, both powdered and monolithic, was reacted with stoichiometric amounts of AsF_5 under 2 atmospheres pressure of F_2 normally for a 12 hour period. Reactions were followed by both gravimetry and tensimetry. Representative results for both As-rich and As-poor are given in Tables VI-3 and VI-4, respectively. Because of the large quantities of graphite necessary for accurate tensimetries, tensimetry was not followed on HOPG samples. A typical HOPG sample was 5 mm square (ab-plane) and 1/2 mm thick along c and weighed ca. 30 mg. Powder samples were analyzed by routine CHN analysis. Because the HOPG samples were intended for other studies destructive analysis was not performed, but t/t_o values are given in Table VI-5 which are indicative of the degree of fluorination (see Fig. VI-3). Gravimetric findings for HOPG samples are also given where available. The graphite/AsF_6 was observed to be stable to vacuum at room temperature. The findings from the removal of arsenic species at elevated temperatures are presented in Table VI-6.

C_xAsF_6 salts were also obtained by the fluorination at 2 atmospheres pressure of C_xAsF_5 materials, produced as outlined in section 1 above. The color of the resulting C_xAsF_6 salt was in all cases a much deeper blue than the original C_xAsF_5 material. Also, an increase in the sample thickness upon fluorination was noted and is illustrated in Fig. VI-3.

3. Graphite/AsF_6 + AsF_3

Graphite/AsF_6 salts were immersed in liquid AsF_3 in quartz vessels for 12 hours at room temperature to produce materials which, from several tests, appeared to be the same as the graphite/AsF_5 materials.[8] At high arsenic content, C_xAsF_6 ($x < 36$), the materials resulting from the

reaction with AsF_3 lost both AsF_5 and AsF_3, as determined by infrared spectroscopy, to vacuum in a manner typical of $C_{2/3x}AsF_5$. At low arsenic content, C_xAsF_5 ($x \geqslant 36$), the resulting materials, from interaction with AsF_3, lost only AsF_3 to vacuum; again in harmony with the behavior of materials of similar stoichiometry derived directly from graphite and AsF_5. The results are summarized in Table VI-7.

In a separate series of experiments, low arsenic content graphite salts (section 2) were observed to incorporate an excess of fluorine up to a maximum uptake (after pumping) represented by the equation

$$C_xAsF_5 + F_2 \rightarrow C_xAsF_6 \cdot 1/2\ F_2 \qquad (5)$$

This "excess F_2" could be titrated with either AsF_3 or AsF_5 to produce a vacuum stable graphite salt according to the equations:

$$C_xAsF_6 \cdot 1/2\ F_2 + 1/2\ AsF_5 \rightarrow C_{2/3x}AsF_6 \qquad (6)$$

$$C_xAsF_6 \cdot 1/2\ F_2 + 1/3\ AsF_3 \rightarrow C_{3/4x}AsF_6 \quad . \qquad (7)$$

As illustrated in Fig. VI-3, the resulting salts show an increase in t/t_o with titration. Further AsF_3 incorporation produced materials which behaved like graphite/AsF_5. Typical results for these arsenic-poor systems are given for both powder and HOPG samples in Table VI-8.

Finally, general reaction schemes for both arsenic-rich and arsenic-poor systems with respect to fluorination and subsequent reaction with AsF_3 are given in Figs. VI-4 through VI-6.

C. X-Ray Diffraction Studies

1. HOPG X-Ray Diffraction Studies

The experimental details are described in Chapter II, section C.1. c-spacing values for C_8AsF_5 and $C_{12}AsF_6$ were observed to be 8.05(3) Å and 8.04 Å, respectively. C_8AsF_6 was observed to have a c-spacing of 7.86(3) Å. For C_xAsF_5 the composition-staging relationships are presented in Table VI-1. For C_xAsF_6 the composition-staging relationships are given in Table VI-5. The stages presented in a given HOPG sample were obtained from 00ℓ data. Comparison of the graphite/AsF_6 and graphite/AsF_5 systems is illustrated in Fig. VI-3.

2. Single-Crystal Precession Photography Data for C_8AsF_6 at Room Temperature

Zero-layer precession photographs of graphite single crystals (~1 mm in any dimension) (Chapter II, section B.1.) established the graphite to be hexagonal with a = 2.46(1), c = 6.70(2) Å. The intercalation technique for graphite single crystals is outlined in Chapter II, section C.3.

Zero-layer precession photographs of C_8AsF_6 at room temperature indicated hexagonal symmetry with c = 7.84(2) Å. The hk0 reflections were identical to that of the parent graphite, a = 2.46(1) Å. This suggests a long-range disorder in the AsF_6^- anion placements from one gallery to the next. Other single crystal studies[9] undertaken in this lab have shown that freshly prepared, C_8MF_6 single crystals, photographed at liquid nitrogen temperatures, are hexagonal and well ordered with respect to the MF_6^- anion placement, a = 4.92(2) Å. However, over 1-2 days at room temperature, the diffraction became less sharp, the hk-indexed spots eventually spreading to rings.

D. Results and Discussion

Intercalation of AsF_5 into pyrolytic graphite[10] produces an excellent metal[1] and there has been much speculation on the nature of the guest species. This laboratory's interest in related AsF_6^- salts[11] prompted the examination of the AsF_5 materials and from synchrotron-radiation As-absorption edge studies it was concluded[4,5] that AsF_5 was entering graphite by oxidation according to the equation:

$$3AsF_5 + 2e^- \rightarrow 2AsF_6^- + AsF_3 \qquad (1)$$

The observation[2] that AsF_5 can be recovered from the intercalate, implied reversibility of (1), but the As-absorption edge studies[4] did indicate essentially complete conversion to AsF_6^- and AsF_3. There has been much reluctance to accept this interpretation. Some of this has derived from failure to find AsF_3 in the gases from graphite-AsF_5.[6] The failure to observe more than one ^{19}F nmr resonance,[3] and the large electron withdrawal from graphite (which extensive conversion to AsF_6^- requires) have also presented difficulties.[12]

Our investigation of the volatiles from C_xAsF_5 shows that the earlier findings[2] were misleading. A sample of C_8AsF_5, was prepared from powdered high-purity pyrolytic graphite, which had been well dried, and pretreated with fluorine to remove any reducing species. Infrared spectroscopy showed other infrared-active components to be absent from the AsF_5 used in the preparation. The volatiles from a C_8AsF_5 sample at 20^o, held under vacuum, were monitored by infrared spectroscopy as a function of pumping time (see Fig. VI-2). Within the first minute

the volatiles were largely AsF_5, but AsF_3 was detected. As the composition of the intercalate approached $C_{10}AsF_{(5-6)}$, the volatiles proved to be approximately equimolar quantities of AsF_5 and AsF_3. From $C_{10}AsF_{(5-6)}$ to $C_{14}AsF_6$ (several hours of pumping) the only volatile detected was AsF_3 (see Table VI-2). Removal of AsF_3 requires an increase in the AsF_6^- fraction of the arsenic species remaining in the graphite and all indications are that the vacuum stable product is an AsF_6^- salt. Although, at 20°, the major volatile from C_8AsF_5 is AsF_5, the only volatile from the third-stage compound $C_{24}AsF_5$ is AsF_3 (see Table VI-2). This is consistent with a higher positive charge and electron affinity of the carbon network of the first-stage compound, in comparison with the third-stage material. Of course the reversal of (1), to produce AsF_5, requires that the carbon network should recapture electrons from the AsF_6^-.

In a separate series of experiments, graphite was intercalated by AsF_5/F_2 mixtures to yield C_xAsF_6. At the intercalation limit, tensimetry of the F_2 and AsF_5 consumption satisfies the equation: $8C + AsF_{5(g)} + 1/2\ F_{2(g)} \rightarrow C_8AsF_6$ (see Table VI-3). The AsF_6^- salts are stable in a vacuum at 20°. At elevated temperatures, fluoride ion attack on the graphite is apparent with CF_4 and AsF_5 being detected by infrared spectroscopy (see Table VI-6). At lower guest concentrations (e.g. $C_{12n}AsF_6$) the material takes up more fluorine to a limiting composition, $C_{12n}AsF_6 \cdot 1/2\ F_2$ (see Table VI-4). This fluorine presumably occupies vacancies in the galleries (C_8MF_6 is close-packed; Chapter III). This fluorine can be 'titrated' with more AsF_5 or AsF_3 to yield AsF_6^- (see Table VI-8). By monitoring highly oriented (c-axis) pyrolytic-graphite slabs (of thickness t) both by micrometry and x-ray diffraction, it has been

established that the composition for each stage is $C_{12n}AsF_6$ (n the stage), up to the first-stage onset of $C_{12}AsF_6$. This means that each occupied gallery up to first stage, has a composition $C_{12}AsF_6$, as indicated in Figs. VI-3 and VI-8. The micrometer t/t_o (t_o being the thickness of the original graphite) compares closely with the t/t_o (ideal) derived from the x-ray diffraction gallery height measurements (see Table VI-5).

The excess F_2 which occupies the vacancies in the C_{12} structure due to the nature of certain syntheses (2 atmospheres F_2 overpressure) can be disregarded. If this F_2 was present as F_2^- ion, essentially generating a pseudo-C_8X packing, these arguments for a C_{12} packing would be invalidated. But $C_{12n}MF_6$ (n the stage) staging relationships have been observed for M = Os and Ir (see Table VI-9). Here, the possibility of an excess F_2 interference is eliminated (Chapter III). Moreover, if F_2^- was occupying holes in $C_{12n}AsF_6$, a spin-only moment of ~1.86 B.M. would be anticipated, since the F_2^- ion would be $^2\Sigma$. All $C_{12n}AsF_6 \cdot 1/2\ F_2$ materials studied were diamagnetic.

With sufficient AsF_5/F_2 the first-stage composition can be taken from $C_{12}AsF_6$ (with a gallery height, $\underline{c}$ = 8.04(2) Å) to a limit of C_8AsF_6 ($\underline{c}$ = 7.86(2) Å). Single crystal work establishes that the latter is hexagonal with a = 4.92(1), c = 7.86(2), V = 165 $Å^3$, which volume requires that the AsF_6^- be in close-packed 'planar' array. The $\underline{c}$-axis contraction from $C_{12}AsF6$ to C_8AsF_6 can be attributed to the increased Coulomb attraction of guest and host, with the change from C_{12}^+ to $C_8^+AsF_6^-$.

In a gallery occupancy of $C_{12}AsF_6$, each anion need have only three anion neighbors, whereas in C_8AsF_6 each is constrained to have six (see Fig. VI-8). We attribute the $C_{12n}AsF_6$ staging-composition relationship

to the reduced repulsive interactions offered by the $C_{12}AsF_6$ gallery occupancy. Evidently, opening of virgin galleries is preferred over filling beyond $C_{12}AsF_6$, as long as virgin galleries are available.

Treatment of $C_{12}AsF_6$ with AsF_3 leads to consumption of the latter according to the equation (see Table VI-7):

$$2C_{12}AsF_6 + AsF_3 \rightarrow 3C_8AsF_5 \qquad (6)$$

In a vacuum it loses AsF_5 and AsF_3 as for C_8AsF_5 made directly from graphite and AsF_5. Similar conversions can be made at other compositions. There is no perceptable change in t/t_o when AsF_3 is added to or removed from a monolithic sample (see Table VI-8) and x-ray diffraction findings indicate no change in stage. It had previously been observed[7] that the graphite/AsF_5 stages obey the relationship $C_{8n}AsF_5$ where n is the stage (see Table VI-1 and Fig. VI-3). Since C_8AsF_5 can be represented as $C_{12}^{+}AsF_6^{-}\cdot 1/2\ AsF_3$ (if the equilibrium for (1) is far to the right) it is reasonable to suppose that the neutral AsF_3 molecules occupy the vacancies in the $C_{12}AsF_6$ anion arrangement, as proposed in Fig. VI-8(a). The equality (within experimental error) of the c-spacing for C_8AsF_5 (8.05(3) Å) with that for $C_{12}^{+}AsF_6^{-}$ (8.04(3) Å) also agrees with essentially complete conversion of AsF_5 to AsF_6^{-} and AsF_3. Recent EXAFS studies for C_xAsF_5, C_yAsF_6, AsF_5, AsF_3 and a vareity of AsF_6^{-} salts[13] also indicate that there is unlikely to be more than 5% of free AsF_5 in $C_{10}AsF_5$ and are fully consistent with the guest species being AsF_6^{-} and AsF_3.

With the demonstration that AsF_3 can be removed from C_xAsF_5, attention must be paid to the preparative conditions for 'C_xAsF_5' samples,

since AsF_3 departure will result in AsF_6^- salt formation. The residual compounds are apparently such salts.

Finally, the general interconversions possible between the graphite/AsF_6 and graphite/AsF_5 systems are presented in Figs. VI-5 through VI-7).

References

1. E. R. Falerdeau, G. M. T. Foley, C. Zeller and F. L. Vogel, J.C.S. Chem. Comm., 389 (1977).

2. H. Selig, M. J. Vasile, F. A. Stevie and W. H. Sunder, J. Fluorine Chem., 10, 299 (1977).

3. L. Ebert and H. Selig, Mat. Sci. Eng., 31, 177 (1977).

4. N. Bartlett, R. N. Biagioni, B. W. McQuillan, A. S. Robertson and A. C. Thompson, J.C.S. Chem. Com., 200 (1978).

5. N. Bartlett, B. W. McQuillan and A. S. Robertson, Mat. Res. Bull., 13, 1259 (1978).

6. D. D. Gibler, Ph.D. thesis, Unversity of California, Berkeley, LBL-1157 (1973).

7. E. R. Falerdeau, L. R. Hanlon and T. J. Thompson, Inorg. Chem., 17, 301 (1978).

8. The materials are chemically indistinguishable, but their conductivities differ: $\sigma(G/AsF_5) > \sigma(G/AsF_6 + 1/2\ AsF_3)$ (see Chapter VIII).

9. N. Bartlett, E. M. McCarron, B. W. McQuillan and T. E. Thompson, Syn. Metals., 1 (1980).

10. Lin Chun-Hsu, H. Selig, M. Rabinovitz, I. Agranat and S. Sarig, Inorg. Nuclear Chem. Letters, 11, 601 (1975).

11. T. J. Richardson and N. Bartlett, J.C.S. Chem. Comm., 427 (1974); and N. Bartlett, R. N. Biagioni, E. M. McCarron, B. W. McQuillan and F. Tanzella, Molecular Metals, W. E. Hatfield, Ed., Plenum Pub. Corp., New York, 293 (1979).

12. M. J. Moran, J. E. Fischer and W. R. Salaneck, personal communication.

13. A. S. Robertson, Ph.D. thesis, University of California, Berkeley, LBL-9840 (1979).

Table VI-1. Evidence for the composition-staging formula, $C_{8n}AsF_5$ (n being the stage), in the system, graphite/AsF_5.

x†	t/t_o ‡ (ideal)	t/t_o (from micrometer measurements)
8 (1st stage)	2.40	----
10.3	2.20	2.21
13.1	1.95	1.96
14.2	1.82	1.82
16 (2nd stage)	1.70	----
16.4	1.69	1.70
17.9	1.65	1.68
18.1	1.64	1.67
20.2	1.58	1.61
23.9	1.48	1.49
24 (3rd stage)	1.47	----

† x is the C/As ratio, C_xAsF_5.

‡ $8 \leqslant x \leqslant 16$: $\frac{t}{t_o}(x) = \left(1 - \frac{x-8}{8}\right) \frac{t}{t_o}$ [1st stage] + $\left(\frac{x-8}{8}\right) \frac{t}{t_o}$ [2nd stage]

$16 \leqslant x \leqslant 24$: $\frac{t}{t_o}(x) = \left(1 - \frac{x-16}{8}\right) \frac{t}{t_o}$ [2nd stage] + $\left(\frac{x-16}{8}\right) \frac{t}{t_o}$ [3rd stage]

Pure stage t/t_o values are based on a measured c-spacing of 8.05(3) Å for C_8AsF_5 and a parent-graphite gallery height of 3.35 Å.

$$\frac{t}{t_o}\text{ [1st stage]} = \frac{8.05\text{ Å}}{3.35\text{ Å}} = 2.40$$

$$\frac{t}{t_o}\text{ [2nd stage]} = \frac{8.05\text{ Å} + 3.35\text{ Å}}{2(3.35\text{ Å})} = 1.70$$

$$\frac{t}{t_o}\text{ [3rd stage]} = \frac{8.05\text{ Å} + 2(3.35\text{ Å})}{2(3.35\text{ Å})} = 1.47$$

Table VI-2. Removal of As-containing species from graphite/AsF_5

Graphite/AsF_5 compositon	pumping temp.-time	volatiles	composition after pumping from	
			gravimetry	CHN analysis
$C_{8.8}AsF_5$	25°, 1 minute	$AsF_5 \gg AsF_3$	---	---
	25°, 1/2 hour	AsF_5, AsF_3	$C_{12.2}AsF_6$	---
	25°, 1-1/2 hour	AsF_3	$C_{12.9}AsF_6$	---
	25°, 12 hours	AsF_3	$C_{14.0}AsF_6$	$C_{14.5}AsF_6$
$C_{16.4}AsF_6$	25°, 3 hours	$AsF_3 > AsF_5$	$C_{25.0}AsF_6$	$C_{25.5}AsF_6$
$C_{23.3}AsF_6$	25°, 3 hours	$AsF_3 \gg AsF_5$	$C_{34.0}AsF_6$	$C_{34.6}AsF_6$
$C_{24.1}AsF_6$	25°, 3 hours	AsF_3	$C_{34.1}AsF_6$	$C_{34.9}AsF_6$
$C_{36.3}AsF_6$	25°, 1-1/2 hours	AsF_3	$C_{42.0}AsF_6$	---
	100°, 1/2 hour	$AsF_3 > AsF_5$	$C_{45.1}AsF_6$	---
	250°, 3/4 hour	$AsF_5 > AsF_3 \gg CF_4$	$C_{52.8}AsF_6$	$C_{54.0}AsF_6$

Table VI-3. Fluorine uptake by graphite/AsF_5: arsenic-rich systems.

Gravimetry						
material	mmol graphite	mmol AsF_5	mmol F·	rnx time		
HOPG					t/t_o	t/t_o(ideal)
$C_{13.1}AsF_6$	3.92	0.30	0.26	12 hr	2.28	2.38
$C_{14.7}AsF_6$	1.77	0.11	0.09	12 hr	2.19	2.21
Powder					CHN analysis	
$C_{8.1}AsF_6$	27.3	3.37	3.32	72 hr	$C_{8.4}AsF_6$	
$C_{9.6}AsF_6$	30.8	3.21	3.13	72 hr	$C_{10.0}AsF_6$	
$C_{10.9}AsF_6$	12.4	1.16	1.20	72 hr	$C_{10.7}AsF_6$	

Tensimetry				
material	torr AsF_5	torr F_2	rnx time	CHN analysis
$C_{8.6}AsF_6$	690	335	72 hr	$C_{9.0}AsF_6$
$C_{13.1}AsF_6$	1706	860	72 hr	$C_{13.8}AsF_6$

Table VI-4. Fluorine uptake as a function of time by graphite/AsF_5: arsenic-poor systems.

Tensimetry				
Starting material	rnx time	Pressures of intercalates consumed at constant volume, temp. torr AsF_5	torr F_2	resultant stoichiometry (see gravimetry)
Graphite (19.70 mmol)	24 hr	500	585	$C_{23.8}AsF_6 \cdot 2/3\ F_2$
	48 hr	---	800	$C_{23.8}AsF_6 \cdot F_2$
Graphite (33.60 mmol)	6 hr	300	289	$C_{70.0}AsF_6 \cdot 1/2\ F_2$
	18 hr	---	607	$C_{70.0}AsF_6 \cdot 3/2\ F_2$

Gravimetry (after pumping)				
mmol graphite	mmol AsF_5	mmol F_2	stoichiometry	CHN analysis
19.70	0.82	0.86	$C_{23.8}AsF_6 \cdot 1/2\ F_2$	$C_{24.3}AsF_6 \cdot 1/2\ F_2$
33.60	0.48	0.50	$C_{70.0}AsF_6 \cdot 1/2\ F_2$	$C_{70.4}AsF6 \cdot 1/2\ F_2$

Table VI-5. Evidence for the composition-staging forumula, $C_{12n}AsF_6$ (n being the stage), in the system graphite/AsF_6.

x†	t/t_o‡ (ideal)	t/t_o (from micrometer measurements)
11.6	2.40(5)	2.38
12 (ideal)	2.40	----
13.1	2.34(5)	2.28
13.9	2.29(5)	2.23
14.6	2.25(5)	2.20
16.2	2.16(5)	2.17
16.6	2.13(5)	2.15
18.3	2.03(5)	2.12
19.7	1.95(5)	2.11
22.8	1.77(5)	1.89
24 (ideal)	1.70	----
28.3	1.62(5)	1.62
30.9	1.57(5)	1.59
36 (ideal)	1.47	----

†x is the C/As ratio, C_xAsF_6.

‡$12 \leqslant x \leqslant 24$: $\frac{t}{t_o}[C_xAsF_6] = \left(1 - \frac{x-12}{12}\right)\frac{t}{t_o}[C_{12}AsF_6] + \left(\frac{x-12}{12}\right)\frac{t}{t_o}[C_{24}AsF_6]$

$24 \leqslant x \leqslant 36$: $\frac{t}{t_o}[C_xAsF_6] = \left(1 - \frac{x-24}{12}\right)\frac{t}{t_o}[C_{24}AsF_6] + \left(\frac{x-24}{12}\right)\frac{t}{t_o}[C_{36}AsF_6]$

t/t_o for $C_{12}AsF_6$ calculated from x-ray diffraction data on HOPG:

$$\frac{\text{c-space } C_{12}AsF_6}{\text{c-space graphite}} = \frac{8.05\ \text{Å}}{3.35\ \text{Å}} = 2.40$$

for C_{24}: $\frac{8.05\ \text{Å} + 3.35\ \text{Å}}{2 \times 3.35\ \text{Å}} = 1.70$

for C_{36}: $\frac{8.05\ \text{Å} + (3.35\ \text{Å} \times 2)}{3 \times 3.35\ \text{Å}} = 1.45$

Table VI-6. Removal of As-containing species from graphite^{+}/AsF_6^{-}.

material	temp	time	volatiles	final gravimetry	CHN analysis
$C_{10.9}AsF_6$	25°	72 hr	none	$C_{10.9}AsF_6$	
	100°	1/2 hr	AsF_5	$C_{11.1}AsF_6$	
	250°	1 hr	$AsF_5 > CF_4$	$C_{12.9}AsF_6$	$C_{13.1}AsF_6$
$C_{16.1}AsF_6$	250°	1 hr	$AsF_5 > CF_4$	$C_{18.5}AsF_6$	----
$C_{24.3}AsF_6 \cdot 1/2\ F_2$	100°	1 hr	$AsF_5 > CF_4$	$C_{24.7}AsF_6$	----
	250°	1-1/2 hr	$AsF_5 > CF_4$	$C_{25.1}AsF_6$	$C_{26.0}AsF_6$

Table VI-7. Graphite hexafluoroarsenate salts + AsF_3.

POWDER					
Starting material, POWDER	+ AsF_3	tensimetry torr	pumped to hard vacuum	analysis	% As loss
$C_{13.1}AsF_6$	$C_{7.8}AsF_5$ (wet)	333 (317 ideal)	AsF_5,AsF_3	$C_{13.8}AsF_6$	0.6%
$C_{14.0}AsF_6$	$C_{7.9}AsF_5$ (wet)	179 (165 ideal)	AsF_5,AsF_3	$C_{14.7}AsF_6$	0.5%

HOPG							
Starting material, HOPG	t/t_o prior to AsF_3 uptake	+ AsF_3	t/t_o following AsF_3 uptake	volatiles pumped to hard vacuum	final material	t/t_o	% As loss
$C_{10.1}AsF_6$	2.39 (2.38)	$C_{7.7}AsF_5$	2.40 (2.40)	$AsF_3 > AsF_5$	$C_{10.8}AsF_6$	2.41 (2.39)	0.6%
$C_{15.2}AsF_6$	2.19 (2.21)	$C_{11.7}As_{F5}$	2.19 (2.21)	$AsF_3 > AsF_5$	$C_{16.3}AsF_6$	2.11 (2.15)	1.8%
$C_{36.1}AsF_6$	1.47 (1.47)	$C_{23.4}AsF_5$	1.48 (1.46)	AsF_3	$C_{31.2}AsF_6$	1.47	--

Table VI-8. Typical fluorination-titration cycle for graphite/AsF_{5-6}.

GRAPHITE POWDER				
			RT	
Graphite 40.25 mmol	+	AsF_5 1.61 mmol 1015 torr	→	$C_{25}AsF_5$ 1.61 mmol
$C_{25}AsF_5$ 1.61 mmol	+	F_2 1.63 mmol 1028 torr	→	$C_{25}AsF_6 \cdot 1/2\ F_2$[a] 1.61 mmol
$C_{25}AsF_6 \cdot 1/2\ F_2$ 1.61 mmol	+	AsF_3 0.55 mmol 325 torr	→	$C_{18.8}AsF_6$ 2.15 mmol
$C_{18.8}AsF_6$ 2.15 mmol	+	F_2 1.06 mmol 670 torr	→	$C_{18.8}AsF_6 \cdot 1/2\ F_2$[a] 2.15 mmol
$C_{18.8}AsF_6 \cdot 1/2\ F_2$ 2.15 mmol	+	AsF_3 0.705 mmol 420 torr	→	$C_{14.1}AsF_6$[a] 3.19 mmol
$C_{14.1}AsF_6$ 3.19 mmol	+	excess AsF_3	→	$C_{9.4}AsF_5$[b] 4.79 mmol
HOPG				
$C_{24.0}AsF_6 \cdot 1/2\ F_2$ $t/t_o = 1.71$ 2nd stage t/t_o ideal = 1.71	+	excess AsF_3	→	$C_{12.6}AsF_5$[b] $t/t_o = 2.09$ mix 1st and 2nd stage t/t_o(ideal) = 2.10
$C_{36.5}AsF_6 \cdot 1/2\ F_2$ $t/t_o = 1.48$ 3rd stage t/t_o(ideal) = 1.47	+	excess AsF_3	→	$C_{18.7}AsF_5$[b] $t/t_o = 1.62$ mix 2nd and 3rd stage t/t_o(ideal) = 1.63

[a] vacuum stable at RT

[b] loses AsF_5 + AsF_3 to vacuum

Table VI-9. Evidence for the composition-staging formula, $C_{12n}MF_6$ (n being the stage) in graphite/MF_5 systems.

x†	M	t/t_o (ideal)‡	t/t_o (from micrometer measurements)
8.0	Ir	2.41	2.41
13.1	Os	2.35	2.37
17.5	Os	2.09	2.10
19.0	Os	2.00	2.02
19.9	Os	1.95	1.97
20.1	Ir	1.89	1.93
20.8	Os	1.90	1.92
33.0	Os	1.61	1.63

†x is the C/M ratio, C_xMF_6.

‡based on c-spacings for 1st stage C_8MF_6; Os, 8.10 Å and Ir, 8.06 Å. This introduces an error (values too small) since the value for $C_{12}MF_6$ should be used; the $C_{12}MF_6$ c-spacing should be larger due to the decreased charging effect, C_{12}^+ vs. C_8^+.

$12 \leqslant x \leqslant 24$:

$$\frac{t}{t_o}(x,M) = \left(1 - \frac{x-12}{12}\right) \frac{t}{t_o}[\text{1st stage(M)}] + \left(\frac{x-12}{12}\right) \frac{t}{t_o}[\text{2nd stage(M)}]$$

$24 \leqslant x \leqslant 36$:

$$\frac{t}{t_o}(x,M) = \left(1 - \frac{x-24}{12}\right) \frac{t}{t_o}[\text{2nd stage(M)}] + \left(\frac{x-24}{12}\right) \frac{t}{t_o}[\text{3rd stage(M)}]$$

where

$$\frac{t}{t_o}(\text{nth stage}) = \frac{MF_6 \text{ intercalated gallery height} + (n-1)\ 3.35\,\text{Å}\ [\text{graphite}]}{n(3.35\ \text{Å})}$$

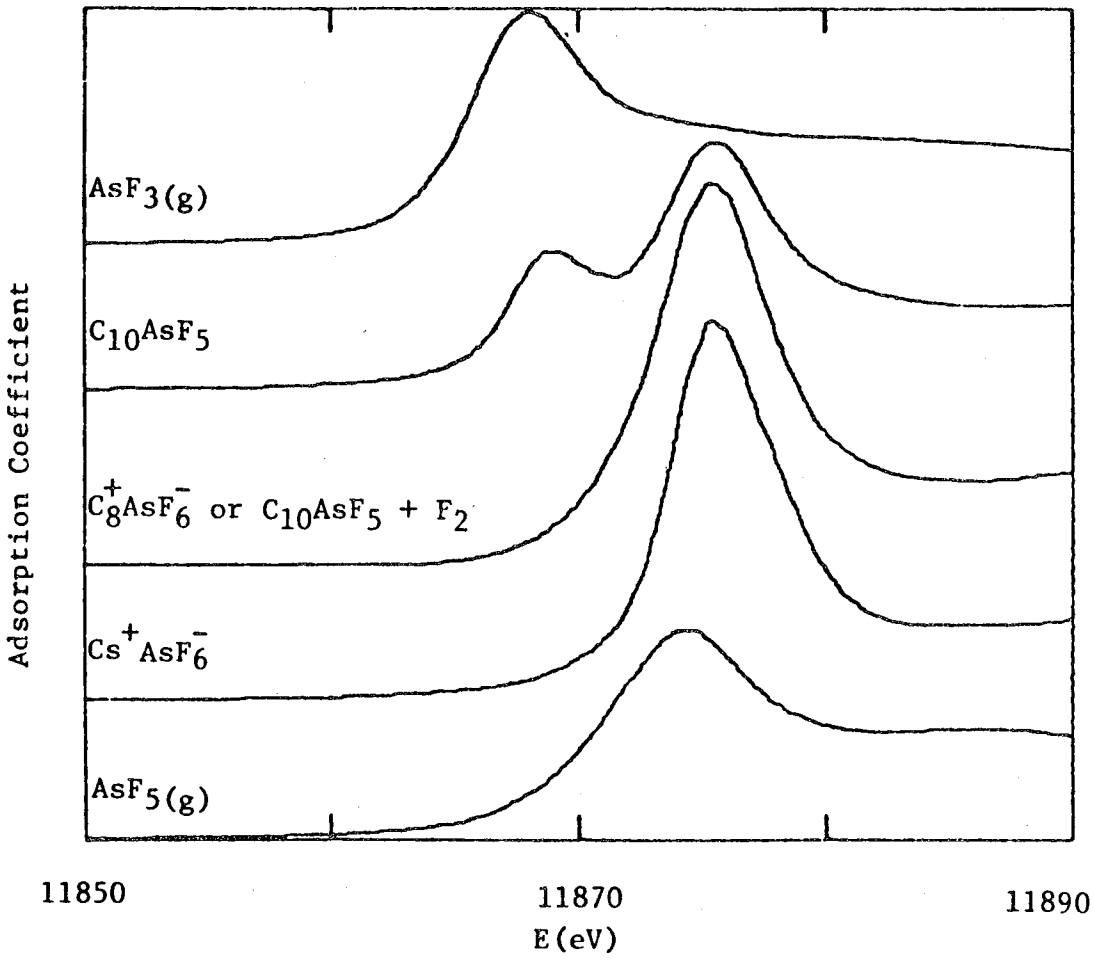

Figure VI-1. Arsenic K-shell pre-absorption edge spectra.

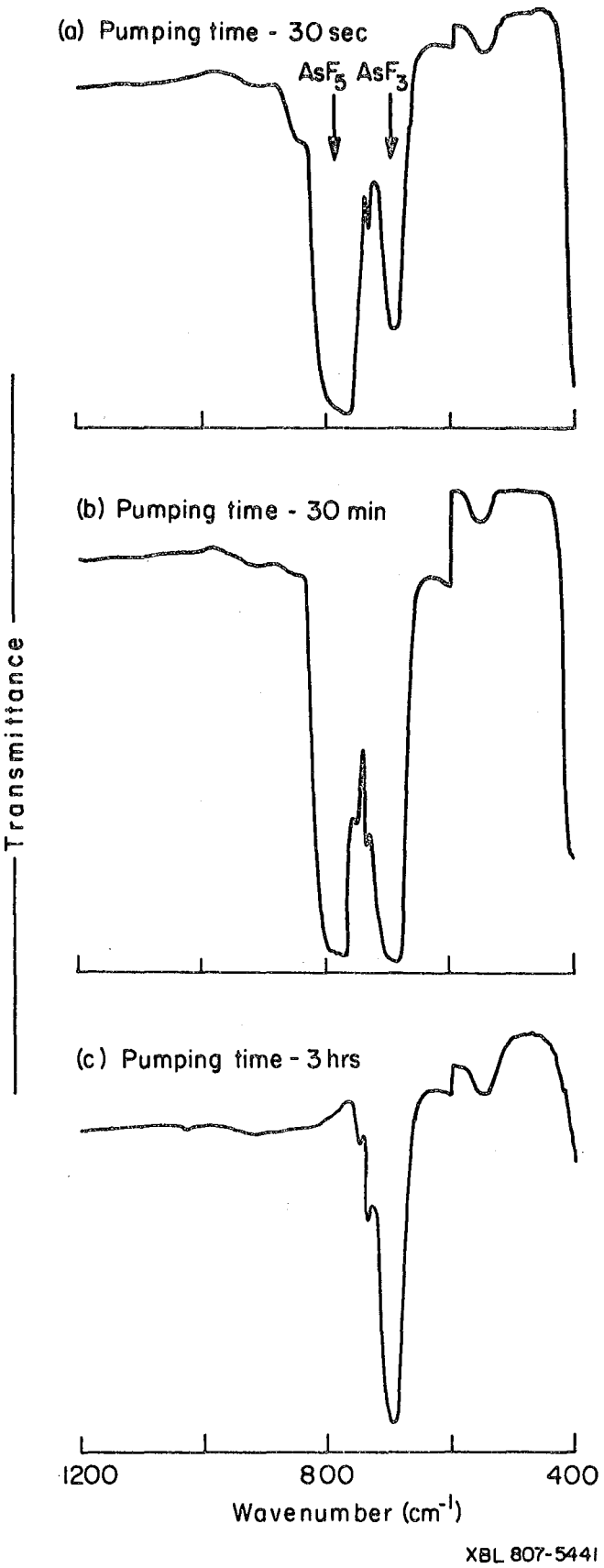

Figure VI-2. Infrared spectra of volatiles removed from C_8AsF_5.

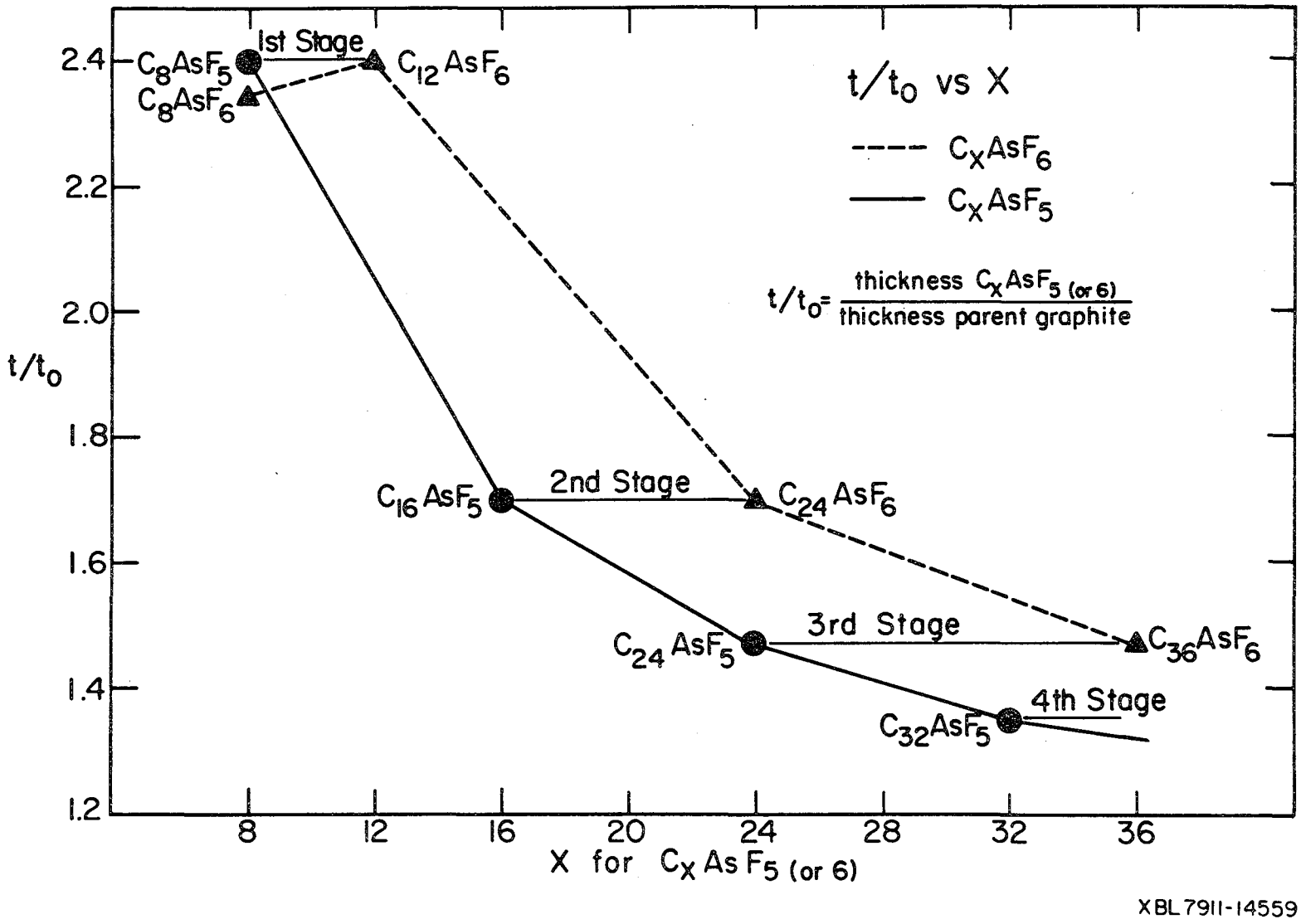

XBL7911-14559

Figure VI-3. Composition/staging relationships for C_xAsF_5 and C_xAsF_6.

ARSENIC RICH SYSTEMS ($x < 24$)

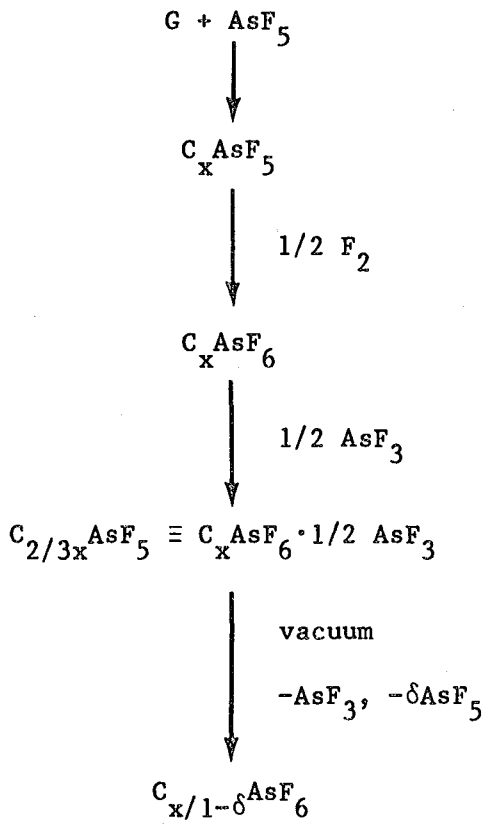

Figure VI-4. Generalized reaction scheme for arsenic-rich (mole ratio C/As = $x < 24$) graphite/AsF_5 systems.

ARSENIC POOR SYSTEMS ($x > 48$)

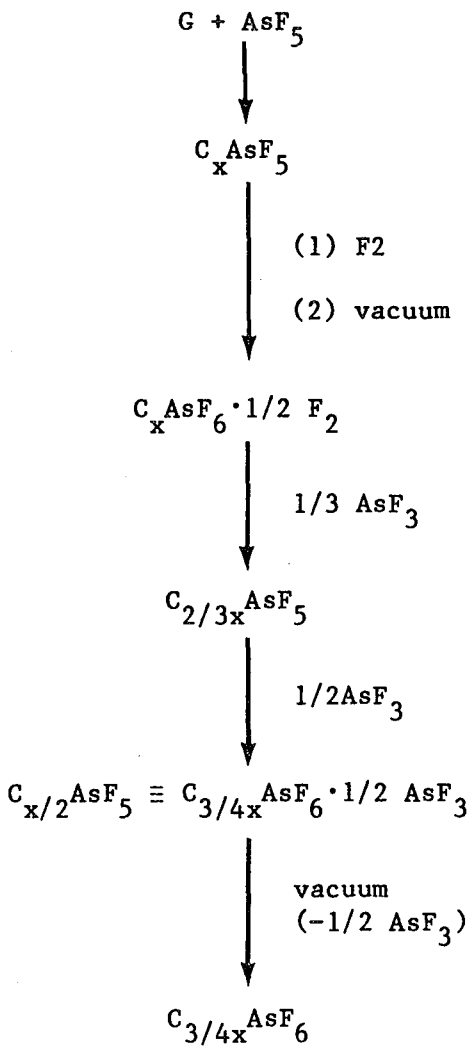

Figure VI-5. Generalized reaction scheme for arsenic-poor (mole ratio C/As = $x > 48$) graphite/AsF_5 systems.

SYSTEMS WITH INTERMEDIATE ARSENIC CONTENT ($24 < x < 48$)

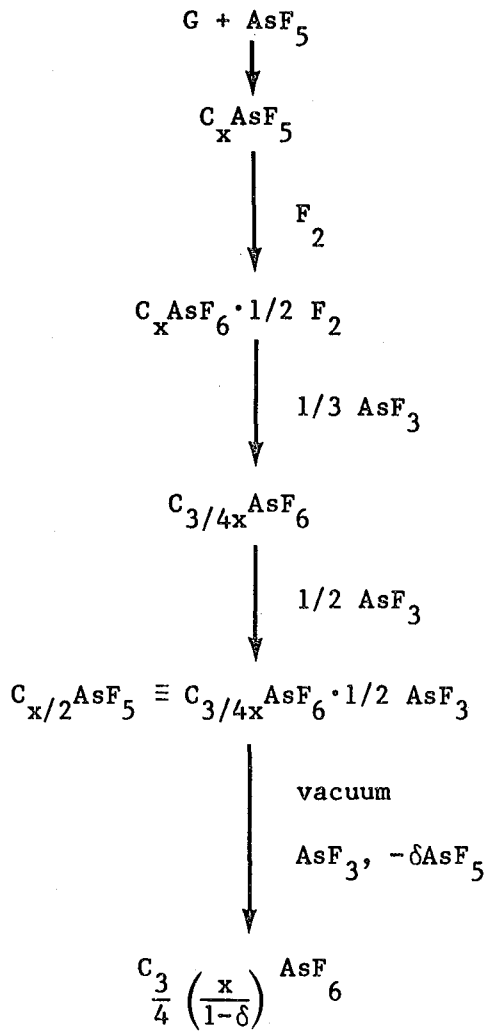

Figure VI-6. Generalized reaction scheme for graphite/AsF_5 systems with a mole ratio C/As = ($24 < x < 48$).

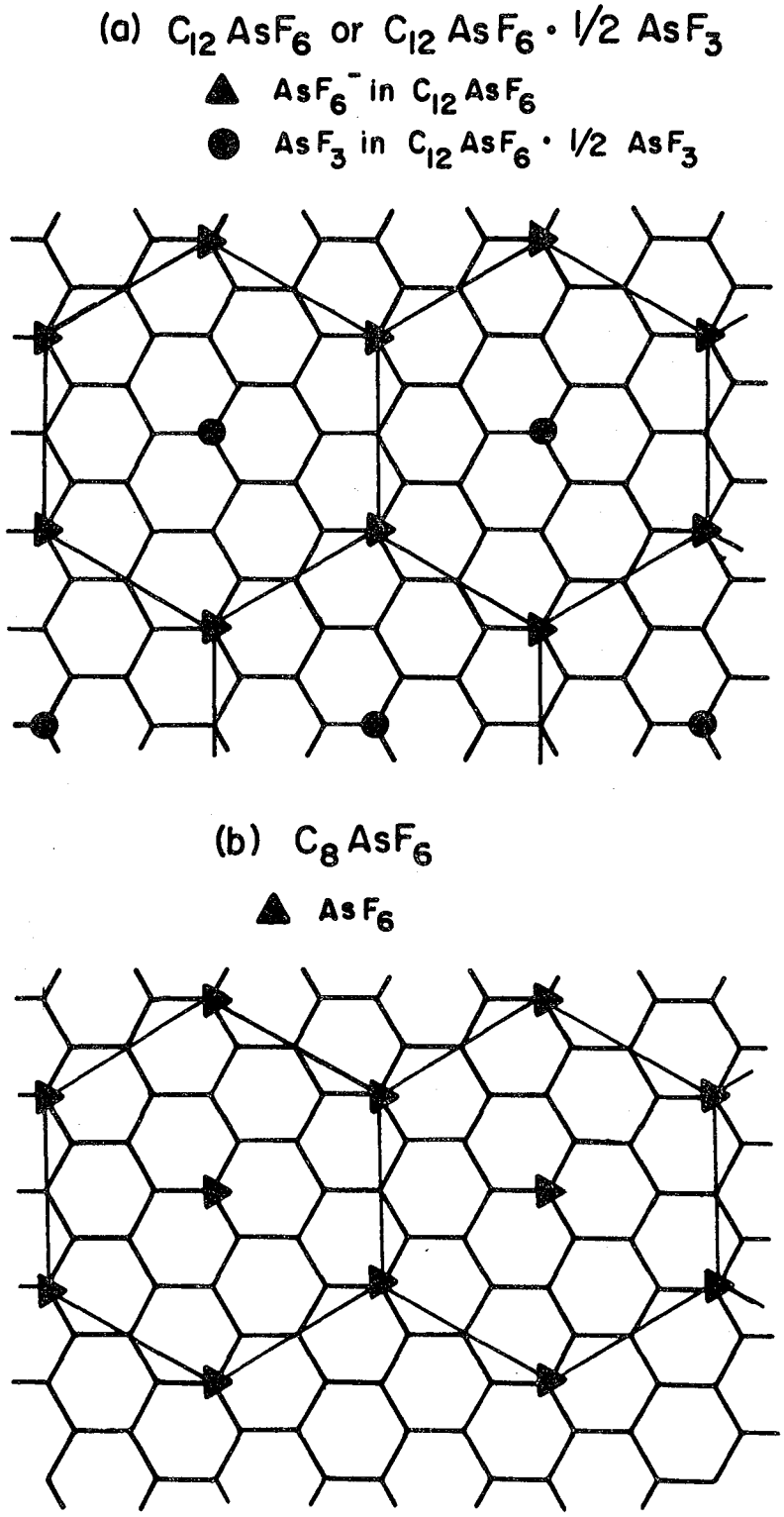

Figure VI-7. Structural models for (a) $C_{12}AsF_6$ or $C_{12}AsF_6 \cdot 1/2\ AsF_3$ and (b) C_8AsF_6.

CHAPTER VII

FLUOROGERMANIUM (IV) SALTS OF GRAPHITE--A SYSTEM IN EQUILIBRIUM WITH ELEMENTAL FLUORINE

A. Introduction

The observation that intercalated PtF_6 does not close-pack within the graphite galleries (Chapter III), as result, perhaps, of: (1) a prohibitive increase in the work function associated with oxidation of the graphite beyond C_6^+; and (2) a large increase in the electrostatic repulsion between doubly charged anions, led to a search for an analogous system.

It was seen in Chapter V that the Group V pentafluorides all reacted with graphite to produce first-stage salts, C_8MF_6. This was attributed to the large fluoride ion affinities of the Group V pentafluorides, MF_5 (M = P, As, Sb). It should be noted that all Group V hexafluoro-anions, MF_6^-, stabilize O_2^+.[1-3] O_2AsF_6 was shown to react (Chapter IV) with graphite

$$\text{Graphite} + O_2AsF_6 \rightarrow C_nAsF_6 + O_2\uparrow \qquad (1)$$

to give the hexafluoroasenate graphite salt with liberation of oxygen. This salt is an analogue of the hexafluoroplatinum-metal graphite salts, C_8MF_6 (M = Os, Ir).

Likewise, the high fluoride affinity of the Group IV tetrafluorides made them excellent candidates for producing a $C_{12}^{++}PtF_6^{=}$ analogue via,

$$\text{Graphite} + MF_4 + F_2 \rightarrow C_{12}MF_6 \quad . \qquad (2)$$

In particular, GeF_4 appeared to be an outstanding candidate, since GeF_4 is a superior fluoride ion acceptor. It stabilizes the O_2^+ ion[4] and NF_4^+ ion[5] in salts. Moreover, in the case of reaction of NOF with GeF_4,[6] by controlling the stoichiometry of the gas mixture, 1:1 and 1:2 adducts can be obtained ($NOGeF_5$ and $(NO)_2GeF_6$). That a dioxygenated salt[4] of germanium fluoride, O_2GeF_5, was known indicated that a graphite salt should be preparable:

$$\text{Graphite} + O_2GeF_5 \rightarrow C_nGeF_5 + O_2\uparrow \quad . \tag{3}$$

It also seems likely that the second fluoride affinity of GeF_4 would be sufficiently favorable to stabilize a $GeF_6^=$ salt. On the basis of the graphite hexafluoroplatinate study (Chapter III) a limiting composition, $C_{12}GeF_6$, seemed probable:

$$C_{12}GeF_5 + 1/2\ F_2 \rightarrow C_{12}GeF_6 \tag{4}$$

but how stable $C_{12}GeF_6$ would be relative to $C_{12}GeF_5$ and fluorine was an open question.

B. Experimental

1. Graphite/GeF_4

Graphite was not observed to react with GeF_4 gas at pressures up to 2 atmospheres at room temperature.

2. Graphite/GeF_4/F_2

i) Low Pressure F_2: Graphite, both powder ($\sim$1/2 gram) and HOPG ($\sim$30 mg), which was vacuum dried and pretreated with fluorine, was reacted at room temperature with GeF_4/F_2 gas mixtures. At no time did the total pressure within the reaction system exceed 1 atmosphere nor the partial

pressure of fluorine exceed 380 torr. The results of the reactions, followed by both gravimetry and tensimetry, are given in Table VII-1. The blue graphite salts which resulted had a stoichiometry of $C_{12}GeF_{5.5}$ and the value of the t/t_o ratio (Chapter VI) was 2.44. Fluorine uptake, by tensimetry, also suggested a GeF_4/F_2 ratio 4/3, consistent with a $C_{12}GeF_{5.5}$ stoichiometry. Pumping on $C_{12}GeF_{5.5}$ samples resulted in the loss of a noncondensible gas, with the resultant gravimetry suggesting $C_{12}GeF_5$:

$$C_{12}GeF_{5.5} \xrightarrow{\text{pump}} C_{12}GeF_5 + 1/4\ F_2 \quad . \qquad (5)$$

No infrared active species were detected in the volatiles removed by pumping (i.e., no GeF_4 loss).

ii) Higher Pressure F_2: Either placing a 2 atmosphere F_2 pressure over $C_{12}GeF_{5.5}$, or reacting graphite, either powder (~1/2 gram) or HOPG (~30 mg), with a GeF_4/F_2 gas mixture, in which the partial pressure of F_2 was maintained at 2 atmospheres (by placing a 1 liter ballast in the reaction system), produced, at room temperature, blue graphite salts of composition $C_{12}GeF_6$. Table VII-2 gives stoichiometric[7] and tensiometric data. The t/t_o value for this material measured using a traveling microscope so as to maintain the F_2 overpressure was 2.32.

Immediately upon removing this material to an ambient nitrogen atmosphere, $C_{12}GeF_6$ would lose mass slowly. Pumping on this material in a dynamic vacuum produced a material, $C_{12}GeF_5$, by stoichiometry. No GeF_4 was detected. The gas evolved was noncondensible at liquid nitrogen temperature. This presumed F_2 loss was accompanied by an expansion of t/t_o to 2.47. Moreover, reintroduction of a 2 atmosphere

overpressure of F_2 at room temperature, produced a mass increase consistent with again a composition, $C_{12}GeF_6$, and a t/t_o ratio decrease to 2.33. These facts indicate an equilibrium:

$$C_{12}GeF_6 \rightleftharpoons C_{12}GeF_5 + 1/2\ F_2 \quad . \tag{6}$$

iii) X-Ray Diffraction Studies: The x-ray diffraction results are depicted in Fig. 1. From the second-stage 00ℓ reflections obtained from a HOPG sample of composition, $C_{15}GeF_{5+\delta}$ (i.e., a sample containing both first-stage (75%) and second-stage (25%) components), the c-spacing listed below were obtained:

$C_{12}GeF_6$ - 7.80 Å

$C_{12}Ge_{5.5}$ - 8.10 Å

$C_{12}GeF_5$ - 8.23 Å

These c-spacing agree well with the observed t/t_o measurements:

	t/t_o(calculated)	t/t_o(measured)
$C_{12}GeF_6$	$\frac{7.80\ Å}{3.35\ Å} \cdot 2.33$	2.32
$C_{12}GeF_{5.5}$	$\frac{8.10\ Å}{3.35\ Å} \cdot 2.42$	2.44
$C_{12}GeF_5$	$\frac{8.23\ Å}{3.35\ Å} \cdot 2.46$	2.47

Comparison of this $C_{12}GeF_{5-6}$ diffraction data with diffraction data obtained for the graphite/MF_6 (M = Os, Ir, Pt) systems (Chapter IV) suggests that the following salt formulations hold:

$$C_{12}^{++}GeF_6^{=}$$

$$C_{12}^{1.5+}GeF_{5.5}^{1.5-} \equiv C_{24}^{3+}(GeF_6^{=} \cdot GeF_5^{-})$$

$$C_{12}^{+}GeF_5^{-}$$

Any correlation between the c-spacing and the charging (Coulombic attraction between guest and host) is necessarily complicated by the changing geometry of the guest anions, $GeF_6^{=}$ versus GeF_5^{-}.

3. $C_{12}GeF_5 + GeF_4$

$C_{12}GeF_5$, obtained as outlined in section 2.ii. above, was reacted with excess GeF_4 at room temperature. The results are given in Table 3. The reaction to produce $C_{12}GeF_5 \cdot 1/2\ GeF_4$[7] or $C_8GeF_{4.67}$ was facile. Subsequent pumping removed GeF_4 (identified by infrared spectroscopy) and restored the $C_{12}GeF_5$. Addition of GeF_4 had no perceptible effect on the t/t_o ratio of 2.47 of the parent $C_{12}GeF_5$.

4. $C_{12}GeF_5 \cdot 1/2\ GeF_4 + F_2$

Placing $C_{12}GeF_5 \cdot 1/2\ GeF_4$ (section 3) under 2 atmosphere pressure of F_2 at room temperature produced $C_{12}GeF_6$ (t/t_o = 2.33) with liberation of GeF_4 (identified by infrared spectroscopy) according to the equation:

$$C_{12}GeF_5 \cdot 1/2\ GeF_4 + 1/2\ F_2 \rightarrow C_{12}GeF_6 + GeF_4 \qquad (7)$$

5. $C_{12}GeF_5 + SiF_4$

$C_{12}GeF_5$ (section 2.ii.) underwent a facile reaction with SiF_4 at room temperature to produce $C_{12}GeF_5 \cdot 1/2\ SiF_4$. The details are given in Table VII-3.[7] No discernable effect on the t/t_o ratio of the HOPG sample with SiF_4 uptake was observed.

6. $C_{12}GeF_5 + SF_6$

$C_{12}GeF_5$ (section 2.ii.) underwent a sluggish reaction with 2 atmospheres SF_6 overpressure to produce $C_{12}GeF_5 \cdot 1/6\ SF_6$[7] (see Table VII-3) after 24 hours at room temperature. This material lost SF_6 to vacuum readily at room temperature.

C. Results and Discussion

Germanium tetrafluoride is a superior fluoride ion acceptor since it can stabilize the O_2^+ ion[4] and NF_4^+ ion[5] in salts. It is this superior fluoride-ion acceptor capability which must account for the observation that pyrolytic graphite readily intercalates GeF_4 in the presence of fluorine, but does not do so, even with high pressures of GeF_4, if fluorine is absent. Similar experiments, in which SiF_4 (see Chapter V) was substituted for GeF_4, failed to bring about any silicon fluoride intercalation. In has long been known[9] that GeF_4 is a superior fluoride ion acceptor to SiF_4 since, with SF_4, the former yields the salt $(SF_3^+)_2GeF_6^{2-}$, whereas the silicon analogue is not stable at ordinary temperatures and pressures (in spite of the lattice energy of the silicon analogue being slightly more favorable by virtue of the smaller size of SiF_6^{2-}).

Treatment of either powder or pieces of highly oriented pyrolytic graphite (HOPG), with GeF_4/F_2 mixtures, results in a GeF_4 uptake which is dependent upon the quantity of F_2 available. The quantity of F_2 determines the stage. A given $C_{12n}GeF_5$ stage takes up GeF_4 to reach a limiting composition $C_{12n}GeF_5 \cdot 1/2\ GeF_4$ (see Table VII-3). In a dynamic vacuum this material loses GeF_4, but not fluorine. Likewise, SiF_4 can be taken up to reach a limiting composition, $C_{12}GeF_5 \cdot 1/2\ SiF_4$ (see Table VII-3). The SiF_4 can subsequently be removed by pumping. In both the GeF_4 and SiF_4 containing materials, the possibility of fluorine bridging exists between GeF_5^- anions and neutral MF_4 species. Of course, the MF_4 may simply be occupying vacancies in the C_{12} - packing structure (see Fig. VII-2) with $C_{12}GeF_6 \cdot 1/2\ MF_4$ representing the packing limit, analogous to $C_{12}AsF_6 \cdot 1/2\ AsF_3$ (see Chapter VI). To distinguish between these two possibilities, SF_6 was similarly reacted, since there is no chance of fluorine bridging taking place with the inert SF_6 molecule. Apparently, $C_{12}GeF_5$ reacts sluggishly with SF_6 to fill approximately 1/3 of the vacancies, with a resultant composition, $C_{12}GeF_5 \cdot 1/6\ SF_6$ (see Table VII-3). The SF_6 is easily removed by pumping. Therefore, neutral species are presumed to occupy the vacancies.

When the F_2/GeF_4 ratio is 1:1 (at a total pressure of 2 atmospheres), the limiting composition of the graphite intercalate is $C_{12}GeF_6$ (see Table VII-2). But if the F_2/GeF_4 ratio is 1:1 but at a lower pressure (total pressure $\leqslant$ 1 atmosphere), the limiting composition is $C_{12}GeF_{5.5}$ (see Table VII-1). Also, if a first-stage material, which is richer in germanium than $C_{12}GeF_5$, is fluorinated, GeF_4 is eliminated and fluorine consumed to again yield $C_{12}GeF_6$:

$$C_{12}GeF_5 \cdot xGeF_4 + 1/2\ F_2 \rightarrow C_{12}GeF_6 + xGeF_4 \quad . \tag{8}$$

The first-stage material $C_{12}GeF_6$, at 20°, loses F_2 in a dynamic vacuum, but not GeF_4, to yield $C_{12}GeF_5$. The change is reversed by applying a 2 atmospheres pressure of fluorine at 20°, the consumption (by tensimetry) being appropriate for the conversion expressed in equation (9):

$$C_{12}GeF_{5(c)} + 1/2\ F_{2(g)} \rightarrow C_{12}GeF_{6(c)} \quad . \tag{9}$$

Similarly, $C_{12}GeF_{5.5}$ is intermediate between $C_{12}GeF_6$ and $C_{12}GeF_5$, resulting from a lowering of the fluorine partial pressure to less than 1/2 an atmosphere (see Fig. VII-1). These observations imply that the free-energy change for equation (9), at ~20°, is close to zero.

It is probable that the formulations for the graphite compounds are $C_{12}^{2+}GeF_6^{2-}$, $C_{12}^{1.5+}GeF_{5.5}^{1.5-}$ $\left[\equiv C_{24}^{3+}(GeF_6^{2-} \cdot GeF_5^-)\right]$ and $C_{12}^{+}GeF_5^-$. Note the preference to adopt a C_{12} packing within the graphite galleries for the germanium salts. Indeed, it is possible to achieve, theoretically, the same degree of oxidation of the carbon network with a C_8 packing of fluorogermanium anions via uptake of 1/2 mole of GeF_4, viz.:

$$\left[C_{12}^{2+}GeF_6^{2-} \equiv C_{24}^{4+}(GeF_6^{2-})_2\right] + 1/2\ GeF_4 \rightarrow$$

$$\left[C_{24}^{4+}\ (GeF_6^{2-})(GeF_5^-)_2 \equiv C_8^{4/3+}\ GeF_{5.33}^{4/3-}\right] \tag{10}$$

and

$$\left[C_{12}^{1.5+}GeF_{5.5}^{1.5-} \equiv C_{24}^{3+}(GeF_6^{2-})(GeF_5^-)\right] + 1/2\ GeF_4 \rightarrow$$

$$\left[C_{24}^{+3}(GeF_5^-)_3 \equiv C_8^+GeF_5^-\right] \qquad (11)$$

This preference for a C_{12} anionic packing must simply be Coulombic, since the site occupancy is more favorable for a C_{12} than a C_8 packing by a factor of 1/3 -- the nearest neighbor repulsions per anionic specie being equal for the two structures.[10] Therefore, if the experiments outlined in equations (10) and (11) were carried out, any GeF_4 consumed would be expected to simply occupy vacancies in the C_{12} structure as neutral GeF_4 to give $C_{12}GeF_6 \cdot 1/2\ GeF_4$ and $C_{12}GeF_{5.5}$ 1/2 GeF_4 [$\equiv C_{24}(GeF_6)(GeF_5)(GeF_4)$], respectively. Unfortunately, the vacuum instability of $C_{12}GeF_6$ and $C_{12}GeF_{5.5}$ as well as the expected instability of the products present some very challenging experimental difficulties. X-ray diffraction data, from intercalated HOPG pieces, show that the gallery height, "c", (i.e., the graphite-network to next graphite-network spacing) is 7.80 for $C_{12}GeF_6$ and 8.23 Å for $C_{12}GeF_5$, which is consistent with marked increase in the Coulombic attraction between guest and host for $C_{12}^{2+}GeF_6^{2-}$ compared with $C_{12}^+GeF_5^-$. The $C_{12}^{2+}GeF_6^{2-}$ formulation is related to that proposed for the limiting composition[11] of the PtF_6 intercalate, $C_{12}PtF_6$. The platinum salt, being diamagnetic, must be $C_{12}^{2+}PtF_6^{2-}$, which contrasts with the iridium hexafluoride limiting-composition salt which is $C_8^+IrF_6^-$.[11] The ordered structure for $C_{12}GeF_6$ is probably as indicated in the Figure VII-2. An ordered structure for

$C_{12}GeF_{5.5}$ $\left[C_{24}^{+3}(GeF_6^{=})(GeF_5^{-})\right]$ is proposed in Fig. 3. The gallery height for $C_{12}GeF_{5.5}$(8.10 Å) is intermediate between $C_{12}^{2+}GeF_6^{2-}$ and $C_{12}^{+}GeF_5^{-}$, which is consistent with a guest-host charging effect. But caution must be exercised with respect to any attempts to correlate the charging to the gallery height due to changes in anion geometries.

The remarkable equilibrium[2], must be a consequence of a close balancing of the fluoride ion affinities of GeF_4, the lattice energies of $C_{12}^{2+}GeF_6^{2-}$ and $C_{12}^{+}GeF_5^{-}$ and the work function of the graphite. There is no such equilibrium for $C_{12}PtF_6$, undoubtedly because of much higher stability of PtF_6^{2-}, compared with GeF_6^{2-}. Even PF_5, which is a poorer F^- acceptor than AsF_5, intercalates in graphite, in the presence of fluorine (see Chapter V), to yield at the limit C_8PF_6, but this, like its arsenic and transition metal analogues, is vacuum stable at ~20°.

Clearly $C_{12}GeF_6$ is a solid which must have an oxidizing and fluorinating capability close to that of elemental fluorine itself.

References

1. I. J. Solomon, R. I. Brabets, R. K. Uenishi, J. N. Keith and J. M. McDonough, Inorg. Chem. 3, 457 (1964).
2. A. R. Young, T. Hirata and S. I. Morrow, J. Amer. Chem. Soc. 86, 20 (1964).
3. a) J. Shamir and J. Binerboym, Inorg. Chem. 2 (1968), 37.
   b) J. B. Beal, C. Pupp and W. E. White, Inorg. Chem. 2, 828 (1969).
4. K. O. Christe, R. D. Wilson and I. A. Goldberg, Inorg. Chem. 15, 1271 (1976).
5. K. O. Christe, C. J. Schack and R. D. Wilson, Inorg. Chem. 15, 1275 (1976).
6. T. Mallouk and N. Bartlett, unpublished results; S. Kigoshi, Thermochim. Acta. 29, 147 (1979).
7. The stoichiometry of pressure sensitive materials (at room temperature) was determined by cooling the entire reaction vessel to -78°C and pumping off excess volatiles. The graphite/GeF_{5-6} materials themselves are stable to pumping at -78°C. Weighing the entire reaction vessel/ contents at room temperature then allows for a gravimetric determination of stoichiometry.
8. The staging formula is $C_{12n}GeF_{5-6}$ (n being the stage) (see Chapter VI). For $12 \leqslant x \leqslant 24$, the percentage of first and second stage are given by: $C_xGeF_{5-6} = (1 - (x-12)/12)C_{12}GeF_{5-6} + ((x-12)/12)C_{24}GeF_{5-6}$. Thus for x = 15; 75% $C_{12}GeF_{5-6}$ (first stage) and 25% $C_{24}GeF_{5-6}$ (second stage) are expected.
9. N. Bartlett and P. L. Robinson, J. Chem. Soc. 1961, 3417; and unpublished observations.

10. For example, the nearest neighbor repulsive terms for $C_{12}^{2+}GeF_6^{2-}$ and $C_8^{4/3+}\left[(GeF_6^{2-})(GeF_5^{-})_2\right]_{1/3}$ would be proportional to, respectively, 2/3[3 x 2 x 2i] and (1/2[6 x 2 x 1i] + 1/2[6 x 1 x 2j]); the ratio is simply that of site occupancy, 2/3:1, since repulsions per anion are equivalent for the two formulations (compare via Chapter VI, Fig. 4). The notation represents: site occupancy [(# of nearest neighbors) x (charge of nearest neighbor) x (charge of ith anion)].

11. N. Bartlett, E. M. McCarron, B. W. McQuillan and T. E. Thompson, Synthetic Metals 1, 221 (1980).

Table VII-1. Stoichiometry of Graphite Salts Intercalated with a GeF_4/F_2 -- Excess Mixture at Low Pressure (total pressure $\leqslant$ 1 atmosphere). $12C + GeF_4 + 3/4\ F_2 \rightarrow C_{12}GeF_{5.5}$.

GRAVIMETRY				
material	Initial Quantities (mmol) graphite	GeF_4	F_2 uptake (mmol) F_2	mmol F_2/mmol GeF_4
1) HOPG	4.75	0.40	0.30	0.75
2) HOPG	2.07	0.17	0.13	0.76
3) powder	35.37	2.94	2.20	0.75

TENSIMETRY				
	Uptake of Gases (measured as a pressure change, ΔP, in a constant volume at a fixed temperature)			
graphite (mmol)	ΔP GeF_4 (torr)	ΔP F_2 (torr)	ΔP $F_2/\Delta P$ GeF_4	CHN analysis
1) powder (34.91)	475	375	0.79	$C_{12.3}GeF_{5.5}$
2) powder (23.52)	320	240	0.75	$C_{12.1}GeF_{5.5}$

Table VII-2. Stoichiometry of graphitic salts intercalated with a GeF_4/F_2 -- Excess mixture at higher pressures (total pressure $\geqslant$ 2 atmospheres). $12C + GeF_4 + F_2 \rightarrow C_{12}GeF_6$.

GRAVIMETRY				
	Initial Quantities (mmol)		F_2 uptake (mmol)	
material	Graphite	GeF_4	F_2	mmol F_2/mmol GeF_4
1) HOPG	4.75	0.40	0.30	0.98
2) HOPG	2.07	0.17	0.17	1.00
3) Powder	35.37	2.94	2.96	1.01

TENSIMETRY				
	Uptake of Gases (measured as a pressure change, ΔP, in a constant volume at a fixed temperature)			
graphite (mmol)	ΔP GeF_4 (torr)	ΔP F_2 (torr)	ΔP $F_2/\Delta P$ GeF_4	CHN analysis
1) powder (34.91)	475	485	1.02	$C_{12.4}GeF_6$
2) powder (23.52)	320	320	1.00	$C_{12.2}GeF_6$

Table VII-3. Uptake of neutral molecules, MF_x, by $C_{12}GeF_5$ to form $C_{12}GeF_5 \cdot \delta MF_x$.

mmol $C_{12}GeF_5$	Reaction time	MFx uptake	$\frac{MF_x \text{ mmol}}{GeF_5 \text{ mmol}}$	volatiles removed under vacuum	(mmol)
3.13	10 min	GeF4 (1.57)	0.49	GeF4	(0.49)
2.84	1/2 hour	SiF_4 (1.42)	0.50	SiF_4	(0.48)
2.54	12 hours	SF_6 (0.97)	0.38	SF_6	(0.97)

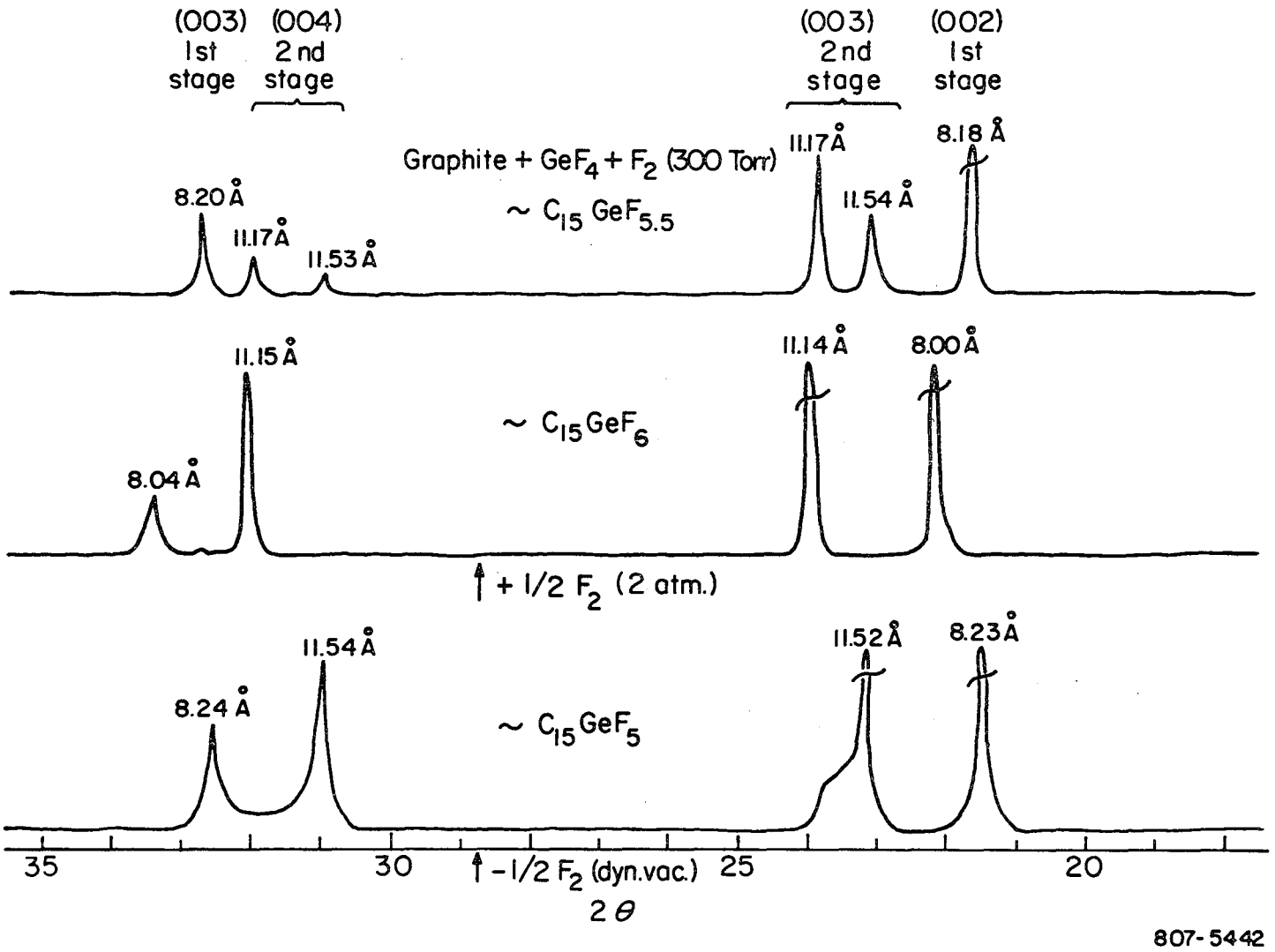

Figure VII-1. X-ray diffraction tracings of $C_{15}GeF_{5-6}$ as a function of fluorine content.

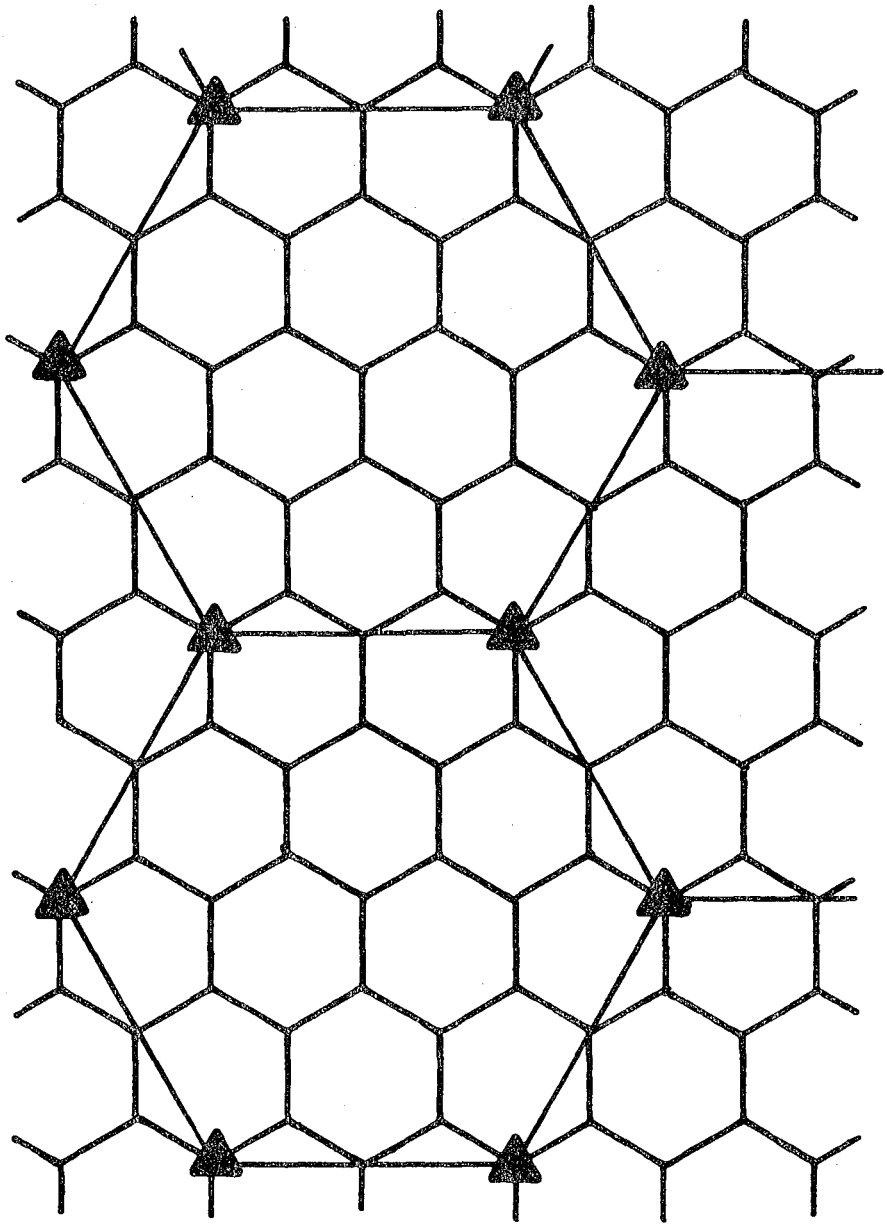

Figure VII-2. Proposed ordered structure for $C_{12}GeF_6$.

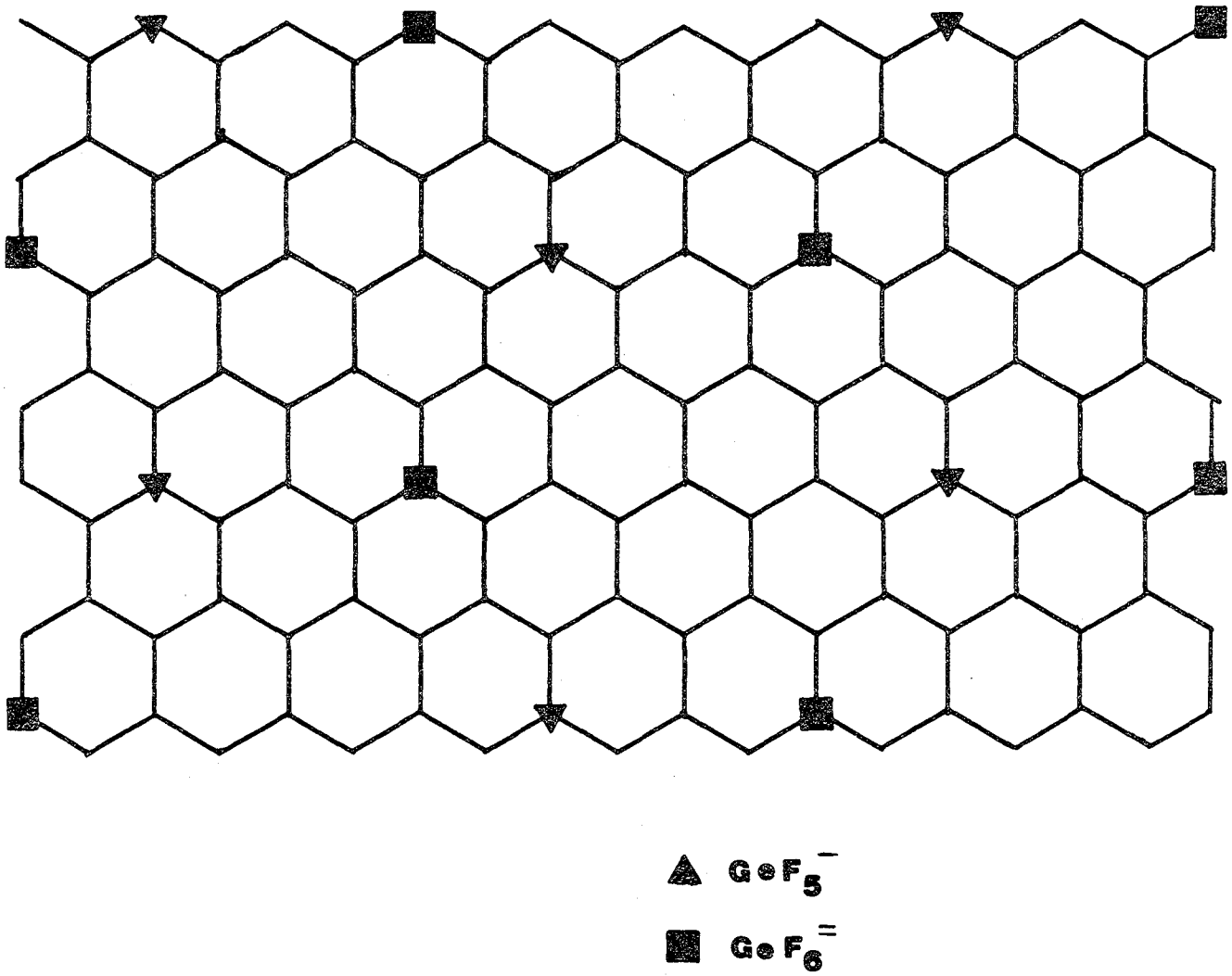

Figure VII-3. Proposed ordered structure for $C_{12}GeF_{5.5} \equiv C_{24}^{3+}(GeF_6^=)(GeF_5^-)$.

CHAPTER VIII

ELECTRICAL CONDUCTIVITIES OF NOVEL GRAPHITE SALTS

A. Introduction

The electrical transport properties of graphite are essentially those of a two dimensional semimetal; the conductivity being parallel to the basal plane ($\sigma_{ab} \sim 25\ (m\Omega - cm)^{-1}$).[1] Ubelhode proposed the term, synthetic metals,[2] to describe the enhanced electrical transport properties of graphite salts relative to the parent graphite. In 1977, Foley and coworkers[3] reported electrical conductivity for second-stage graphite/AsF_5 samples to be in excess of that for silver metal. Bartlett and coworkers,[4] and more recently Interrante and coworkers,[5] independently reinvestigated the graphite/AsF_5 system, and while the absolute value of the conductivities measured are lower by a factor of 2, the shape of the conductivity versus stage curve agrees quite well with that of Foley et al. These data are presented in Fig. VIII-1.

These plots of specific conductivity, σ, versus stage (Fig. VIII-1) obscure what may well be a simple basis for the enhanced conductivity of graphite in its salts.

With respect to specific conductivity, $\sigma(\Omega - cm)^{-1}$, the maximum in conductivity is found at the second stage, $C_{8n}AsF_5$ (n = 2). If allowance is made for the c-axis expansion, which accompanies intercalation, and the data in Fig. VIII-1 are now normalized[6] to give the conductivity per graphitic plane, k, and replotted (Fig. VIII-2), an approximately linear dependence of k upon 1/n (n being the stage) is observed. This implies that the normalized conductivity, k, is proportional to the intercalant, X, density per graphite plane,

$$k \propto \rho(X)_{GP} \quad . \tag{1}$$

In terms of the simple Drude model[7] of conductivity,

$$\sigma \propto n \times \mu \tag{2}$$

(where n is the number of charge carriers per unit volume and μ the carrier mobility), this implies that, for constant mobility, the intercalant density is directly proportional to the charge carrier density normalized per graphite plane,

$$\rho(X)_{GP} \propto n_{GP} \quad . \tag{3}$$

For graphite/acceptor salts, electron transfer from the graphite to the intercalating acceptor provides a carrier by creation of a hole in the filled π_{p_z} band of the graphite. In the case of unit charge transfer to the acceptor, X, equation (3) simply becomes an identity:

$$\rho(X)_{GP} \equiv n_{GP} \tag{4}$$

Hence, the conductivity ratios per graphite plane, k, for first-, second- and third-stage salts should be 1:1/2:1/3, respectively.

Therefore, if the contention of Bartlett and coworkers[8] is correct and AsF_5 oxidizes graphite according to the equation,

$$3AsF_5 + 2\bar{e} \rightarrow 2AsF_6^- + AsF_3 \tag{5}$$

$$\text{i.e., } \rho(AsF_5)_{GP} = 2/3\ n_{GP} \tag{6}$$

then first stage graphite/AsF_5, C_8AsF_5, is in fact $C_{12}^{+}AsF_6^{-}\cdot 1/2\ AsF_3$. Thus, one hole carrier is generated for every 12 carbon atoms. It seemed reasonable then that the graphite/AsF_5 conductivities would be exceeded by $C_8^{+}MF_6^{-}$(Os, Ir) and $C_{12}^{++}PtF_6^{=}$ since the formal charge on the carbon, hence, the carrier density, is greater. But caution must be exercised, since constant mobilities are being assumed.

Moreover, if the model proposed for graphite/AsF_5 is correct, namely, $C_{12n}^{+}\ AsF_6^{-}\cdot 1/2\ AsF_3$, it should be possible to remove AsF_3 (for $n \geqslant 3$, see Chapter VI) without grossly changing the conductivity of the sample, if k is indeed simply related to the charge transfer. In other words, an equivalence of the conductivity for $C_{12n}MF_6$ and $C_{8n}MF_5$ is expected, providing there is no change in carrier mobility.

B. Experimental

1. General Conductivity Measurement

i) Sample Preparation: Blocks of HOPC approximately 5 x 5 (ab) x 1 mm were cleaved and abraided from larger sheets for use in the conductivity studies. Except for the work with PtF_6, it was usual for the intercalation to be carried out in a quartz tube with a Monel Whitey valve provided with Swagelok compression fittings with teflon ferrules. Weighing of this assembly before and after the intercalation gave a composition, but in the first experiments in each series the gravimetric composition was always checked by elemental analysis. In the PtF_6 experiments, weighed graphite was exposed overnight to PtF_6, or to $O_2^{+}PtF_6^{-}$, in a Monel can provided with a teflon-gasketed lid. Since all of the intercalates were unstable in moist air they were all handled in the dry atmosphere of a Vacuum Atmospheres Corporation Dri-Lab.

ii) Electrical Conductivity Measurements: Measurements of basal plane electrical conductivities was made by the contactless radio frequency inductive technique recently described by Zeller, Denenstein and Foley,[9] and illustrated in Fig. II-6. For this purpose HOPG was cut into pieces each roughly square, approximately of 5 mm edge and 0.5 mm thickness (along the c-axis). The graphite was compared with a calibrated copper standard of nearly the same size. The induced eddy current was sensed ion a secondary circuit and the conductivity was derived from the empirically evaluated relationship $\Delta V = K\,(\text{area})^2 t \cdot \sigma$, where ΔV represents a voltage change, t the thickness of the sample, σ the specific conductivity, area the ab-plane area, and K the proportionality constant. With the arrangement represented in Fig. II-6 it was possible to monitor the conductivity of a sample in the course of intercalation. It was possible, by detaching and weighing the tube (complete with valve) containing the sample, to check the composition gravimetrically. Moreover, a traveling microscope (with the sample in place) or a micrometer (with the sample in the Dri-Lab) were used to determine the thickness of the sample. Occasionally a sample was subjected to an x-ray diffraction scan to determine which stage or stages were present. See also Chapter II, Section 8.

2. Graphite/MF_6 (M = Os, Ir) Conductivities

The vacuum dried graphite (HOPG pieces), in its quartz container was exposed to either OsF_6 or IrF_6 vapor (at 15 and 11 torr, respectively) at ~25°. In each case, the conductivity increased rapidly with MF_6 uptake as represented in Fig. VIII-3 and attained a maximum value somewhat above the MF_6 content appropriate for a second stage material (i.e.,

$C_{24}MF_6$). The ratio of the thickness of the sample to that of the original graphite, and the gravimetry, are consistent with a mixed phase which is 25% first and 75% of the second stage at this point of maximum conductivity. The occasional x-ray diffraction evidence also supports this. At this position of maximum conductivity there was a marked slowing in the rate of intercalation of MF_6 and an increase in pressure (to ~200 torr) of the intercalant was required to bring about renewal of MF_6 uptake. This renewed MF_6 uptake appears to be coincident with the development of a first stage material. There was detectable exothermicity, occasionally the sample, which had remained intact to this point, cleaved. The most dramatic effect, however, was the decrease in conductivity, which became progressively lower, with MF_6 uptake, beyond this point. It was also observed that whereas a steady value for the conductivity was quickly obtained (usually within one minute or so) at all compositions up to $C_{24}MF_6$, for MF_6 incorporation richer than $C_{24}MF_6$, (and in association with the catastrophic conductivity decrease) the conductivity value became markedly time dependent. Data are given in Table VIII-1. Thus for a composition $C_{13}MF_6$ the conductivity would continue to decrease significantly over a period of several hours.

3. Graphite/PtF_6 Conductivities

The conductivity work for Graphite/PtF_6 was hampered by two factors. First, the highly reactive nature of PtF_6 complicated the gravimetric work and although x-ray data provided a convenient check on the stage produced, it was not possible to determine the extent of the gallery occupancy. Secondly, the reaction of PtF_6 with HOPG is extremely slow. This is probably a consequence of the double-charged PtF_6^{2-} anion

having a low mobility relative to singly charged species (OsF_6^-, IrF_6^-). An HOPG/PtF_6 sample with the composition $C_{12}PtF_6$ has not yet been prepared; this limit having been achieved with graphite powder. Yet even in second stage ($C_{24}PtF_6$) material, low (ab-plane) conductivities have been observed (Table VIII-1). This is in contrast with the OsF_6 and IrF_6 results.

4. Graphite/AsF_6 versus Graphite/AsF_5 Conductivities

Measurements of the conductivities of $C_{8n}AsF_5$ (n being the stage) were made prior to those recently reported by Interrante and coworkers[5] and agree quite well. Unlike the graphite/MF_6 (M = Os, Ir) cases which display a conductivity per graphite plane, k, maximum at the second stage followed by a catastrophic decrease in conductivity as the first-stage composition, C_8MF_6, is approached (see Fig. VIII-3), the conductivity per plane of graphite is observed to increase smoothly up to the second-stage limiting composition of $C_{16}AsF_5$ (with a slight departure from linearity at the first stage, C_8AsF_5 (see Fig. VIII-2). Conversion of C_8AsF_5 to C_8AsF_6 by treatment of the former with fluorine gas at ~25° (2 atmospheres pressure) until the sample no longer consumed it, led to a marked drop in conductivity as shown by the data given in Table VIII-1. On the other hand, a sample of HOPG of composition $C_{24}AsF_6$, prepared by treating the graphite with a AsF_5/F_2 mixture, exhibited a graphite plane conductivity close to a the maximum value observed in the OsF_6 and IrF_6 systems.

In accord with the experimental results presented in Chapter VI, simple loss of AsF_3 from $C_{8n}AsF_5$ ($n \geqslant 3$) to form the corresponding $C_{12n}AsF_6$ salt did not significantly change the conductivity nor did the

reintroduction of AsF_3 (again generating $C_{8n}AsF_5$). The data are listed in Table 2. For $C_{8n}AsF_5$ ($n < 3$) loss of AsF_5 (along with AsF_3) resulted in a drop in the conductivity per graphite plane, k. Along with this conductivity drop, loss of AsF_5 produced a decrease in the ratio of t/t_o (see Table VIII-2).

C. Results and Discussion

The ab-plane electrical conductivity data are presented in Table VIII-1. The conductivity per plane of graphite relative to the conductivity of a plane of the parent graphite, as a function of iridium hexafluoride uptake, is shown in Fig. VIII-3 (the behavior for OsF_6 intercalation is essentially the same). With the pressures of OsF_6 and IrF_6 used in this work, all HOPG tablets quickly, and with proper MF_6 uptake, assumed the thickness appropriate for a second stage (i.e., $t/t_o \sim 1.7$). The uptake of MF_6 but slowed significantly after the second stage composition was attained. Up to this point (see Fig. VIII-3) the conductivity per plane increased. Note from Table VIII-3 that the conductivity is approximately the same for the IrF_6 and OsF_6 systems close to $C_{20}MF_6$. To carry the intercalation towards the first stage it was necessary to increase the pressure of the intercalant. This had to be done with caution since the change to a first stage material, once initiated, proved to be a highly exothermic process and extensive cleavage could then occur. For both the OsF_6 and the IrF_6 systems the conductivity dropped catastrophically with MF_6 uptake beyond $C_{24}MF_6$. Indeed, for MF_6^- salts, formation of first-stage material appears to be associated with decreased conductivity. With PtF_6^{2-} salts however, even second stage $C_{24}^{2+}PtF_6^{2-}$ is a poor conductor. Therefore, poor conductivity is

associated with high positive charge in the graphite sheets. No doubt the cooperative effect of two anions (one on each side of the graphite sheet) or the double charge of an MF_6^{2-} ion is more likely to localize high positive charge at a carbon atom than a single MF_6^-. Positively charged carbon atoms will tend to be boron-atom like and will make more bonds than the neutral atoms and this probably leads to distortion from the regular trigonal graphite net. Thus the structure for C_8MF_6, shown in Fig. VIII-4 may not be the stable one. Indeed this may account for the loss of long-range order initially observed in single crystals of C_8MF_6 (see Chapter VI). A structural change, involving distortion of the graphite sheets and slow relocation of the MF_6^- species, would also account for the observation that the conductivity of first-stage materials, at constant composition, decreased steadily over a period of several hours. This fits in with the time scale for the apparent loss of long-range order in the single-crystal diffraction studies previously alluded to (see Chapter VI, section C.2).

The comparison of the graphite/AsF_5 with the graphite/AsF_6^- system is particularly interesting. We have found that it is possible to convert incompletely-intercalated first-stage graphite/AsF_5 to its AsF_6^- counterpart, by treating the former with fluorine gas. In this way a sample of composition $C_{12.7}AsF_5$ was converted to $C_{12.7}AsF_6$. The excellent conductivity of the former was replaced by a conductivity more like that of the first stage OsF_6^- and IrF_6^- salts and not very different from that of graphite itself. This could mean that the conversion represented by equation (5) is not extensive and that the continuous increase in conductivity per plane of graphite on intercalation, up to and

including the first stage, is simply a consequence of the concentration of charged guests never being high enough to produce large charge localization effects. In the face of other evidence,[10] however, another explanation may apply. The coexistence of AsF_3 with AsF_6^- (and even some AsF_5) within the galleries is more likely to result in a less ordered and less periodic charge distribution than in the MF_6^- cases. Thus it may be that the guest species in graphite/AsF_5 are never in commensurate register with the graphite lattice. Indeed it may even be that the MF_6^- anions in second-stage $C_{24}MF_6$ are not commensurate with the graphite sheet either.

Whereas some doubt remains as to the exact nature of the graphite-intercalant electronic interactions (possibility of charge localization) in first-stage graphite/AsF_5 materials, second and higher stages are well behaved. For $C_{8n}AsF_5$ ($n \geqslant 3$) the observation that only AsF_3 is removed with pumping (see Table VI-2) implies that equation (5) is completely to the right. Hence, the materials can be viewed as $C^+_{12n}AsF_6^- \cdot 1/2\ AsF_3$ ($n \geqslant 3$) salts, with neutral AsF_3 occupying 1/3 of the sites in a graphite hexafluoroarsenate salt structure (Chapter VI - Fig. VI-8). Simple removal of AsF_3 neither significantly changes the conductivity nor the ratio of t/t_o (see Table VIII-2). This is in agreement with the conductivity being dependent on the charge transfer for high stage compounds.

For lower stage compounds, $C_{8n}AsF_5$ ($n = 1$ or 2), AsF_5 (along with AsF_3) is removed by pumping on these materials. Loss of AsF_5 is reflected in a decrease in the conductivity per graphitic plane along with a decrease in the t/t_o ratio. This loss of AsF_5 is equated with decreasing the number of hole carriers (h_G^+) in the graphite network:

$$2\ AsF_6^- + AsF_3 + 2h_G^+ \rightarrow 3\ AsF_5 \quad . \qquad (7)$$

Thus the loss of AsF_5 decreases the conductivity per plane since the hole carrier population is reduced by 2/3 h_G^+ per AsF_5 molecule removed. Likewise, the decrease in t/t_o with AsF_5 removal results from a degradation of the $C_{12n}^+AsF_6^-$ salt 'backbone' (2/3 AsF_6^- per AsF_5; equation (7)). The low stage material is driven toward a higher stage by the AsF_5 loss (see Chapter VI, Figure VI-3).

Finally, whereas C_8AsF_5 has a high k (Fig. VIII-2) and $C_{12}AsF_6$ an order of magnitude lower k (Table VIII-1), addition of AsF_3 to $C_{12}AsF_6$ does not appreciably change the k value:

$$C_{12}AsF_6 + 1/2\ AsF_3 \rightarrow C_8AsF_5 \quad . \qquad (8)$$

Hence, there exists two chemically equivalent yet electronically different first-stage graphite/AsF_5 materials. This fact lends support to the previously discussed disorder phenomena, since disorder would tend to be found in the simple graphite + AsF_5 reaction. Therefore, it must be assumed that in the $C_{12}AsF_6$ case, once order is established, promoting charge localization (decreased mobility (equation (2)), introduction of AsF_3 will not upset that order to give high conductivity. Gentle heating of the low conductivity C_8AsF_5 to induce disorder, hence high conductivity, has not as yet been performed.

References

1. I. L. Spain, Chemistry and Physics of Carbon, P. L. Walker and P. A. Thrower, eds., Marcel Dekker Inc., N. Y., 1973.

2. A. R. Ubbelhode, Nature 210, 404 (1966).

3. G. M. T. Foley, C. Zeller, E. R. Falardeau and F. L. Vogel, Solid State Commun. 24, 371 (1977).

4. N. Bartlett, R. Biagioni, B. McQuillan, A. S. Robertson and A. C. Thompson, J. C. S. Chem. Comm., 200 (1978).

5. L. V. Interrante, R. S. Markiewicz and D. W. McKee, Syn. Metals 1, 287 (1980).

6. The curve which is observed when specific conductivity is plotted versus stage (Fig. VIII-1) is simply a result of the expansion of the graphite along c with increasing intercalant density (lower stage). The expansion reduces the number of graphite planes per unit volume while the number of charge carriers per plane increases. For first, second, and third stages the number of planes per unit area are in the ratio $(t/t_o)_n^{-1}$ $[(2.40)^{-1}:(1.71)^{-1}:(1.47)^{-1}]$ while the charge carriers per plane are in the ratio 1/n [1, 1/2, 1/3]. So the conductivity per plane would be 1:1/2:1/3, resp., while the specific conductivity ratio would be 1:0.71:0.55, resp., since $\sigma_n = k_n \times (t/t_o)_n^{-1}$.

7. P. Drude, Annalen der Physik 1, 566 (1900), and 3, 369 (1900).

8. N. Bartlett, E. M. McCarron, B. McQuillan and T. E. Thompson, Synthetic Metals 1, 221 (1980).

9. C. Zeller, A. Denenstein and G. M. T. Foley, Rev. Sci. Inst. 50, 602 (1979).

10. N. Bartlett, R. N. Biagioni, E. M. McCarron, B. W. McQuillan and F. L. Tanzella, Molecular Metals, W. E. Hatfield, Ed., Plenum Pub. Corp., N.Y., p. 293 (1979).

Table VIII-1. Composition and electrical conductivity data for HOPG/MF_6 and HOPG/AsF_5/F_2 intercalates.

Sample	Composition (Gravimetric)	σ/σ_G †	t/t_o ‡	k^{**}/k_G	Comments
1	C_xOsF_6	8.0	----	13.7	conductivity maximum
	$C_{9.9}OsF_6$	1.0	2.48	2.4	deep blue
2	$C_{19.3}OsF_6$	8.2	2.00	14.0	deep blue
	$C_{11.6}OsF_6$	1.3	2.45	3.1*	deep blue
3	C_xIrF_6	6.2	----	10.6	conductivity maximum
	$C_{8.0}IrF_6$	1.2	2.41	2.9	deep blue
4	$C_{21.0}IrF_6$	8.0	1.81	13.7	deep blue
	$C_{8.1}IrF_6$	0.6	2.68	1.5*	deep blue
5	$C_{8.1}IrF_6$	0.4	2.45	1.0*	deep blue
6	$C_{10.6}IrF_6$	0.6	2.41	1.4*	deep blue
7	$C_{30}PtF_6$	1.0	1.68	2.4	green-blue
8	$C_{24}PtF_6$	0.8	2.00	1.3	green-blue
9	$C_{16.0}AsF_5$	11.7	1.96	20.0	steel blue
	$C_{12.7}AsF_5$	11.3	2.41	28.2	steel blue
	$C_{12.7}AsF_6$	0.5	2.41	1.2*	fluorinated deep blue
10	$C_{20}AsF_5$	9.7	1.85	16.6	
	$C_{11}AsF_6$	2.2	2.48	5.2*	addition of $AsF_5 + F_2$
	$C_{7.8}AsF_6$	1.5	2.48	3.7*	addition of $AsF_5 + F_2$

*denotes the time dependent values. Samples 5 + 6 are representative of $t = \infty$ values for conductivity (~3 weeks). Multiple entry samples are approx. time = 12 hrs.

† $\sigma_g = (26 \pm 3) \times 10^3 \Omega^{-1}\ cm^{-1}$.

‡ t represents the thickness of sample and t_o the thickness of the HOPC piece from which it was derived; 1st stage $t/t_o \sim 2.4$, and 2nd stage $t/t_o \sim 1.7$.

**Specific conductivity normalized per plane of graphite, simply $(\sigma/\sigma_g \times t/t_o) = k/k_G = \Delta V_{sample}/\Delta V_{graphite}$.

Table 2. Effect on the per plane conductivity, k, with the removal/addition of arsenic-containing species from Graphite/AsF5-6 materials.

initial material stoichiometry t/t_o*; k/k_G†	volatiles lost to vacuum	resulting material	after addition of AsF_3	after removal of AsF_3	after AsF_3 addition
1) $C_{15.8}AsF_5$	$AsF_3 > AsF_5$	$C_{27.2}AsF_6$	$C_{18.1}AsF_5$	$C_{28.1}AsF_6$	$C_{18.1}AsF_5$
1.76; 22.3		1.67; 19.0	1.71; 19.7	1.69; 19.6	1.70; 19.3
2) $C_{22.9}AsF_5$	$AsF_3 \gg AsF_5$	$C_{36.6}AsF_6$	$C_{24.4}AsF_5$	$C_{39.2}AsF_6$	$C_{26.4}AsF_5$
1.53; 18.9		1.49; 18.7	1.51; 18.7	1.44; 17.8	1.48; 16.7
3) $C_{24.8}AsF_5$	AsF_3	$C_{37.2}AsF_6$	$C_{25.4}AsF_5$	$C_{37.2}AsF_6$	$C_{25.0}AsF_5$
1.48; 18.3		1.46; 17.5	1.48; 17.9	1.43; 17.2	1.48; 16.3

*t represents the thickness of sample and t_o, the thickness of the HOPG piece from which it was derived; 2nd stage, $t/t_o \sim 1.71$; 3rd stage, $t/t_o \sim 1.47$.

†Specific conductivity normalized per plane of graphite, simply $(\sigma/\sigma_G \times t/t_o) = k/k_G = \Delta V_{sample}/\Delta V_{graphite}$.

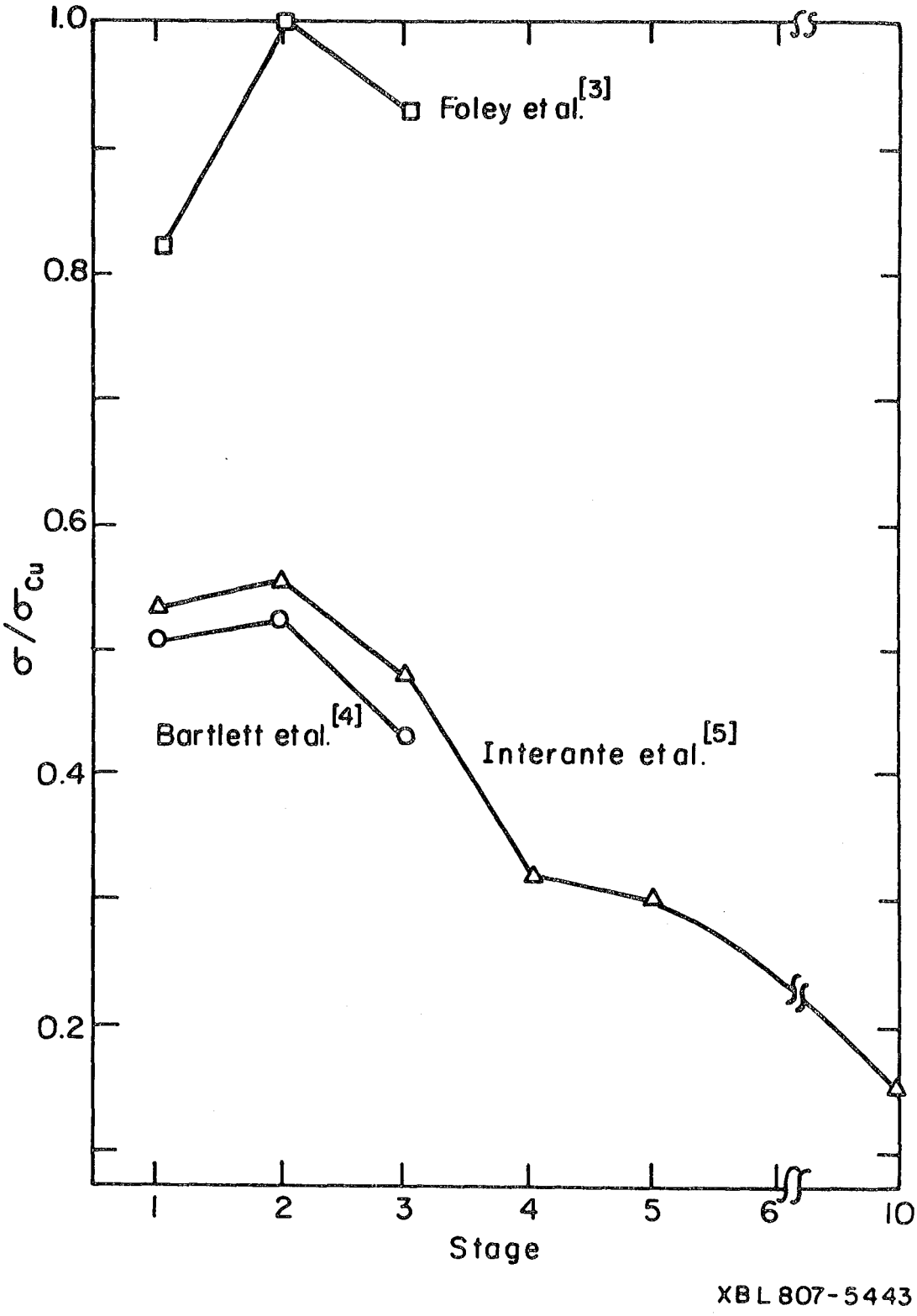

Figure VIII-1. Plots of specific conductivity, σ, versus state, n, for $C_{8n}AsF_5$.

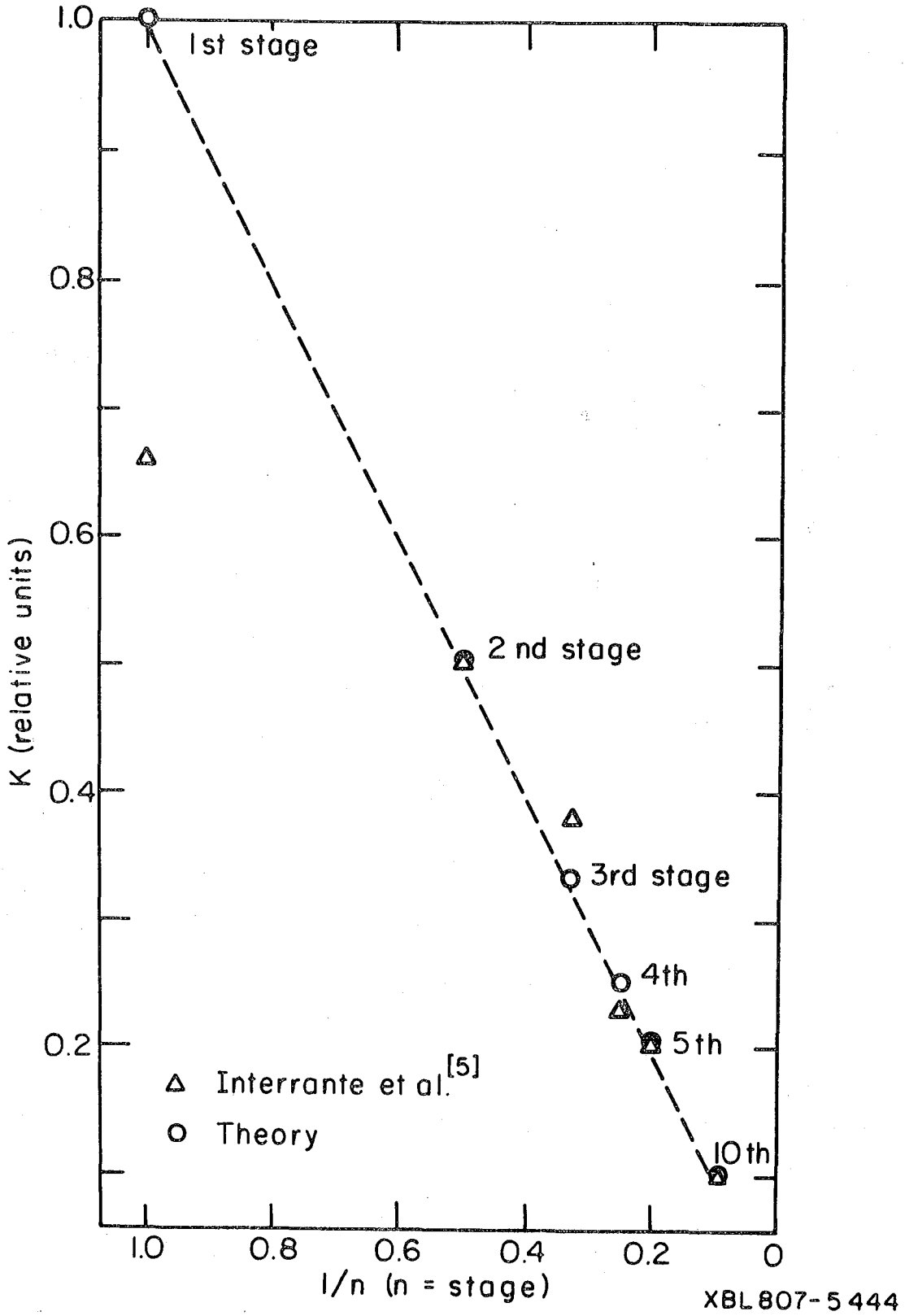

Figure VIII-2. Plots of the conductivity per graphite plane, k, versus 1/n (n = stage) for $C_{8n}AsF_5$.

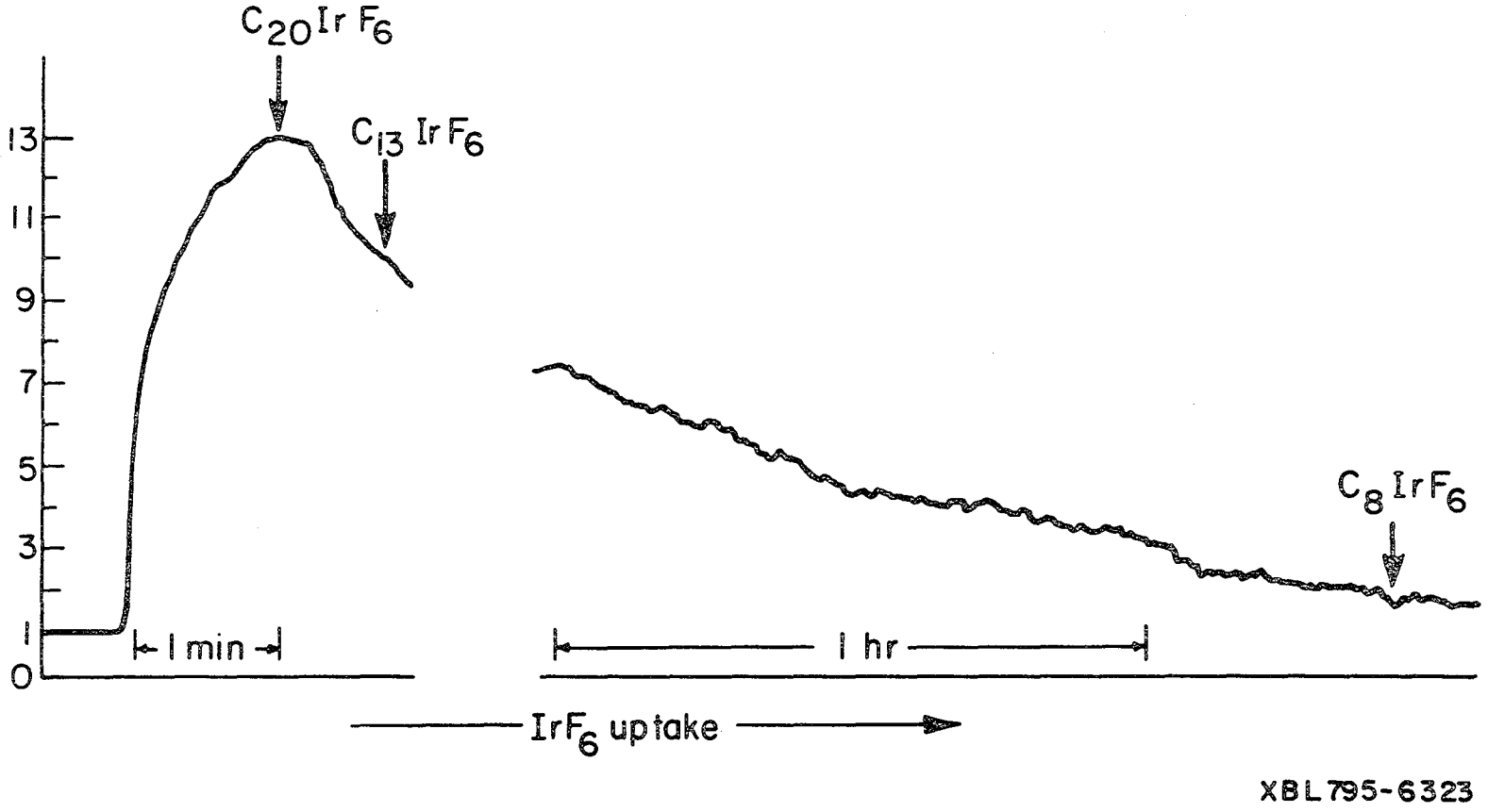

Figure VIII-3. Response of conductivity of HOPG-IrF_6 intercalates as a function of IrF_6 uptake.

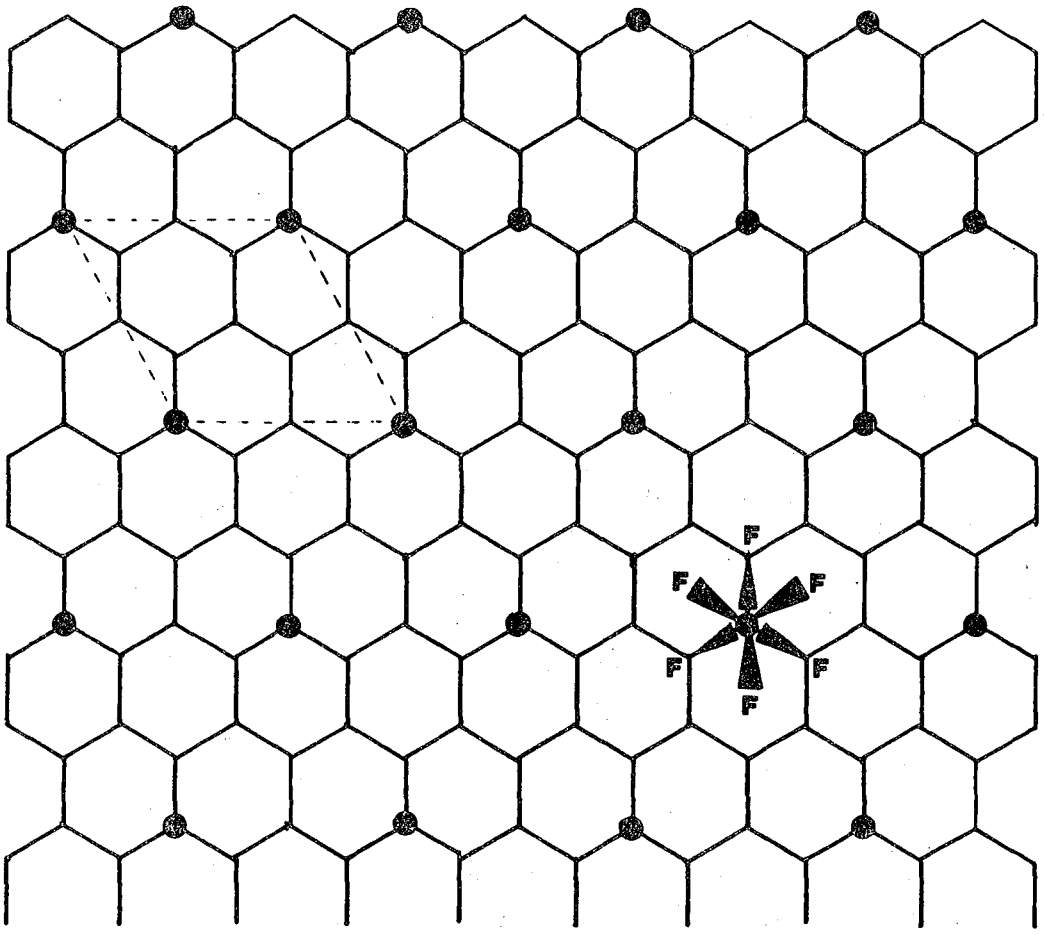

Figure VIII-4. Projection of the C_8MF_6 (M = Os, Ir, As) unit cell in relation to the graphite lattice.

CHAPTER IX

A POSSIBLE ELECTRICAL-ENERGY-STORAGE BATTERY UTILIZING GRAPHITE SALTS

A. Introduction

Ubbelohde in 1966 pointed out[1] that when graphite is intercalated by anions of strong acids (i.e. oxidized with incorporation of HSO_4^-, ClO_4^-, etc.) the in-plane conductivity of the graphite is greatly increased and the graphite becomes a good metal. By exploiting powerful oxidizers such as[2] $O_2^+MF_6^-$, $C_6F_6^+MF_6^-$, the third transition series hexafluorides,[3] MF_6 (M = Os, Ir, Pt), and strong fluoride ion acceptors in combination with elemental fluorine[4] (e.g. AsF_5 + 1/2 F_2; PF_5 + 1/2 F_2 and GeF_4 + F_2) Bartlett and his coworkers have now extended this series of compounds.

The salts of formulation $C_x^+MF_6^-$ or $C_y^{2+}MF_6^{2-}$ conduct electricity at least as well as graphite and when x is ~24 the $C_x^+MF_6^-$ salts are good metals.[3] These materials are therefore suitable for application as electrodes and since the salts can be reduced, and again oxidized, (e.g.,

$$C_{24}^{3+}(AsF_6^-)_3 + 3e^- \rightarrow C_{24}^{2+}(AsF_6^-)_2AsF_3 + 3F^-) \qquad (1)$$

without loss of guest and without gross change in the gallery spacing, the expansion and contraction ("concertina effect") is minimal.

B. Fluoride-Ion Conductors

In particular, fluorides with the CaF_2-type structure have been investigated. In this structure, there exists a central vacancy which facilitates fluoride ion diffusion. Conductivities at 20°C and 150°C and also activation energies for some recently studied fluorides are listed in Table IX-1.

C. Solid Galvanic Cells

1. Experimental

The galvanic cells studied were constructed as shown in Fig. IX-1. The cells consisted of a sandwich of two electrodes with the solid electrolyte in between. $Pb_{0.75}Sb_{0.25}F_{2.25}$ was chosen as the electrolyte since it is both an acceptable ionic conductor and is thermodynamically stable with respect to the graphite intercalation compounds. The anodes used were either a mixture of Sb metal and $Pb_{0.75}Sb_{0.25}F_{2.25}$ powder or C_xSbF_5. The following cathodic materials were studied: C_xIrF_6, C_xPtF_6, $C_{11.5}AsF_5$, C_xSbF_5 and C_xSbF_6. In the Ir, Pt, and Sb fluoride intercalation compounds it was assumed that the limiting compositions had been reached (x = 8, 12, 8, respectively), although the actual compositions were not determined. C_xSbF_6 was produced according to the equation:

$$C_xSbF_5 + 1/2\ F_2\ (2\ atm) \rightarrow C_xSbF_6$$

The voltages were measured with a Keithley 210 electrometer possessing a high input impedence ($\simeq 10^{-10}\Omega$). The measurements were done at both 25°C and 60°C.

2. Results

The voltages obtained with the various galvanic cells are shown in Table IX-2. The supposed electrochemical reactions are given for each electrode system studied.

$\underline{SbC_xIrF_6}$

$$Sb + 3/y\ C_xIrF_6 \rightarrow SbF_3 + 3/y\ C_xIrF_y$$

In this and all following studies the resultant graphitic materials were not analyzed. Although the reaction scheme is probably correct, diffraction studies are needed.

Sb/PtF_6

$$Sb + 3/y\ C_xPtF_6 \rightarrow SbF_3 + 3/y\ C_xPtF_y$$

Sb/$C_{11.5}AsF_5$ and Sb/C_xSbF_5

The electrochemical reactions are probably as follows:

$$2Sb + 3C_{11.5}AsF_5 \rightarrow 2SbF_3 + 3C_{11.5}AsF_3$$

$$2Sb + 3C_xSbF_5 \rightarrow 2SbF_3 + 3C_xSbF_3$$

The corresponding voltages are close to those calculated approximately from the available thermodynamic data on the molecular arsenic and antimony pentafluorides (see Table IX-2).

$$Sb/SbF_5 \simeq 0.7\ v$$

$$Sb/AsF_5 \simeq 1.0\ v$$

This coincidence of observed and calculated voltages implies low thermodynamic stability for the intercalates. This fits the facile loss of guest molecules to vacuum in both C_xAsF_5 and C_xSbF_5.

C_xSbF_5/C_xSbF_6 and Sb/C_xSbF_6

The first case represents a concentration cell:

$$C_xSbF_5 + C_xSbF_6 \rightarrow C_xSbF_{5.5}$$

but for the second the net reaction is:

$$Sb + C_xSbF_6 \rightarrow SbF_3 + C_xSbF_3$$

It should be noted here that the voltage predicted by joining the couples Sb/C_xSbF_5 and C_xSbF_5/C_xSbF_6 (0.850 v + 0.480 v = 1.330 v) is not far from the observed value for Sb/C_xSbF_6 (1.510 v).

$\underline{C_xSbF_5/C_xSbF_5}$

Obviously the voltage obtained is zero. But after applying a voltage of 5 volts to the cell, a very stable voltage of 1.525 volts corresponding to the previous cell was observed, suggesting that the following reactions had occurred:

(positive pole) $\quad C_xSb^{V}F_5 + 1/2\ F_2 \rightarrow C_xSb^{VI}F_6$

(negative pole) $\quad C_xSb^{V}F_5 \rightarrow XC + Sb^{0} + 5/2\ F_2$

This experiment indicates that the cells studied are reversible.

3. Discussion

This study can be compared to previous studies[5] (see Table IX-3). The voltage obtained in the case of the Sb/SbF_6 cell is the highest ever obtained in such cells. The present study demonstrates the superiority of the $C_x(MF_6)$ compounds over the graphite fluoride, $(CF)_n$ (Table IX-3) which is thermodynamically more stable and consequently less oxidizing. Furthermore, $(CF)_n$ is a molecular compound and therefore an electronic insulator, whereas the fluoride intercalation compounds are both ionic (F^-) and electronic conductors.

D. Conclusion and Prospects for Future Work

The demonstrated reversibility of the redox processes in the Graphite/$MF_6(MF_5)$ electrodes and the compatibility of such electrodes with the F^- ion conductors such as PbF_2/SbF_3 already provides a possible basis for an electrical-energy-storage system. It is probable however that an even more valuable cell can be constructed in which one electrode is of graphite intercalated with alkali metal (e.g. C_6Li), and the other of oxidized graphite (e.g. $C_{12}GeF_6$). The remaining problem is to find a solid electrolyte which is compatible with such a pair of electrodes and which will provide both for F^- ion transport and alkali cation transport.

References

1. A. R. Ubbelohde, Nature, 210, 404 (1966).

2. N. Bartlett, R. N. Biagioni, E. M. McCarron, B. W. McQuillan and F. L. Tanzella, Molecular Metals, W. E. Hatfield, Ed., Plenum Publishing Corp. (1979); see also this thesis, Chapter IV.

3. N. Bartlett, E. M. McCarron, B. W. McQuillan and T. E. Thompson, Synthetic Metals, vol. 1, 221 (1980); see also this thesis, Chapter VIII.

4. E. M. McCarron and N. Bartlett, J.C.S. Chem. Comm., 009 (1980); E. M. McCarron, Y. J. Grannec and N. Bartlett, J.C.S. Chem. Comm., in press; see also this thesis, Chapters V, VI and VII.

5. P. Hagenmuller and W. van Gool, Solid Electrolytes, Academic Press (1980).

Table IX-1. Conductivities of some solid electrolytes at 20° and 150°C and their activation energies.

Compound	σ@20°C (r^{-1} cm^{-1})	σ@150°C (r^{-1} cm^{-1})	ΔEa (E_v)
$Pb_{0.75}Bi_{0.25}F_{2.25}$ [1]	$6 \cdot 10^{-5}$	$8 \cdot 10^{-3}$	0.39
$Pb_{0.75}Sb_{0.25}F_{2.25}$ [2]	$2 \cdot 10^{-4}$	$2.5 \cdot 10^{-2}$	0.32
$Pb_{0.875}Th_{0.125}F_{2.25}$ [1]	$2 \cdot 10^{-4}$	$2.5 \cdot 10^{-2}$	0.32
$KBiF_4$ [1]	$1 \cdot 10^{-4}$	$2 \cdot 10^{-2}$	0.32
$RbBiF_4$ [1]	$2 \cdot 10^{-4}$	$3 \cdot 10^{-2}$	0.37
$\alpha T\ BiF_4$ [1]	$1 \cdot 10^{-5}$	$1 \cdot 10^{-3}$	0.38
$\alpha PbSnF_4$ [1]	$1 \cdot 10^{-3}$	----	0.42
$\beta PbSnF_4$ [1]	----	$8 \cdot 10^{-2}$	0.14

[1] J. M. Reau, J. Portier, A. Leuasseur, G. Villinenaie and M. Pouchard, Mat. Res. Bull., vol. 13, pp. 1415-1423 (1978).

[2] Unpublished work.

Table IX-2. Galvanic cells studied.

Sample	Anode	Electrolyte	Cathode	Voltage (V)
1	Sb	$Pb_{0.75}Sb_{0.25}F_{2.25}$	$C_8(IrF_6)$	0.6-0.7
2	Sb	$Pb_{0.75}Sb_{0.25}F_{2.25}$	$C_{12}(PtF_6)$	0.5-0.6
3	Sb	$Pb_{0.75}Sb_{0.25}F_{2.25}$	$C_{11.5}(AsF_5)$	0.9-1
4	Sb	$Pb_{0.75}Sb_{0.25}F_{2.25}$	$C_8(SbF_5)$	0.8-0.9
5	Sb	$Pb_{0.75}Sb_{0.25}F_{2.25}$	$C_{11.5}(AsF_6)$	1.5-1.6
6	Sb	$Pb_{0.75}Sb_{0.25}F_{2.25}$	$C_8(SbF_6)$	1.5-1.6
7	Sb	$Pb_{0.75}Sb_{0.25}F_{2.25}$	$C_{12}(GeF_6)$	1.9-2
8	$C_8(SbF_5)$	$Pb_{0.75}Sb_{0.25}F_{2.25}$	$C_8(SbF_6)$	0.4-0.5

Table IX-3. Galvanic cells previously reported.

Cell	Authors	Year	Voltage (v)
$Pb/PbF_2/CuF_2$	Kennedy	1976	0.61 - 0.70
$Pb/PbF_2 \cdot AgF/Bi(O,F)_{3.9}$	Schoonma	1976	0.33
$Pb/PbF_2 \cdot KF/(CF)_n$	Varta	1974	0.5
$Pb/PbF_2 \cdot BiF_3/AgF$	Bordeaux group	1973	1.24
$Pb/PbF_2/BiF_3$	Bordeaux group	1976	0.3

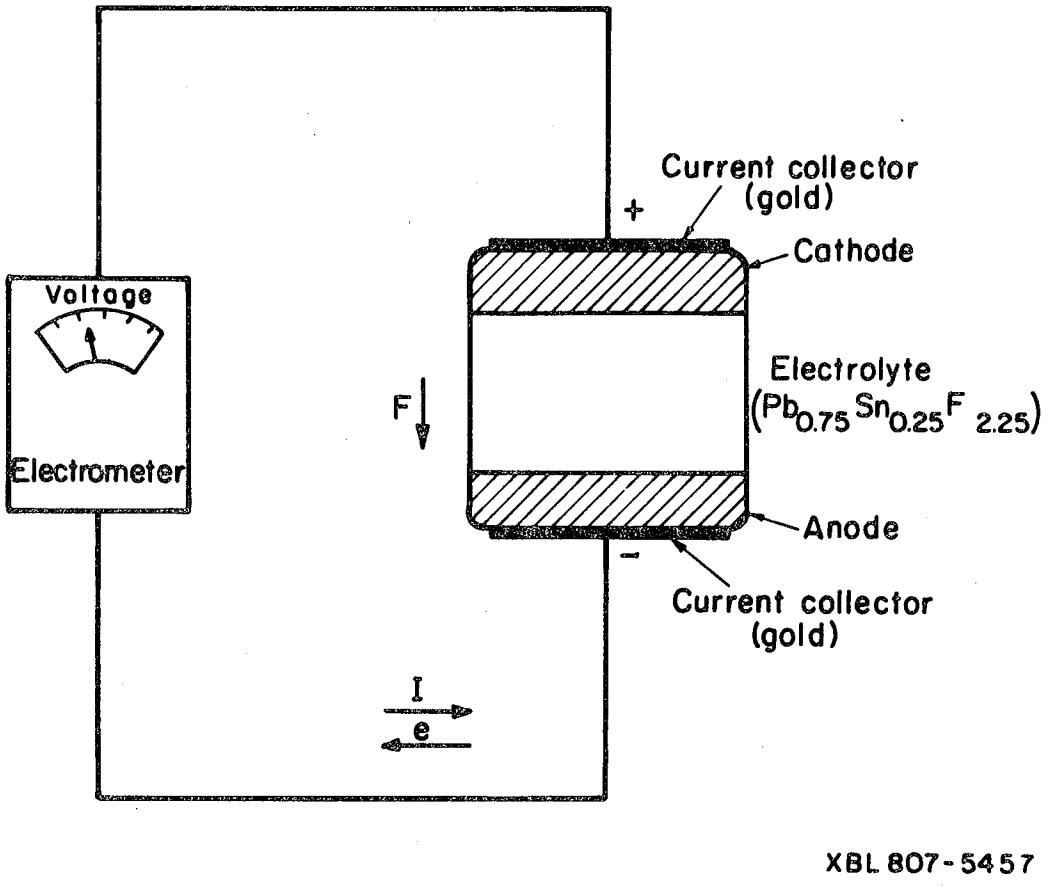

Figure IX-1. Typical galvanic cell utilizing a solid electrolyte.

APPENDIX

A GLOSSARY OF TERMS PECULIAR TO GRAPHITE INTERCALATION CHEMISTRY

1) Intercalation: The uptake of guest (intercalating specie) by the host material (graphite) with a consequent swelling of the material along its unique axis (c-axis).

2) Gallery: The graphite plane-graphite plane spacing.

3) Staging: A periodic gallery occupancy (illustrated in Fig. A-1). First stage implies all galleries filled; second stage, every other gallery filled; and so on.

4) Graphite-Acceptor Compounds: Graphite intercalation compounds in which electron transfer from the filled π_{Pz} band of the graphite to the intercalant specie (the acceptor) takes place. Hence, the graphite becomes a macro-cation. Graphite-acceptor compounds are characterized by their metallic blue coloration.

5) Synthetic Metal: Any material in which the number of charge carriers in the conduction band is increased by charge transfer to an acceptor or from a donor species to form, essentially, a salt.

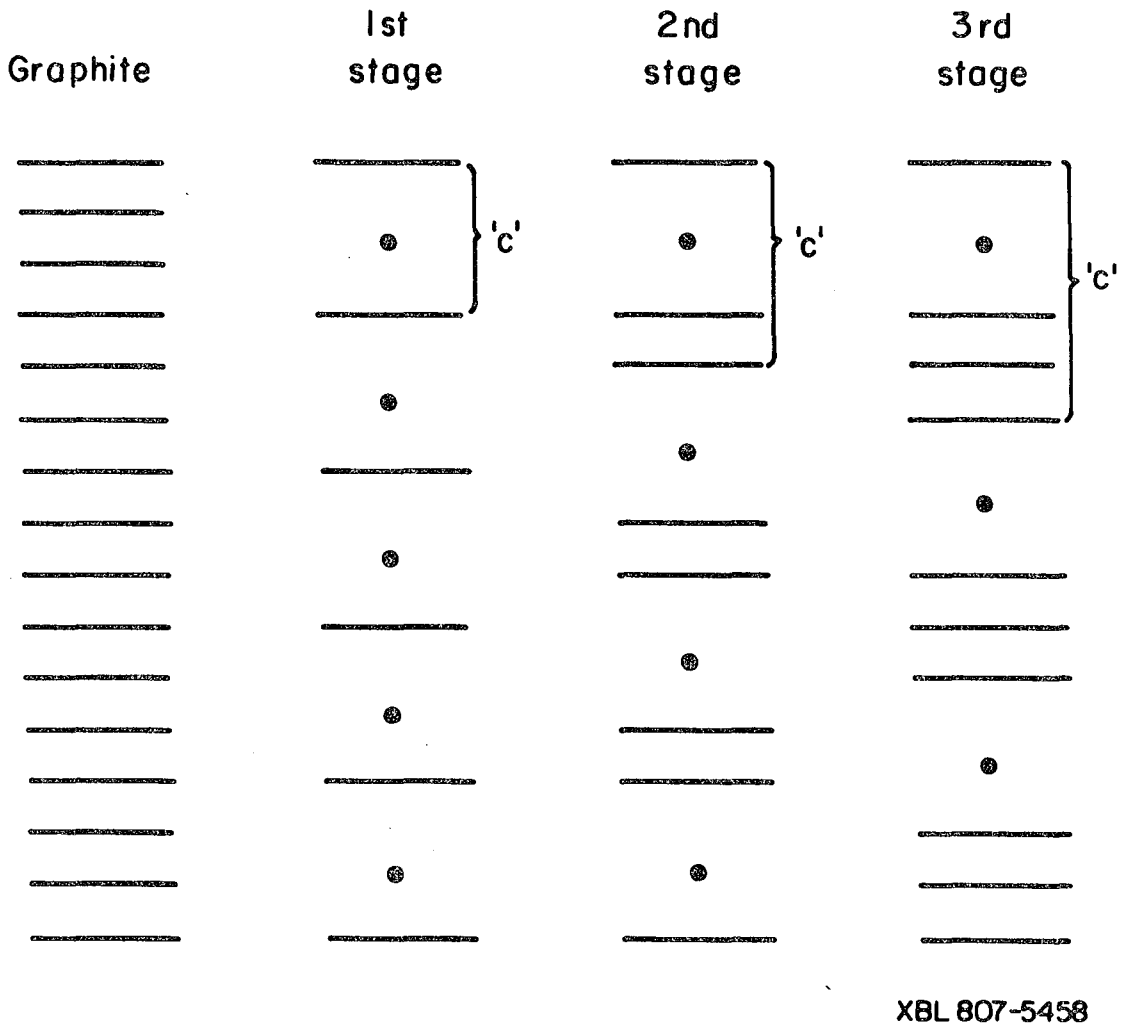

Figure A-1. The concept of staging in graphite intercalation compounds.

This report was done with support from the United States Energy Research and Development Administration. Any conclusions or opinions expressed in this report represent solely those of the author(s) and not necessarily those of The Regents of the University of California, the Lawrence Berkeley Laboratory or the United States Energy Research and Development Administration.